The Pennsylvania State University

The Graduate School

Intercollege Graduate Program in Agricultural and Biological Engineering

A NOVEL MACHINE TO PRODUCE FUEL NUGGETS FROM NON-RECYCLABLE PLASTICS

A Thesis in

Agricultural and Biological Engineering

by

Matthew J. Lawrence

Submitted in Partial Fulfillment
of the Requirements
for the Degree of

Doctor of Philosophy

August 2007

The thesis of Matthew J. Lawrence was reviewed and approved* by the following:

Dennis R. Buckmaster
Associate Professor of Agricultural and Biological Engineering
Purdue University
Thesis Advisor
Co-Chair of Committee
Special Member

Dennis E. Buffington
Professor of Agricultural Engineering
Co-Chair of Committee

James W. Hilton
Associate Professor of Agricultural Engineering

Ronald C. Hedden
Assistant Professor of Materials Science and Engineering

William J. Lamont, Jr.
Professor of Vegetable Crops

Roy E. Young
Professor and Head
Department of Agricultural and Biological Engineering

Signatures are on file in the Graduate School

ABSTRACT

The potential for energy reclamation from non-recyclable plastics is significant and particularly timely. A plastic-derived fuel production process was developed and has been shown to be effective for non-recyclable plastics that are normally discarded. A machine was designed, constructed and evaluated with regard to energy balance and fuel nugget production. The hydraulically driven machine processed dirty, non-recyclable plastics by first compacting and then extruding them through four internal channels of a heated die. The process produced plastic fuel nuggets with a thin, melted exterior which trapped unmelted plastic in the interior. The plastic nuggets, called Plastofuel™, were 3.8 cm (1.5 in) wide, 3.8 cm (1.5 in) high, and were cut to a length of 5.1 cm (2 in).

All aspects of machine operation, with the exception of feedstock loading, were automated and controlled by an onboard microprocessor. The machine was equipped with two data loggers to collect hydraulic system metrics and electrical energy usage. Component positions, electric power consumption, and hydraulic system pressure were recorded and converted to total energy consumption for all production runs.

Energy content of the Plastofuel™ formed using clean household plastic and unused mulch film was 45.5 MJ/kg (19500 BTU/lb). Plastofuel™ formed with used mulch film and used plastic pots and trays had an energy content of 38.8 MJ/kg (16700 BTU/lb). The average density of the individual Plastofuel^{TM} nuggets formed was 708 kg/m^3 (44.1 lb/ft^3). The bulk density of Plastofuel^{TM} was 378 kg/m^3 (23.6 lb/ft^3).

An energy ratio was determined by dividing the combined hydraulic and electric energy used for Plastofuel^{TM} formation into the potential energy stored in all plastic nuggets formed for a single test run. The highest energy ratio (E_{out}/E_{in}) from all test runs

was 47. During this test run, the electrical system consumed 30% of the total input energy to melt the Plastofuel™ perimeter, and the hydraulic system consumed 70% of the total input energy to process the plastic feedstock. The maximum Plastofuel™ production rate achieved with the machine was 27.6 kg/hr (61 lbs/hr).

A mathematical model was derived to predict a relationship between the die surface temperature, the plastic residence time in the die, and melt depth achieved around the Plastofuel™ exterior. The 99% confidence interval on the mean difference between actual and predicted melt depth was -0.08 mm (-0.003 in) to 0.1 mm (0.004 in) ($P = 0.8$).

Twelve additional test runs were run to isolate the effect of temperature and residence time on melt depth. Both factors significantly affected ($P < 0.05$) melt depth. Increasing die residence time with a fixed temperature was shown to increase melt depth, and increasing die temperature with a fixed residence time was shown to increase melt depth.

A theoretical analysis of electrical energy used to heat the unmelted interior of each nugget was performed and indicated that 18% of the total electrical energy consumed by the machine was used to heat the nugget interior.

TABLE OF CONTENTS

LIST OF FIGURES

LIST OF TABLES

LIST OF EQUATIONS

ACKNOWLEDGEMENTS

Successfully completing a graduate degree requires far more than the efforts of one student. Throughout my graduate experience I have had tremendous support from many individuals: far more than I can name here. However, I would like to acknowledge those with whom I have been in almost daily contact. I had the privilege of conducting graduate research on the principles of machinery and power transfer with someone who literally wrote the book on agricultural machinery engineering: Dr. Dennis Buckmaster. He is patient, understanding, accessible, and knowledgeable - all of the qualities required for a superior major professor and committee chairman.

The idea of Plastofuel™ is not my own, but rather that of James Garthe. In his tireless efforts to make the world a more livable, resourceful, and efficient place, I believe that he has invented something in Plastofuel™ that has done just that. He secured the grant from the Pennsylvania Department of Agriculture for this research and welcomed me to the Plastofuel™ team. He has been a great mentor and friend to me throughout my research, and I thank him for that.

My committee members are ideally suited for exploratory Plastofuel™ research, and I was extremely fortunate to have their input throughout this process. Dr. Dennis Buffington, co-chair of my committee, is a specialist in energy systems and alternative fuels. Dr. William Lamont, Jr. is world renowned in the science of plasticulture. Dr. Ronald Hedden has a great understanding of polymer behavior and science and was a major contributor to the mathematical model to predict melt depth. Dr. James Hilton is an expert in agricultural machine design. All committee members have contributed much more than their time to this research.

Jared Puvak, an undergraduate engineer, was hired in the summer of 2006 to help with machine fabrication. He proved to be a very accomplished young engineer and quickly expanded his role to become a great contributor to machine design through the spring semester of 2007. Dr. Roderick Thomas, our resident electrical expert, and Randall Bock, our resident machining expert, also contributed greatly and were always willing to offer their time and guidance.

Finally and most importantly, I want to thank my family. My parents have been supportive of my education throughout my life, and graduate school was no exception. Leaving industry for graduate school required a fairly significant lifestyle adjustment – one that my wife Renee was graciously willing to make. Her support and encouragement has been constant on this journey, and I thank her for that. Our son, Owen, was born while I was in graduate school, and he probably has no idea that his future was the reason I decided to return for an advanced degree.

1.0 Introduction

The use of plastics in agriculture has increased dramatically since their introduction to the industry in the 1950s. Termed plasticulture, this practice is widespread and used for such on-farm applications as round bale covers, nursery trays and pots, mulch films, drip tape, trench silo and greenhouse covers, and chemical containers. Unfortunately, due to their contaminated condition, most agricultural plastics are used only once and then discarded rather than reused or recycled. Piles of used plastic products on farms are an eyesore and environmental hazard; however, they also may be an opportunity.

Nearly all plastic materials in use today are petroleum-based products with a high heating value. If these waste plastics could be transformed to fuel nuggets and burned in a specially designed high-temperature furnace, this alternative energy source would alleviate the burden of disposal and may also provide an additional revenue stream to farmers. Alternatively, further research with plastic burning technology may someday result in a system in which plastic fuel pellets could provide heat for greenhouses and/or other farm structures.

The problem of waste agricultural plastic disposal coupled with the potential of waste plastic as an alternative fuel is a great opportunity to obtain value from what is currently considered a waste product and an expensive liability. Continued research in this area is in the best interest of farmers, the environment, and our communities as a whole.

Forming Plastofuel™ (Figure 1) fuel nuggets made from waste plastics has been under development since the mid-1990s (Garthe, 2004).

Figure 1: Plastofuel™ Nuggets

A prototype Plastofuel™ formation process and machine (Figure 2) exist for low volume production. This machine has produced fuel pellets from a wide variety of used plastics: mulch film, greenhouse coverings, nursery trays and pots, drip tape, and several other non-farm waste plastics. This research expanded on the prototype design to produce an automated, instrumented Plastofuel™ production machine.

Figure 2: First Prototype Plastofuel™ Machine in Operation

Although a prototype machine to create the fuel pellets is in existence, it is very labor intensive and is not suitable to transform large quantities of waste agricultural plastics. With the prototype machine the initial feedstock size reduction, compaction, and nugget cut-off processes require the continuous effort of an operator to produce approximately 2.3 kg (5 lb) of nuggets per hour.

The ultimate research goal for this work was the design, construction, and analysis of an automated, mobile Plastofuel™ production system. Machine performance statistics were collected to determine the ratio of potential energy stored in the Plastofuel™ nuggets to the hydraulic and electric energy used in their formation. Design considerations began with a review of current literature pertaining to waste agricultural plastic availability, current disposal methods, and plastic physical properties.

2.0 Research Hypothesis, Goals, and Objectives

2.1 Hypothesis

An optimized electro-hydraulically powered machine can produce plastic derived fuel nuggets that have a potential energy approximately 100 times higher than the energy used to form them.

2.2 Research Goals and Objectives

The goals of the research were the design and fabrication of a mobile Plastofuel^{TM} production machine as well as the quantification of the energy used to produce the fuel pellets and the energy stored in the fuel pellets. The objectives in support of the goals and hypothesis were to:

1. Develop a predictive thermal model to set system parameters sufficient to form plastic derived fuel nuggets.
2. Design and fabricate a system to form plastic derived fuel nuggets from waste agricultural plastics.
3. Use the machine fabricated in Objective 2 to determine maximum plastic fuel nugget production rate.
4. Optimize, using an electro-hydraulic circuit and feedback mechanisms, the energy input settings to produce plastic fuel nuggets at the maximum rate.
5. Determine the energy balance of the system by comparing energy used to form plastic fuel pellets and the potential energy stored in the nuggets.

3.0 Literature Review

This literature review will begin with a discussion of the role of plastics in agriculture. The advantages of using plastics for improved agricultural production and storage are well known and widely publicized; however, this review will discuss the relatively brief useful life of plastic products in outdoor environments and their requisite disposal. The difficulties and hazards of disposal for both agricultural and consumer plastics are lesser known and will be the focus of the review. Finally, this section will discuss the physical properties of plastic products to show that waste plastic holds a significant energy value and poses a minimal environmental risk when properly incinerated.

3.1 Plastic Use in Agriculture

Many different types of plastic can be found in use for nearly every crop and at nearly every stage of production in modern agriculture (Figure 3). Grain, forage, and horticultural crops can benefit in some ways from plastic utilization. For example, plastics in grain and forage crops are used for fertilizer and herbicide storage, silage bale wrapping, and trench silo coverings. Horticultural farmers use plastics for such applications as nursery trays and pots, drip irrigation tubing, mulch film, row covers, and high tunnel and greenhouse coverings.

There are two general categories of agricultural plastics: films and containers. The obvious difference is rigidity: plastic film products are less rigid than plastic container products. Agricultural films are primarily low density polyethylene (LDPE)

but can also be polypropylene (PP). Agricultural containers are primarily high density polyethylene (HDPE) but can also be polystyrene (PS) or PP.

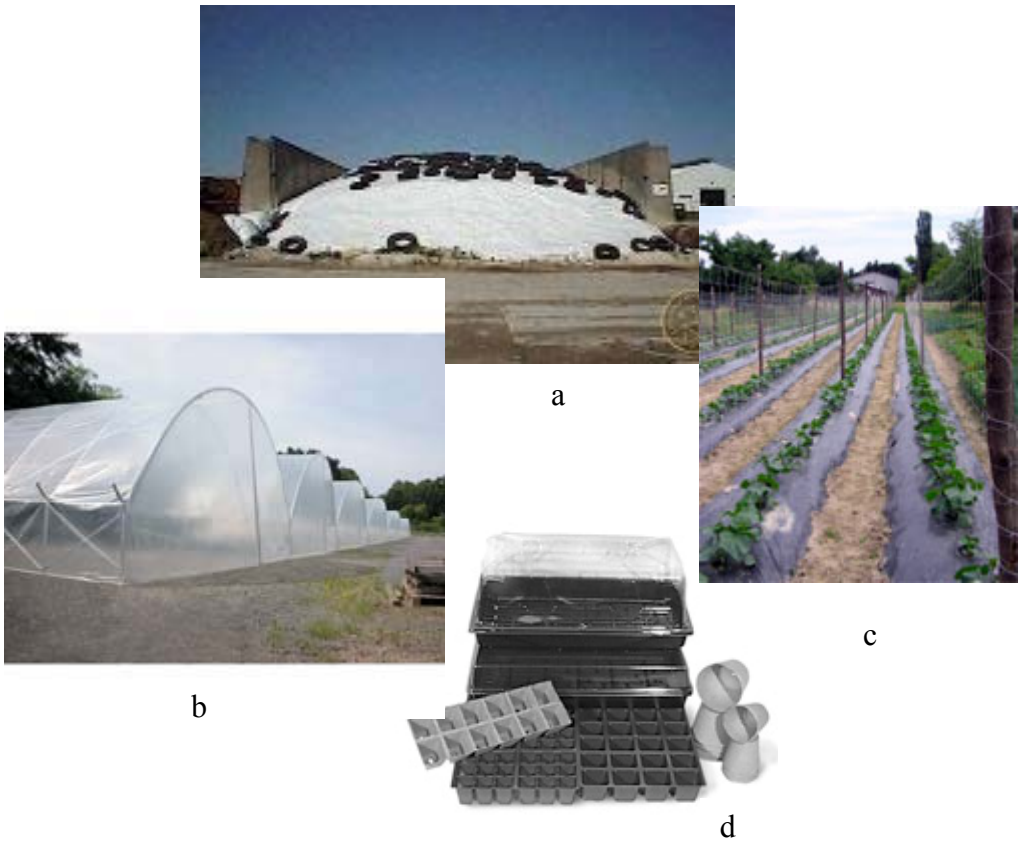

Figure 3: Examples of Plastics Used in Agriculture

a: LDPE bunker silo cover, b: PP high tunnel covering, c: LDPE mulch film, d: PS nursery trays

At the current annual consumption rate of $2.25(10^6)$ Mg ($4.96(10^9)$ lbs), the amount of plastic used in agriculture worldwide is staggering (Hussain and Hamid, 2003). The only published comprehensive study of plastic use in American agriculture was completed by Amidon Recycling at the request of the American Plastics Council (APC) (APC, 1994). The 1994 study not only categorized and quantified the plastic use annually in the US agricultural sector, but also indicated the type of plastic used in each application. A summary of these findings is shown in Table 1.

Table 1: Estimated Quantities of Agricultural Plastics Used Annually in the US (APC, 1994)

Agricultural Application	Primary Plastic Type	Thousands of Mg (Millions of Pounds)
Film		
Greenhouse and Nursery Film	Low-Density Polyethylene (LDPE)	11.3 (25.0)
Mulch Film	LDPE	27.2 (60.0)
Fumigation Film	LDPE	5.7 (12.5)
Degradable Mulch Film	LDPE	1.4 (3.0)
Irrigation Tubing	LDPE	6.1 (13.5)
Silage Bags	LDPE	3.6 (8.0)
Hay and Silage Bale Stretch Wrap	LDPE	11.3 (25.0)
Haysleeve Covers	LDPE	1.1 (2.5)
Nursery Containers		
Blow-Molded Pots	High-Density Polyethylene (HDPE)	40.8 (90.0)
Injection-Molded Pots	HDPE	45.4(100.0)
Injection-Molded Pots	Polypropylene (PP)	38.6(85.0)
Pots, Packs, and Flats	Polystyrene (PS)	31.8 (70.0)
Agricultural Pesticide Containers		
Blow-Molded less than 2.5 gallon	HDPE	3.6 (8.0)
Blow-Molded 2.5 gallon	HDPE	5.4 (12.0)
Extrusion Blow-Molded 30-gallon	HDPE	0.7 (1.5)
Injection-Molded 5-gallon	HDPE	0.7 (1.5)
Rotational-Molded Returnable/Refillable	HDPE	0.7 (1.5)
Total		235 (518.5)

Since this study was completed in 1994, subsequent studies completed by the same author but not released to the public have determined that the amount of plastics

used in U.S. agriculture increased to $3.86(10^5)$ Mg ($8.5(10^8)$ lbs) in 1998 and $4.54(10^5)$ Mg ($1(10^9)$ lbs) in 2001 (A. Amidon, personal communication, 12 August 2005).

3.2 Plastic Disposal

Statistics specifically regarding the disposal of agricultural plastic were only found in the APC publication released in 1994. Of the more than $2.35(10^5)$ Mg ($5.19(10^8)$ lbs) of plastic used, it was estimated that less than 5% were recycled and less than 5% were incinerated for energy recovery (APC, 1994). That left approximately $2.11(10^5)$ Mg ($4.66(10^8)$ lbs) of plastic disposed in undesirable methods. Currently, there are three primary methods to handle waste agricultural plastic: recycling, incineration (mostly through open burning), or burying in a landfill site (Garthe, 2004; Warner, 2005). Each of these disposal options will be discussed in this section.

The disposal of post-consumer, non-agricultural plastics in the United States is better documented and will also be discussed for reference purposes. Post-consumer plastics, those that have served their intended purpose, make up roughly 9.4% of municipal solid waste (MSW) by weight before recycling. Of this percentage, 3.8% are recycled. Remarkably, the remaining 5.6% of MSW plastics by weight destined for the landfill make up an estimated 16% to 25.1% of the total waste by volume (Harper, 2002; Rathje and Murphy, 1992). Although this research focuses on the recovery of waste plastics from the agricultural sector, the potential for plastic recovery from the MSW stream should not be overlooked.

Plastofuel™, the plastic-derived fuel nuggets that are the focus of this research, is considered the last stop for a waste product, because it will be incinerated for energy

recovery. Plastofuel™ creation should only be considered when product reuse or recycling is not an option.

3.2.1 Post-Consumer Plastic Recycling

There are four categories of plastic recycling defined: primary, secondary, tertiary, and quaternary (Ehrig, 1992; Harper, 2002; Fisher, 2003). Primary recycling is the creation of similar quality products from the recycled source. Secondary recycling is the creation of products from the reclaimed material with less demanding specifications such as the creation of composite lumber from waste plastics. Tertiary recycling is the use of a recycled product as a chemical raw material. Finally, quaternary recycling is considered by some not recycling at all. It is the incineration of a plastic as an energy source. Plastofuel™ represents a form of quaternary recycling.

The methods used to recover the $1.1(10^6)$ Mg ($2.4(10^9)$ lbs) of post-consumer plastics recycled annually in the United States (Harper, 2002) must overcome two main hurdles: recovery and separation. Current recovery options (Harper, 2002) include bottle deposit systems (only available in some states), buy-back systems, drop-off systems, and collection systems. The use of collection systems, also known as curbside collection, has become the most popular method of recovery in the United States. In 1990, 15% of the households in the United States had the option of curbside recycling (Ehrig, 1992). By 2002, this number increased to 70% (Harper, 2002).

Separation of the collected plastic is done at material recovery facilities (MRF). MRFs not only separate the various resin types, but also prepare the materials for market (Ehrig, 1992). In some instances, preparation for market can be as simple as baling bulk plastic by type for shipment to, for example, a secondary recycling composite lumber

facility. Alternatively, manual separation of plastics by not only type but also color can be done for primary recycling purposes. The scope and automation of the plastic separation processes generally depend on the size of the facility.

3.2.2 Agricultural Plastic Recycling

There are many references in the literature that point to the difficulties in recycling agricultural plastics. The primary obstacle in recycling used agricultural plastics is the high level of foreign particles (Wittwer, 1993). Hochmuth (1990) points out that recycling agricultural plastics is much more difficult than recycling household plastic items because the agricultural plastics are more contaminated. They may be covered with sand, soil, crop refuse, and possibly agricultural pesticides. However, the virgin resin used in the plastic manufacturing process is made primarily from natural gas and oil, and higher raw material prices increase the economic viability of washing and recycling contaminated plastics (Corr, 1992).

There is little documentation regarding the extent of contamination on typical waste agricultural plastics as they are retrieved from the field. Clearly, the extent of contamination on agricultural plastics can vary widely. Application, contaminant density, plastic type, and collection methods can all affect contaminant levels. Brooks (1997) determined that plastic mulch pulled directly from the raised beds had a dirt content of 36% by weight. Hussain and Hamid (2003) stated that recovered agricultural films can achieve contamination rates as high as 50% by weight. Concentrations this high will exclude the recovered plastic from recycling centers. It is typical that any concentration above 5% by weight will not be accepted by recycling centers (Clarke, 1995).

One type of agricultural plastic, HDPE, is currently recycled under certain conditions. HDPE agricultural containers are collected by members of the Ag Container Recycling Council (ACRC). Regional collectors associated with the not-for-profit ACRC recycle some $3.2(10^3)$ Mg ($7(10^6)$ lbs) of HDPE annually in the United States (ACRC, 2005). The plastics that are collected by the ACRC must first be triple-rinsed or washed out with pressurized water by the farmer. Finally, each container is visually inspected and may be rejected by collectors. These containers are granulated and then recycled into such items as fence posts, marine pilings, railroad ties, and landscape timbers.

There is a patent on a machine that cleans and pelletizes used plastic mulch film (Brooks, 1997). The plastic mulch must first be baled and is then placed on a conveyor belt and transported through a series of shredders and dryers before being strained clean and forced through an extruder to melt it prior to being pelletized. No indication was found during this review that the machine was in production or current use. Additionally, the final use of the pellets was not specified.

An example of secondary recycling for used agricultural plastics is the manufacturing of composite wood materials. One of the leading companies in this industry is Trex Company of Winchester, Virginia (Harper, 2002). Trex Company buys contaminated LDPE from several sources. Daniel Zook, a collection source in Leola, Pennsylvania, collects and bales used agricultural plastic before selling it to Trex Company. Zook seems to be the only collection source of used agricultural plastics in Pennsylvania. Trex Company washes the plastic before incorporating it into their composite lumber (D. Zook, personal communication, 20 September 2005).

Zook also collects and bales used polystyrene greenhouse trays and polypropylene sacks from local farmers. He sells that material to a broker and believed the plastic was shipped overseas to be washed and recycled. It is not uncommon for contaminated film plastics to be shipped overseas where the cheap labor costs make hand sorting an economical option (Harper, 2002).

3.2.3 Post-Consumer Plastic Incineration

The topic of quaternary recycling, the recovery of energy from waste plastics through incineration is fraught with public misconceptions. Plastic incineration instills the thought of thick black smoke and the release of numerous toxins. However, if done correctly, incineration of most waste plastics can be accomplished in a clean and environmentally friendly manner (Garthe et al, 2006, Fisher, 2003 and Ehrig, 1992). Studies begun in the early 1990s by the Association of Plastics Manufacturers in Europe evaluated the co-combustion of plastics with MSW to produce both heat and electricity. The emissions and solid residues released during combustion were in compliance with strict German regulations. Furthermore, a study of the incineration of automotive shredder residue, including plastics mixed with MSW, was carried out in compliance with the U.S. waste-to-energy plant regulations (Fisher, 2003).

The major differentiator between post-consumer and agricultural plastic waste in the combustion debate is polyvinyl chloride (PVC). PVC is not nearly as widely used in the agricultural sector as PE, PS and PP, and therefore is not proposed as a component of Plastofuel^{TM}. The chlorine in PVC has led many to believe that incineration of PVC will lead to the release of hydrochloric acid and dioxins, as chlorine is a constituent of dioxin.

In the case of PVC combustion, stack gas remediation equipment can reduce the release of Cl and dioxins by 90% (Ehrig, 1992).

The key to clean combustion of plastics is elevated temperatures. The current facilities that cleanly burn plastics (cement kilns, industrial boilers, and steel mill blast furnaces) do so at temperatures of approximately 2000°C (3600°F) (Fisher, 2003).

3.2.4 Agricultural Plastic Incineration

Incineration of waste plastic from farms has considerable energy conversion potential, if done correctly; however, field incineration with no energy reclamation is far more common. With high transport costs and tipping fees at most landfills, farmers often pile the used plastic on the farm and openly burn the waste. Low temperature burning and incomplete combustion can generate pollutants. This tactic is generally frowned upon by communities. Since some plastic has chemical residue on it, open burning is not acceptable in many areas (Hochmuth, 1998).

Parish, et al. (2000) developed a machine to collect and simultaneously burn waste plastic mulch in the field. The energy was not reclaimed from the mulch; the research was focused on mulch disposal rather then energy recovery. The machine required two operators: one to drive the tractor, and the other to feed plastic into the machine at the beginning of the row or if the plastic tore. The machine lifted the plastic from the field and forced it through a combustion chamber with four LPG burners rated at 528 MJ/hr (500,000 Btu/hr) each. The researchers discovered that even at slow operating speeds (1.5 km/hr (1.0 mph)) the combustion was incomplete leaving burning globules in the field. They determined that the solution required more research, and no further publications regarding this approach were located.

The potential thermal energy stored in common agricultural plastics is often overlooked. The three most commonly used agricultural plastics – polyethylene (PE), polypropylene (PP), and polystyrene (PS) - are nearly as high in energy value as fuel oil on a mass basis (South, 1992). Waste plastics can be burned at high temperatures in commercial incinerators to generate steam to produce electricity. Most plastic burns cleanly in proper commercial incinerators; however, bundled plastic can actually burn so hot it will damage an unprotected furnace (Corr, 1992). South (1992) identified three key issues to be addressed regarding agricultural plastic incineration:

1. Although studies indicate that PE, PP, and PS can be safely incinerated, effects of residual pesticides are yet unknown.
2. Public misperception of the "noxious" by-products these plastics produce when burned must be corrected.
3. The logistics of collecting the bulk plastic, processing it into a usable form, and transporting it to a suitable facility are yet to be determined.

There are at least three applications where waste agricultural plastics are being successfully burned as fuel (Garthe, 2004 and Fisher, 2003). A full-scale trial of the burning of post-commercial polyethylene greenhouse coverings was successfully demonstrated as a co-fuel in a coal-fired power plant. Also, plastic-derived fuel (PDF) is currently being investigated as a supplemental fuel source for the heating of cement kilns at Lafarge North America. Finally, the Korean company GR Technologies Company, Ltd. (www.highgr.com) manufactures and sells a high temperature burner and boiler system fueled by pea-sized plastic pellets (Figure 4).

Figure 4: Plastic Fuel Pellets for GR Technologies Burner

The GR Technologies system was emissions tested by an independent U.S. company in May, 2005. Three main groups of pollutants were analyzed: 1) gases (sulfur dioxide, oxides of nitrogen, and carbon monoxide); 2) particulate matter; 3) dioxins /furans. Test results proved that this is an extremely clean burning system in all three groups (Garthe et al, 2006). Research is ongoing with this company to adapt their technology to accept the larger and likely more contaminated Plastofuel^{TM} nuggets.

3.2.5 Post-Consumer Plastics in Landfills

From 1989 to 2000, the total amount of MSW generated per year in the United States rose from 1.48(10^8) Mg (3.26(10^{11}) lbs) to 1.95(10^8) Mg (4.3(10^{11}) lbs). Over this time the percentage of plastics in the waste stream has hovered near 9% by weight. There has been, however, an increase in the percentage of plastics recovered from the

waste stream. In 1989, 1% of plastics were recovered, and in 2002, 5.6% of plastics were recovered prior to landfilling. The plastics that are not recovered for recycling but rather are deposited in a landfill contribute up to 25.1% of the total landfill volume (Ehrig, 1992 and Harper, 2002). An interception of plastic in the waste stream prior to landfilling would significantly reduce landfill volume.

Plastics do not degrade in landfills. The very properties of plastic polymers that make them desirable to the consumer (durability, resistance to corrosion, etc.) make them resistant to decay in a landfill.

3.2.6 Agricultural Plastic On-Farm Dumping and Landfilling

There are three methods of agricultural plastic disposal that offer no value other than removing the waste from site. For this reason, these options should be regarded as disposal methods of last resort; however, they are unfortunately the most commonly exercised. Landfilling, on-site stock piling, and burial are the most usual disposal methods for waste agricultural films and containers (APC, 1994). A more recent survey of Pennsylvania vegetable farmers (Garthe, 2004) indicated that burying, stock piling, landfilling, and contracting a local waste hauler account for 72% of plastic disposal.

3.2.7 Plastofuel™

Conversion of dirty, used, agricultural plastics to an energy source through quaternary recycling has been researched by Garthe (2004) since the mid 1990s. Plastofuel™ (Figure 5), is a fuel pellet formed from dirty, unsorted waste agricultural plastics not suitable for primary, secondary, or tertiary recycling. One option for Plastofuel™ incineration is to co-fire the pellets at rates of 5-10% with coal in existing

boilers. An alternative would be to create Plastofuel™ fuel pellets from plastic waste generated on the farm to heat farm structures using a burner like the one available from GR Technologies. Any clean incineration of the Plastofuel™ for the purpose of energy recovery would be far better than burying, stock piling, and landfilling.

A prototype machine does exist and can create roughly 2.3 kg (5 lb) of Plastofuel™ per man-hour (Figure 2). The process is relatively simple. First, waste plastics are fed by hand into a hopper. The rod from a vertically-oriented hydraulic cylinder then drives the plastic through a die in the bottom of the hopper. The plastic forced through the die is heated with band heaters, jacketing the 3.8 cm (1.5 in) diameter extrudate in approximately 2 mm (0.08 in) of melted plastic (Figure 5).

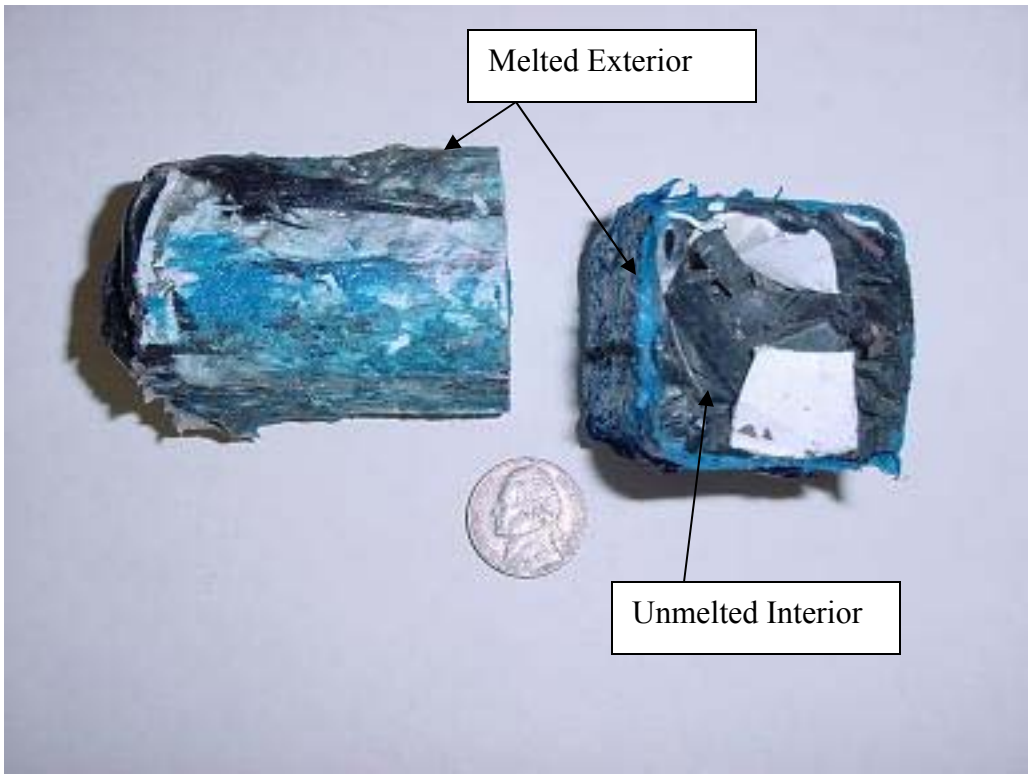

Figure 5: Melted Perimeter and Unmelted Interior of Two Plastofuel™ Nuggets

As the plastic exits the band heaters, the melted exterior of the extrudate cools and hardens, thus locking unmelted plastic in the center and retaining a cylindrical shape.

Finally, using a heated butter knife, the extrudate is cut by hand into nuggets 5 cm (2 in) in length.

Of critical importance is minimal energy input into the nugget formation. Minimizing the energy input during Plastofuel™ formation maximizes the value of the end product in the waste to energy balance. The non-human energy input to the Plastofuel™ formation using the current prototype machine involves electric power. The hydraulic power unit is powered by a 0.75 kW (1 hp) electric motor and the four heating bands each consume 0.38 kW (0.5 hp) for a total continuous power consumption rate of 1.9 kw (2.5 hp). If the energy content of Plastofuel™ is assumed to be 43.9 MJ/kg (18,900 BTU/lb), the average of pure PE, PP, and PS, the energy ratio of the prototype machine is 15.

3.2.8 Current Plastic Derived Fuel Technologies

Current technologies and research regarding plastic derived fuels were not located in peer-reviewed journals during the literature review. A series of Internet searches, however, did provide pertinent results. These technologies are discussed in this section.

Professor Alka Zadgaonkar from the G H Raisoni College of Engineering in Nagpur, India, has been researching energy recovery from waste plastics since 1993 (Good News India Magazine, 2006 and Autocar, 2005). Professor Zadgaonkar reclaims all types of plastic wastes from individual collectors for tertiary recycling. The wastes include plastic bags, buckets, chairs, CD cases, computer keyboards, expanded PS, and PVC. There is no initial sorting or cleaning; all plastics are shredded and melted at low temperature then augered into a degasification chamber. In the chamber, the chlorine in the PVC is bubbled away as hydrochloric acid. The remaining melt then interacts with a

proprietary mix of catalysts to produce three streams of energy: (1) a gaseous cloud which is condensed to form a sulfur-free liquid hydrocarbon, (2) a non-condensable gas which is a liquid petroleum gas equivalent, and (3) a solid fuel called petroleum coke. All three end products can be burned to reclaim energy. The balance of the feedstock is ash and metal fines. The production has transitioned from the research to industrial sector. A single facility is collecting and processing 25 Mg ($5.5(10^4)$ lbs) of plastic daily, and there is the expectation that more facilities will be built in the future. No energy balance for the system was located.

A similar facility in both size and function is manufactured by a company called Ozmotech located in Melbourne, Australia (Ozmotech, 2007). Ozmotech is an environmental technology company and manufactures a modular solution to waste plastic energy recovery. The system is called ThermoFuel™ and processes waste plastics using a gasification process similar to that used by Professor Zadgaonkar. According to the company press release, they construct modular Thermofuel™ plants for shipment around the world. The latest system processes 20 Mg ($4.4(10^4)$ lbs) of dirty, unsorted plastic per day converting it to $18(10^3)$ liters (4800 gal) of sulfur-free diesel fuel. No mention was found regarding an energy balance, but the feedstock did require shredding and melting prior to processing. Ozmotech specifically mentions that used agricultural plastics including "silage wrap and trickle tape" are acceptable feedstocks.

Campbell et al. (2001) performed an economic analysis to quantify the effect of adding plastic feedstock to a coal gasification plant – another example of tertiary recycling. The analysis involved a simulation only; data was not collected from a working facility. The focus of the analysis included the effect of plastic on facility

performance, the avoided landfill cost, and the cost of processing plastic to a form suitable for use. The authors concluded that an addition of 20% plastic to the coal feedstock would equate to a 42% increase in overall system efficiency as compared to a coal-only scenario. There were, however, significant capital investment requirements.

There were two examples of fuel cubes made from a mixture of plastics and other materials (Ore-Cal RC&D, 2006 and Balcones Resources, 2006). Ore-Cal RC&D is a non-profit organization that focuses on resource conservation and rural economic development in northern California and southern Oregon. These areas have a generous supply of two products: (1) waste agricultural film from strawberry production and (2) western juniper – an invasive specie overtaking native grasses.

Balcones Resources is an independent recycler of high grade paper products headquartered in Austin, TX. They also produce fuel cubes from a combination of waste paper and plastic feedstocks in their newest division, Balcones Fuel Technology, located in Little Rock, AR. Balcones fuel cubes consist of pre-consumer baby diapers, surgical gowns, and feminine hygiene products mixed with polyethylene and paper fiber. Balcones stated on their website that the fuel cubes have a heating value of 30.1 MJ/kg (13000 BTU/lb). There was no information on the process energy balance, production rates, or the target customer.

Ore-Cal RC&D and Balcones Resources formed an inter-corporate agreement to explore the possibility of producing fuel cubes from a mixture of 50% waste agricultural film and 50% western juniper. 6.8 Mg (15000 lbs) of each feedstock type were shipped from Ore-Cal RC&D to the Balcones Fuel Technology facility to be ground and processed into cubes measuring 5.1 cm (2 in) on all sides. The cubes formed from the

mixture contained 28 MJ/kg (12000 BTU/lb). There was no documentation found regarding the process energy balance or production rate. Sample cubes were sent to test facilities to determine combustion emissions, but the data was not yet available. When available, the emissions results will be used to begin the search for buyers of the fuel cubes.

3.3 Plastics and Plastic Properties

Reclaiming energy from waste agricultural plastics must begin with an understanding of how much energy can be derived from this currently untapped source. This section focuses on the physical and thermal properties of different types of plastic that are often used in agriculture. These properties are important to the transformation of the waste to a viable energy resource. The types of plastic most commonly found in agricultural settings are polyethylene (PE), polystyrene (PS), and polypropylene (PP) (South, 1992).

The primary raw-material sources of the major plastic and elastomer materials are fossil fuels: natural gas, coal, and crude oil (Harper, 1992). Plastics can be broadly categorized as thermoplastics and thermosets. Both are high molecular weight polymers; however, they differ in the fact that thermoplastic polymers are not cross-linked. Cross-linking is the tying together of polymer chains with covalent bonds (Harper, 2002). This three-dimensional network cannot be undone and renders thermosets a one-time use product. For example, thermoplastic HDPE milk jugs can be recycled by reheating them to the appropriate temperature and reforming them as new milk jugs. Thermosets, such as used automobile tires, cannot be reheated and reprocessed as new tires, but they can be

pulverized and reused in some other application. Polyethylene, polystyrene, and polypropylene are all thermoplastics.

This section will begin with a discussion of the methods used to form plastic films and containers. It will conclude with the thermal and physical properties of typical agricultural plastics pertinent to the formation of Plastofuel™. Because Plastofuel™ may include waste plastics that are not dried or washed, the potential for contamination by soil and water will also be considered.

3.3.1 The Extrusion Process

Each of the manufacturing processes in this section begins with resin and an extruder. The material from which all plastic films and containers originate is called resin. Resin can be termed "virgin resin". Virgin resin is derived from original feedstock, or "regrind", which consists of items that have been extruded and formed but due to rejection have become waste. This regrind is then reduced in size and returned to the manufacturing process. Extruders feed resin from a material hopper to a die via a screw conveyor. The conveyor contains a series of zones where the material is melted and compacted (Moore and Kline, 1984). Finally, the extrudate is forced through a die and exits most commonly as a flexible rod to be later formed into some final product.

Fuel pellets could be made from waste agricultural plastics using an extruder. However, industrial extruders require a feedstock that consists of finely ground particles which are completely free of contamination. Washing contaminated agricultural plastics and then grinding them to fine particles would require energy input and would therefore detract from the net energy realized from burning the extrudate formed. Additionally, the process of completely melting the feedstock would detract from the net energy gain upon

pellet combustion. Extrudate feedstock is completely melted during its path from the hopper to the die (Muccio, 1994). Preliminary calculations shown in Appendix F indicate that melting a 2 mm (0.08 in) jacket around the exterior of the Plastofuel™ nugget requires 500% less energy than melting all of the plastic contained in the nugget.

3.3.2 Plastic Film Formation

Plastic film is defined as a plastic sheet that is less than 0.025 cm (.010 in) thick (Muccio, 1994). It is common for the thickness of polyethylene film used in agriculture to be described using the term "mil". One "mil" is defined as 0.0025 cm (0.001 in). Four mil LDPE plastic mulch film, for example, would be 0.01 cm (0.004 in) thick.

Blown film extrusion is used to form thin film and bags (Moore and Kline, 1984 and Muccio, 1994). For this process, no mold is required; a continuous ring-shaped tube of melted plastic is extruded as a jet of compressed air directed at the center of the extrudate forms a long hollow "oblong balloon". The film cools and sets in the surrounding air and is then wound into rolls. The extrudate can then be sliced to form film or sealed to form bags.

3.3.3 Plastic Container Formation

Rigid plastics used in agriculture are generally formed one of three ways: blow molding, injection molding, or rotational molding. Each will be briefly discussed in this section.

Blow molding begins with the extruder forming a plastic tube that approximates the shape of the finished product. This tube is known as a "parison". The parison is then clamped into a split mold in the shape of the finished product. An air nozzle directed in

the end of the parison injects compressed air into the parison and the material expands to the shape of the clamp and forms the finished product. The clamp is then cooled to set the plastic and released (Moore and Kline, 1984).

Pots, trays, container lids, and drip irrigation plugs are typically injection molded. For a part to be injection molded, the extruder places a charge of softened plastic into a chamber. The plastic in the chamber is then forced into the mold with a hydraulic cylinder and cooled. The formed plastic part is then released and the process repeated (Moore and Kline, 1984).

Finally, another way to produce typically larger rigid plastic items is through the use of rotational molding. In rotational molding, an extruder is not used. Rather, the resin, usually powder or liquid, is placed directly in a mold. The mold is then heated and rotated on two axes coating the inside of the mold. The mold continues to spin as it is cooled; the mold is then stopped, opened, and the object is removed (Moore and Kline, 1984).

3.3.4 Plastic Energy Values

Currently, fossil fuels are the primary source for U.S. electrical energy, as they account for 71% of the total production (USDOE, 2003). The relatively high energy content of fossil fuels makes them the most important single resource for energy production. Fossil fuels, petroleum and natural gas, are the primary feedstock for plastics (Muccio, 1994), so it is to be noted that plastics also carry a high energy content. Table 2 provides heating values for plastics and other common materials.

Table 2: Heating Values of Plastics and Various Materials
(Garthe and Kowal, 1993 and Gupta and Lilley, 2003)

Material	Heating Value, MJ/kg (Btu/lb)
Fuel Oil	48.6 (20,900)
Polyethylene	46.3 (19,900)
Polypropylene	44.1 (19,000)
Polystyrene	41.4 (17,800)
Tires	30.1 (13,000)
Subbituminous Coal	27.3 (11,700)
Wood (pine)	22.3 (9,600)
Wood (oak)	19.3 (8,300)
Municipal Solid Waste (dry)	16.2 (7,000)
Municipal Solid Waste (50% moisture)	7.9 (3,400)

3.3.5 Plastic Properties

As explained in section 3.2.7, the formation of Plastofuel™ involves both thermal and physical alteration of the waste agricultural plastic. This section will focus on the properties of plastics and pertinent equations for Plastofuel™ production. These properties are summarized in Table 3.

Table 3: Properties of Plastofuel™ Components

Material	Density, kg/m^3	Thermal Conductivity, W/m-°K	Heat Capacity, J/°K-kg	Heat of Fusion, J/kg
Liquid Properties				
HDPE*	855[a]	0.26[c]	2228[a]	--
LDPE*	855[a]	0.24[c]	2146[a]	--
PP*	852[a]	0.17[c]	2463[a]	--
PS*	1065[a]	0.17[c] 0.128[a]	1884[a]	--
Solid Properties				
HDPE	950[a] 950[b] 950[c]	0.25[b] 0.49[c] 0.40[d]	1363[a] 2250[b] 2250[c]	280000[a]
LDPE	920[b] 920[c]	0.24[b] 0.32[c] 0.33[d]	1363[b] 2300[c] 2300[d]	290000[a]
PP	905[a] 910[b] 910[c]	0.117[a] 0.15[b] 0.15[c]	1625[a] 2100[b] 2400[c]	209000[a]
PS	1040[a] 1060[b] 1060[c]	0.11[a] 0.12[b] 0.12[c] 0.16[d]	1225[a] 1200[b] 1200[c]	0[a]

* HDPE – High Density Polyethylene; LDPE – Low Density Polyethylene; PP – Polypropylene; PS - Polystyrene

[a]Brandrup et al, 1999

[b]Rao and Schumacher, 2004

[c]Rao and Obrien, 1998

[d]Osswald and Menges, 2003

There are differences in the physical properties of plastic from different sources (Table 3). For example, the thermal conductivity of solid HDPE ranged from 0.29 to 0.49 W/m-°K. All research calculations used the median values from the sources in Table 3 when multiple values were discovered for the same material property.

Plastofuel™ nuggets formed using the prototype machine (Figure 2) have only the outer 2 mm (.08 in) melted of the total 3.8 cm (1.5 in) diameter. This was accomplished by heating the die to a constant temperature of 135º C.

The melting of a semi-infinite solid with constant thermophysical properties and a step change in surface temperature is better known as the Stefan-Neumann problem (Tadmor and Gogos, 1979). Temperature distribution, and therefore depth of melt, can be predicted using an empirically determined value of a constant K in the Stefan-Neumann equation.

Equation 1: Stefan-Neumann
(Tadmor and Gogos, 1979)

$$\frac{(T_m - T_1)k_l e^{-K^2\beta^2/4\alpha_l}}{\sqrt{\pi\alpha_l}\,erf\,(K\beta/2\sqrt{\alpha_l})} - \frac{(T_o - T_m)k_s e^{-K^2/4\alpha_s}}{\sqrt{\pi\alpha_s}\,erfc(K/2\sqrt{\alpha_s})} = \lambda\rho_l \frac{K\beta}{2}$$

where

T_m = melting point of plastic (ºK)

T_1 = surface temperature (ºK)

k_l = thermal conductivity of liquid (W/mºK)

K = unknown constant (m/√s)

β = ratio of solid and liquid densities

α_l = thermal diffusivity of liquid defined as $\frac{k_l}{\rho_l c_l}$ (m^2/s)

c_l = heat capacity of liquid (J/°K-kg)

T_o = initial core temperature (ºK)

k_s = thermal conductivity of solid (W/mºK)

α_s = thermal diffusivity of solid defined as $\frac{k_s}{\rho_s c_s}$ (m^2/s)

c_s = heat capacity of solid (J/°K-kg)

λ = heat of fusion (J/kg)

ρ_l = density of liquid (kg/m^3)

ρ_s = density of solid (kg/m^3)

The constant K can be used to not only determine the depth of melt over time while the plastic is in contact with the heated plate, but it can also be used to calculate the temperature distribution in the Plastofuel™ nugget. Equation 2 can be used to determine the distance of the solid/melt interface from the heated plate.

Equation 2: Distance of Solid-Melt Interface from Heated Plate (Tadmor and Gogos, 1979)

$$X = K\sqrt{t}$$

where

X = distance from heated plate to solid/melt transition (m)

t = time in contact with heated plate (s)

K = constant determined in Equation 1

The temperature distribution within the Plastofuel nugget also requires a solution for the constant K. This temperature distribution is important because any heat delivered to the unmelted portion of the Plastofuel nugget represents wasted energy. Temperature distributions can be calculated in both the melted and solid zones of the plastic in contact with the hot plate.

Equation 3: Temperature Distribution in Melt
(Tadmor and Gogos, 1979)

$$\frac{(T_l - T_m)}{(T_1 - T_m)} = 1 - \frac{erf(x_1 / 2\sqrt{\alpha_l t}}{erf(K\beta / 2\sqrt{\alpha_l}}$$

where

T_l = temperature of liquid at depth x_l after time t (ºK)

x_l = depth in melt at which temp is determined (m)

t = time in contact with hot plate (s)

Equation 4: Temperature Distribution in Solid
(Tadmor and Gogos, 1979)

$$\frac{(T_s - T_m)}{(T_o - T_m)} = 1 - \frac{erfc(x_s / 2\sqrt{\alpha_s t}}{erfc(K / 2\sqrt{\alpha_s}}$$

where

T_s = temperature of solid at depth x_s after time t (ºK)

T_o = initial core temperature (ºK)

x_s = distance from melt/solid transition at which temp is determined (m)

Equations 1-4 apply to a very specific condition to determine melt depth and temperature distributions. These equations apply to a semi-infinite, solid, pure plastic sample in stationary contact with a heated plate. The highly variable properties of Plastofuel™ in addition to conditions within the heated die used for this research deviate

from this model; however, these equations were the closest representation found in the literature to research conditions. Several examples of how the research conditions differ from model assumptions are listed below.

- Nugget Components – The model assumed that the nugget was of a pure, constant plastic type and solid throughout. The Plastofuel^{TM} nuggets consist of several different types of plastic.
- Nugget Size – The model assumed a semi-infinite solid in contact with a flat, hot plate on one surface only. In reality, the nuggets are relatively small (1.5"x1.5") and heated around the entire perimeter.
- Surface Temperature – The model assumed that the surface temperature would be constant the entire time the surfaces are in contact. The research die will likely have a temperature gradient as room temperature feedstock warms throughout its passage through the die.
- Thermal Properties – The model required many thermal properties for the plastic type in contact with the heated die. These included thermal conductivity (W/m^{o}K), thermal diffusivity (m^2/s), heat capacity (J/kg^{o}K), and heat of fusion (J/kg). These values may be inaccurate for a typical Plastofuel^{TM} nugget, because it may also contain air pockets, water, plant debris, and soil.
- Core Temperature – All models assumed a core temperature of 298^{o}K. This may vary based on the initial temperature of the waste plastic.
- Residence Time – The model required a time in contact with the heated surface. The residence times may be variable due to a variety of feedstock types during testing.

- Heat Generation by Surface Friction – Heat generated by friction may increase the melt depth.

4.0 Procedure

One objective of this research was the development of a fluid power system to produce plastic fuel pellets. However, Pennsylvania Department of Agriculture funded this project and dictated that the Plastofuel™ production machine be mobile and not require an external power source to operate. In other words, the system had to include an electric generator to run the hydraulic power unit and the electrical components. The desire to have a mobile unit was two-fold. First, the machine was to be used as an extension tool by Penn State. Realizing the goal of recovering energy from waste begins with a re-education of the public. Ultimately, the acceptance of Plastofuel™ as an alternative energy would require the collection of non-recyclable plastic from those who currently dispose of the plastic using less than ideal methods. A mobile demonstration unit would allow this technology to be on display throughout the commonwealth as an educational tool. Second, a mobile machine was the first step in reaching the ultimate goal of Plastofuel™: collecting and processing waste plastics for incineration. Although a power generation incineration facility willing to accept Plastofuel™ has not yet been located, research is ongoing to find such a plant. Supplying a facility with large volumes of Plastofuel™ may be accomplished with many small, mobile processing units like the one developed for this research traveling from farm to farm collecting and processing waste plastics.

This research began with the design, specification, and construction of a mobile system to transform used agricultural plastic to a form from which energy could be recovered. The design of the system, however, took into consideration that a minimum

amount of energy would be used for the Plastofuel™ formation in order to maximize the net recoverable energy.

The research procedure detailed in this section follows a systematic approach and appears in chronological order including initial system layout and basic machine operation, preliminary experiments and calculations, machine design, data collection and analysis methods, and finally machine testing.

4.1 System Design

Over the course of this research, the system design and fabrication phase was the most time consuming. System design began in January, 2005, and continued through March, 2007. This phase of the research included system layout, preliminary experimentation and calculations, computer aided design (CAD), part manufacturing, and machine assembly. Each of these processes will be discussed in this section.

4.1.1 System Layout

The first step in the system design was the system layout. The mobility requirement was satisfied by placing the machine in a towable trailer. A 2.1 m (7 ft) wide and 4.9 m (16 ft) long merchandising-style trailer manufactured by Pace American was selected. The merchandising-style trailer had five awning doors providing suitable demonstration capabilities. The trailer had a gross vehicle weight of 4500 kg (10000 lb) and could be towed by a common heavy-duty vehicle. The floor area of the selected trailer dictated the initial system layout.

The trailer had to house four large system components: the Plastofuel™ machine, an engine generator, a hydraulic power unit, and a plastic-fueled incineration unit.

Allocation of trailer space began by estimating these machine dimensions. The Plastofuel™ machine was determined to be no more than 1.8 m (6 ft) tall, 0.3 m (1 ft) wide, and 1.8 m (6 ft) long.

An additional design parameter of target machine throughput of 227 kg/hr (500 lb/hr) was also chosen during the initial system layout. With these initial design parameters, the basic machine geometry could be estimated. Machine sizing, component selection, and layout were very involved processes. Several considerations were made during the design phase; some of which are listed below.

- Density and melt depth data had to be collected from Plastofuel™ formed with the prototype machine.
- Data regarding agricultural plastic response to cutting and compaction had to be collected.
- The machine had to be easy to use, safe, and controllable.
- The machine had to adhere to the space requirements of the trailer layout.
- The machine components had to be represented in usable manufacturing drawings, manufactured at a reasonable cost, and produced with readily available components.

The first step was to determine the basic machine layout followed by an analysis of the physical characteristics of the Plastofuel™ nuggets formed with the prototype machine.

4.1.2 Basic Machine Operation

The basic machine operation was loosely based on the prototype machine (Figure 2). The new machine, however, had several key differences. These differences are listed below.

- The new machine had hands-free, automated operation – the only requirements of the operator would be to add feedstock and monitor the machine.
- The new machine was to achieve a higher volume of Plastofuel™ production. The target production rate was 227 kg/hr (500 lb/hr).
- The new machine produced four continuous Plastofuel™ "sausages". Nuggets were formed as these were automatically cut to length. The prototype machine produced only one continuous "sausage" cut to length by hand.
- The new machine added the capability to compact feedstock upon machine entry as well as cut nuggets to length upon machine exit.
- The new machine was instrumented to accurately quantify both hydraulic and electric power consumption.

Feedstock densification prior to extrusion was not done with the prototype machine. A hopper was simply filled with used plastics and the only plastic that was pushed through the die was that which was trapped between the extrusion cylinder rod and the die opening. This plastic was first compressed and then cut as it entered the die. In order to increase machine throughput for this research and reduce the size of large plastic pieces, the decision was made to add a compaction chamber. The compaction chamber was a confined volume into which loose feedstock was loaded. A hydraulic cylinder then drove a compaction plunger into the chamber, simultaneously cutting large feedstock pieces and compressing the waste agricultural plastic. The compaction cylinder continuously cycled as loose plastic was added by an operator. When the density in the compaction chamber matched a density that was empirically determined to be near that at which the plastic cuts, the compaction cylinder held its position. At this

point, the plastic was already compressed to the density that cutting began at the die entrance. However, before reaching the die entrance, a second plunger, the extrusion plunger, cut a portion of the compacted plastic from the compaction chamber and forced the compacted plastic through a linear knife grid and into one of four channels in a heated die. The extrusion plunger was driven by a second hydraulic cylinder. The extrusion plunger would then be retracted to its starting position, and the compaction cylinder would resume cycling and the process repeated. As the extrudate exited the die, each of the four nuggets were cut to length using individual limit switches that activated one of four cutting cylinders. The machine algorithm (Control Algorithm 1) to perform the above processes can be found Appendix H. Detailed drawings and photographs of all major machine components are discussed in section 4.1.5.

4.1.3 Preliminary Experimentation

The thermal and physical properties of plastics common to agriculture are well known and documented in Table 3. Plastofuel^{TM} properties, however, have never been analyzed or documented. Plastofuel^{TM} is a very complex material. It is not only an amalgamation of four types of plastic, but may also contain air pockets, moisture, soil, plant material, and other contaminants. For this reason, design parameters such as force required to densify and cut waste agricultural plastics were determined experimentally.

The first experiment attempted to determine the density at which waste agricultural plastics would cut when forced against a hot knife. This metric was a critical design parameter to determine the size of the extrusion cylinder required. The force of the extrusion cylinder would push compressed, uncut plastic through a linear knife grid and into the heated die.

Experiment 1

A preliminary experiment was performed using knives very similar to those that would provide the cutting surface of the heated die entrance. The purpose of the experiment was to determine the approximate density at which a collection of different types of plastics (PE, PS, PP) would begin to cut. The results of this experiment were used along with the results of a second preliminary experiment to size bore diameters of the compaction and extrusion hydraulic cylinders. To perform the first experiment, a 36 cm (14 in) length of 15 cm (6 in) diameter PVC tube was notched on either side nearly the entire length of the tube as shown in Figure 6.

Figure 6: PVC Tube Used for Density at Cutting and Knife Temperature Relationship

The tube was then filled with a known weight of assorted, used agricultural plastics. The plastics included LDPE drip irrigation, HDPE nursery pots, PS nursery trays, PP greenhouse coverings, and LDPE plastic mulch. A knife was heated with a propane torch

along the cutting surface that spanned the PVC tube. The temperature was recorded using an infrared temperature sensor made by 3M. The model number was IR-500 and it had an accuracy specification of ±2% of the reading within its operating range of -18º to 260ºC at a distance of 1.2 m (4 ft) from the target. The heated knife was placed in the notch and then pushed into the plastic. At regular intervals, the knife was removed and any visual evidence of cutting was recorded; if none was observed, the knife was reheated and pushed further into the plastic. When cutting was observed, the knife was held in position, and the height of the compacted plastic was measured. The weight of plastic divided by the volume at cutting provided an estimation of density at which cutting began. The process was repeated for eight different knife temperatures. The average required density that must be achieved before cutting begins was determined to be 0.28 g/cm^3 (0.01 lb/in^3). A graphical representation of the results is shown in Figure 7, and the experimental data can be found in Appendix A.

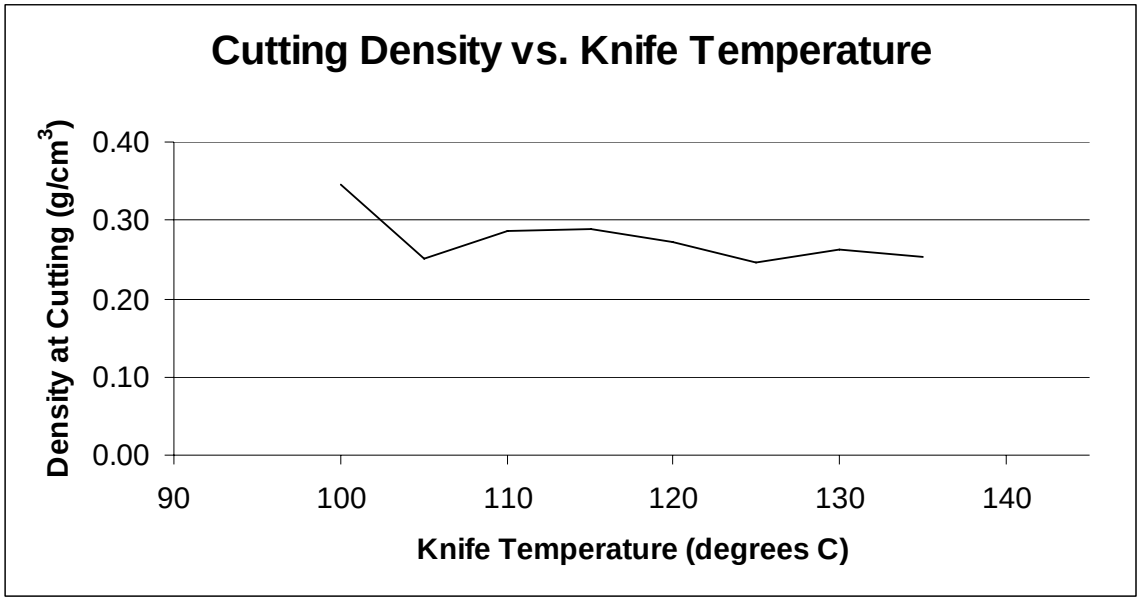

Figure 7: Density of Used Agricultural Plastics at Cutting vs. Knife Temperature

The second experiment determined how the density of waste agricultural plastic changed as pressure was applied to the plastic.

Experiment 2

The goal of the second preliminary experiment was to determine the hydraulic cylinder size required to compress loose plastic to the cutting density determined in experiment 1. The bore sizes of the compaction and extrusion cylinders selected had to exert enough force on the loose plastic to achieve this density.

For this experiment, a hydraulic press (Figure 8) was used to compact a sample of used agricultural plastics. Weighed plastic samples were confined to a hollow PVC tube and a "stamp" attached to a hydraulic cylinder rod compressed the plastic. The PVC tube was 30 cm (11 in) in diameter and 43 cm (17 in) in height and oriented directly under the vertical cylinder. The 25 cm (10 in) diameter "stamp" then extended into the plastic. The change in height of the plastic within the tube was recorded as hydraulic pressure varied from 0 kPa to 12.4 MPa (1800 psi). Two consecutive test runs using the same plastic sample were performed for each of four types of common used agricultural plastics: drip tape, nursery pots and trays, mulch film, and greenhouse coverings.

Figure 8: Test Stand Operated to Measure Used Agricultural Plastic Density With Varying Pressures

The results indicated that nursery trays and pots required the highest pressure to be compacted. The stamp applied a pressure of approximately 520 kPa (75 psi) to this type of plastic before reaching the estimated cutting density predicted in experiment 1. The relationship between pressure applied and density achieved can be seen for all four Plastofuel^{TM} feedstocks in the following graphs.

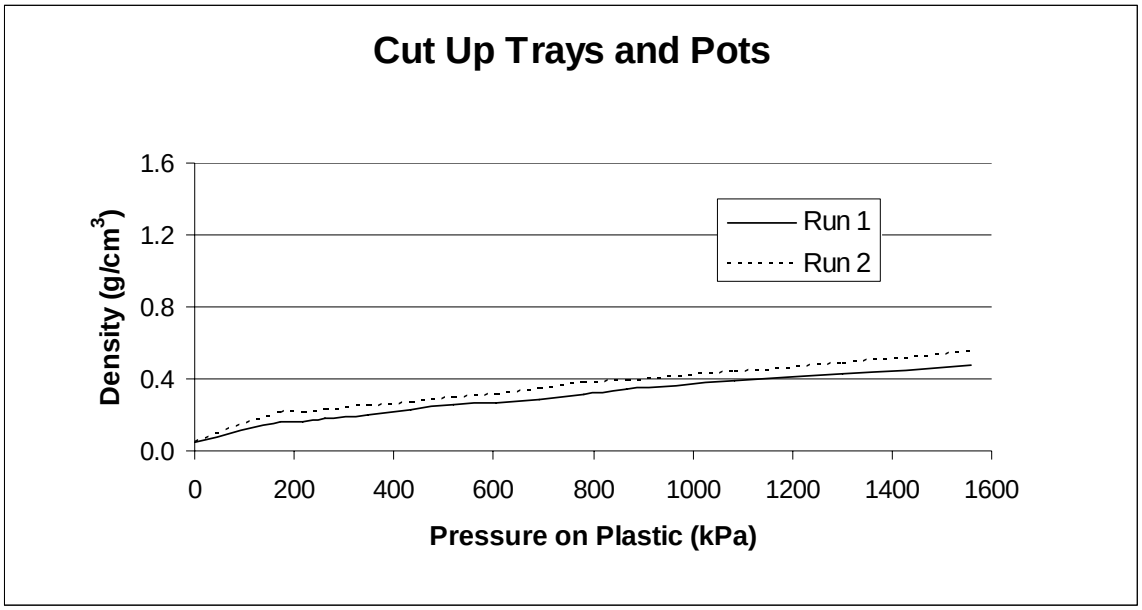

Figure 9: Density vs. Pressure on Plastic for Used Nursery Trays and Pots

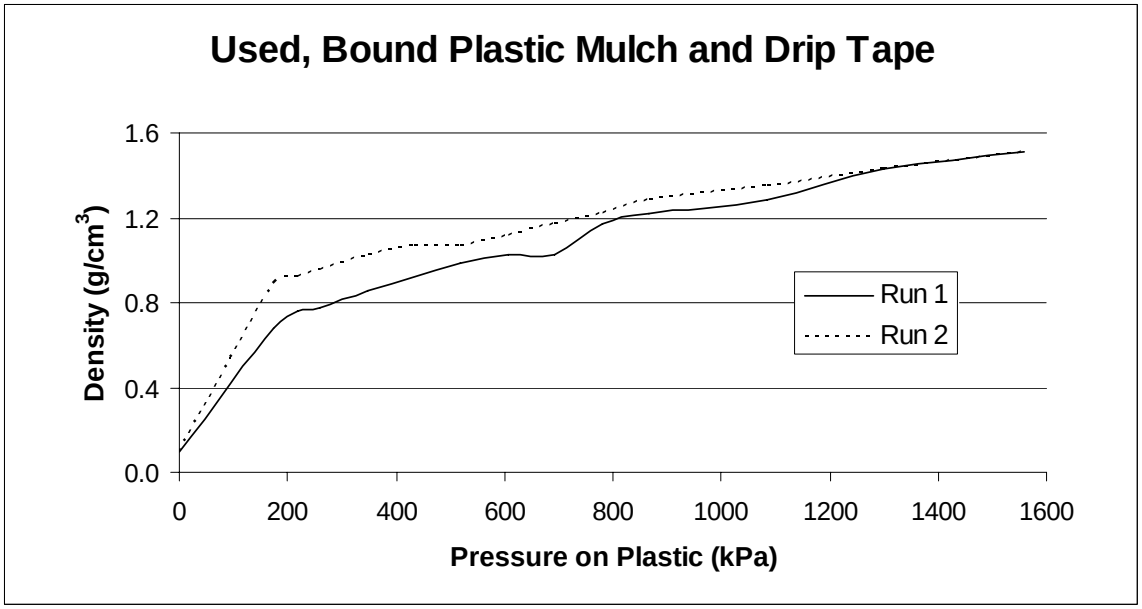

Figure 10: Density vs. Pressure on Plastic for Used, Bound Plastic Mulch and Drip Tape

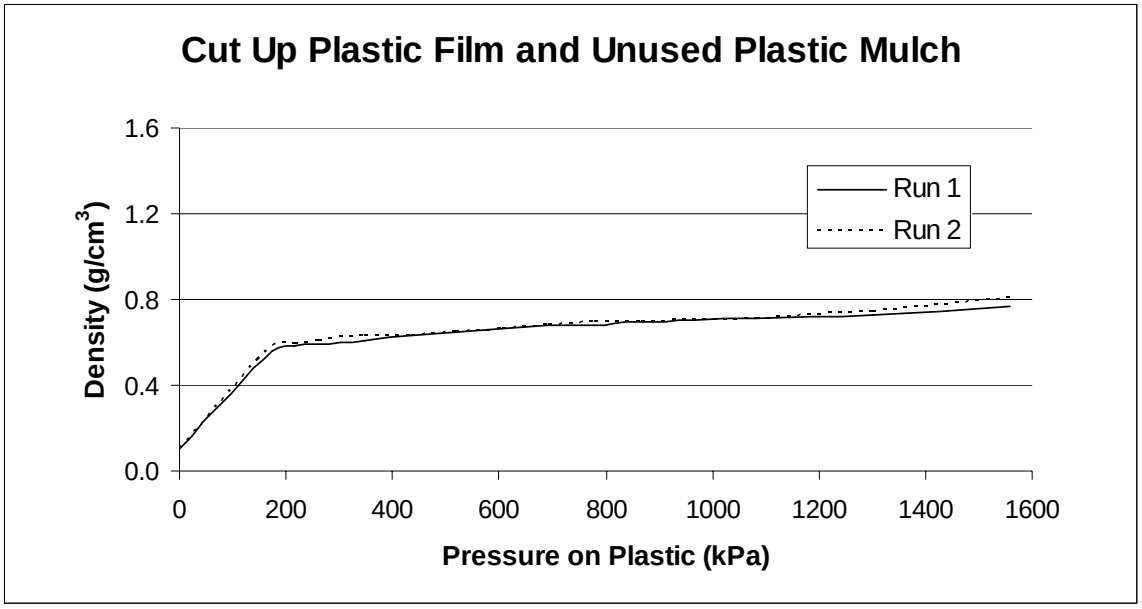

Figure 11: Density vs. Pressure on Plastic for Cut Up Plastic Film and Unused Plastic Mulch

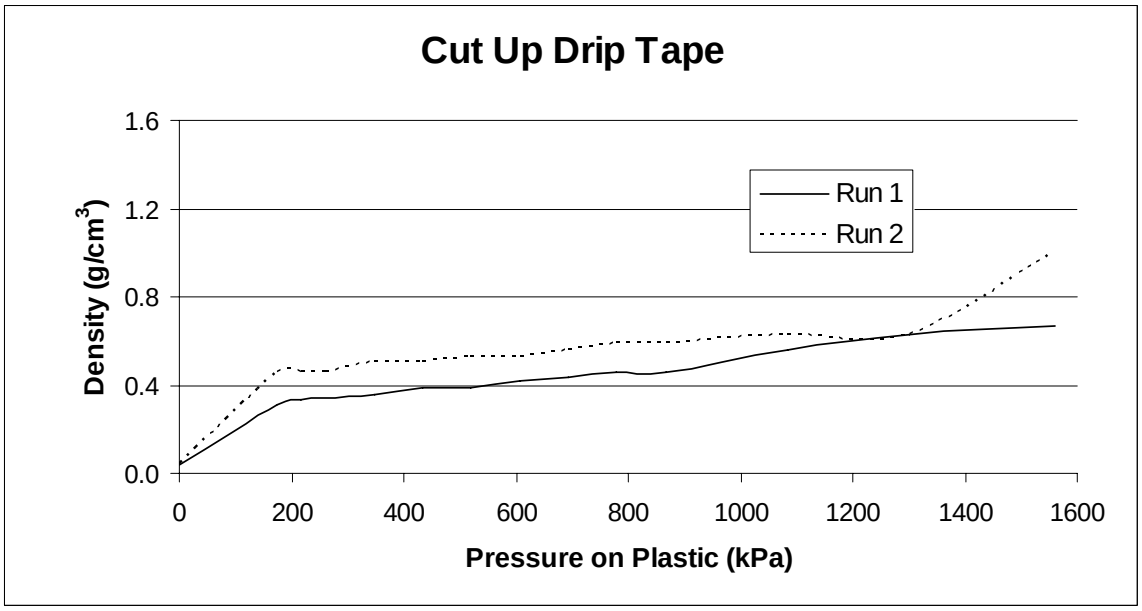

Figure 12: Density vs. Pressure on Plastic for Cut Up Drip Tape

The calculations for these experiments as well as the data collected can be found in Appendix B.

4.1.4 Preliminary Calculations

Hydraulic Cylinder Calculations

Required compaction pressure was used to size the hydraulic cylinder with an assumed hydraulic pressure of 20.7 MPa (3000 psi), and an adjustment was made to accommodate for the compaction plunger face area (Appendix C). An initial density and mass of a typical feedstock "charge" was assumed. As the compaction cylinder extended and decreased the compaction chamber volume, the charge density increased. The cylinder bore selected corresponded to a charge density that matched or exceeded the target Plastofuel^{TM} density. A 5 cm (2 in) bore cylinder was chosen for the compaction plunger. The extrusion plunger face had a smaller area than the compaction plunger face, so it was assumed that a 5 cm (2 in) bore extrusion cylinder would provide more than enough force to cut the plastic and force it into the die.

To achieve a throughput of 227 kg (500 lb), the compaction cylinder needed to cycle approximately twelve times per minute, and the extrusion cylinder needed to cycle four times per minute. At the peak hydraulic system pressure of 20.7 MPa (3000 psi), the power required for the compaction cylinder was calculated to be approximately 8 kW (10 hp). The peak power required for the extrusion cylinder was predicted to be 1.9 kW (2.5 hp). The cycle frequencies, key assumptions, and power calculations for the compaction and extrusion cylinders can be found in Appendix D.

As the extrudate was forced through the die channels, it emerged as four continuous "sausages" with a melted exterior. Each extrudate was cut by one of four cutting cylinders. The cylinders were positioned vertically after the heated die, and cut the nuggets with a "guillotine" type action. When a 5 cm (2 in) length of extrudate was

sensed with a limit switch, a heated blade attached to the cutting cylinder rod end extended into the nugget. Heating the blade eased cutting and melted the nugget face, trapping unmelted contents inside. As with the compaction and extrusion cylinders, the cutting cylinders were assumed to operate at a maximum system pressure of 20.7 MPa (3000 psi), and they had a bore diameter of 5 cm (1.5 in). Given a nugget diameter of 3.8 cm (1.5 in), the stroke of the cutting cylinder was considerably smaller than the compaction and extrusion cylinders. A stroke length of 6.3 cm (2.5 in) was selected. At the throughput goal of 227 kg/hr (500 lb/hr), each cutting cylinder would need to cycle eighteen times per minute. The power requirement of the cutting cylinders was a function of the cylinder size, operating pressure and cycle frequency. At maximum system pressure and target machine throughput, the cutting cylinders were predicted to consume a peak power of 3.1 kW (4.1 hp). The cutting cylinder calculations and assumptions can be found in Appendix E.

Die Heating Calculations

On the prototype machine created by Garthe (2004) four heating bands acting in series and directly attached to the die exterior were adequate to jacket the exterior of the Plastofuel^{TM} nugget in 2 mm (0.08 in) of melted plastic (trapping its unmelted contents). This machine was designed to have four die channels, and electric heating strips fixed to the die exterior. As stated earlier, specific thermal properties of mixed, heterogeneous Plastofuel^{TM} components are unknown, so a simplified calculation was used to estimate power used by the heating strips for generator selection. Assuming a melt depth of 2 mm (0.08 in) depth of melt, a machine throughput of 227 kg (500 lb) per hour, an experimentally determined Plastofuel^{TM} density of 728 kg/m^3, and nugget dimensions of

5.1 cm (2 in) in length and 3.8 cm (1.5 in) in diameter, a continuous electric power requirement of 4.5 kW (6.1 hp) was estimated to melt the exterior of the extrudate. The calculations can be found in Appendix F.

Melt Depth Prediction Calculations

The Stefan-Neumann model was applied to predict Plastofuel™ perimeter melt depth albeit with simplifications. The Stefan-Neumann problem (Tadmor and Gogos, 1979) applied to the melting of a semi-infinite solid with constant thermophysical properties and a step change in surface temperature. The model assumptions and actual research conditions were different.

Plastofuel™ physical properties and components are highly variable, so the model was applied using the properties of pure plastics common in agriculture: HDPE, LDPE, PP, and PS. The melt depth relationship to machine throughput rate and die temperature was established using a spreadsheet solution for a range of operating conditions. The procedure for calculating melt depth was to first calculate a value of the unknown constant "K" in the Stefan-Neumann equation (Equation 1) using plastic properties, a wall temperature, and an initial plastic temperature. The wall temperatures used were 220ºC, 200 ºC, 175 ºC, 165 ºC, 155 ºC, and 145 ºC. Die temperatures at or below 135 ºC were not modeled because they are below the melting temperature of HDPE. The initial plastic temperature was assumed to be 25ºC. The plastic property values used in the Stefan-Neumann equation are listed in Table 4.

Table 4: Plastic Properties Used in Stefan-Neumann Equation

Material	Density (kg/m^3)	Thermal Conductivity (W/m-°K)	Heat Capacity (J/°K-kg)	Heat of Fusion (J/kg)
Liquid Properties				
HDPE*	855[a]	0.26[c]	2228[a]	--
LDPE*	855[a]	0.24[c]	2146[a]	--
PP*	852[a]	0.17[c]	2463[a]	--
PS*	1065[a]	0.17[c]	1884[a]	--
Solid Properties				
HDPE	950[a]	0.40[d]	2250[b]	280000[a]
LDPE	920[b]	0.24[b]	2300[c]	290000[a]
PP	910[b]	0.15[b]	2100[b]	209000[a]
PS	1060[b]	0.12[b]	1200[b]	0[a]

* HDPE – High Density Polyethylene; LDPE – Low Density Polyethylene; PP – Polypropylene; PS - Polystyrene

[a]Brandrup et al, 1999

[b]Rao and Schumacher, 2004

[c]Rao and Obrien, 1998

[d]Osswald and Menges, 2003

The K value was then substituted in Equation 2 to calculate the melt depth for different residence times based on a machine throughput value achieved for each test run. The relationships formed are shown in the following graphs and an example of the spreadsheet solution can be found in Appendix G.

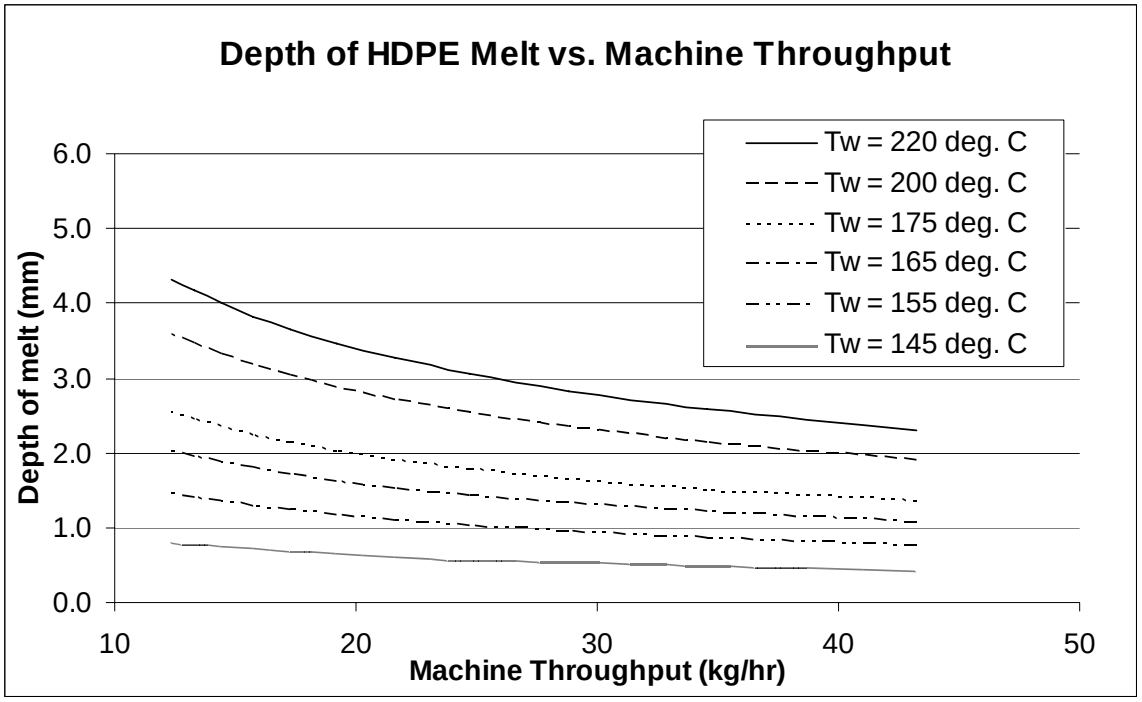

Figure 13: Melt Depth Prediction for High Density Polyethylene

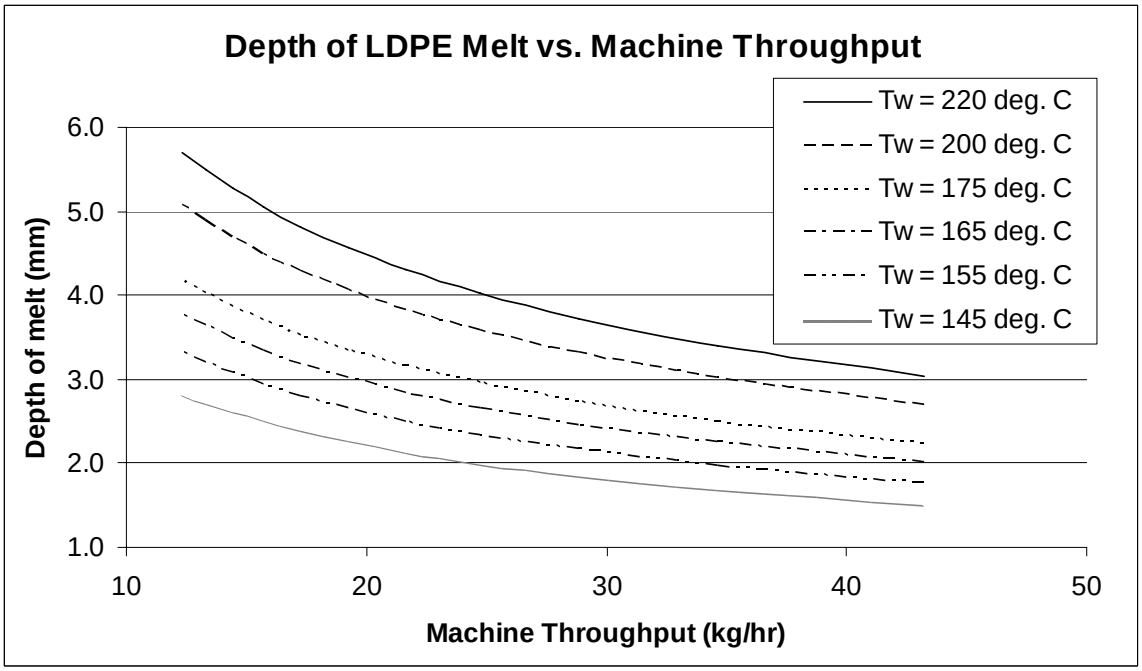

Figure 14: Melt Depth Prediction for Low Density Polyethylene

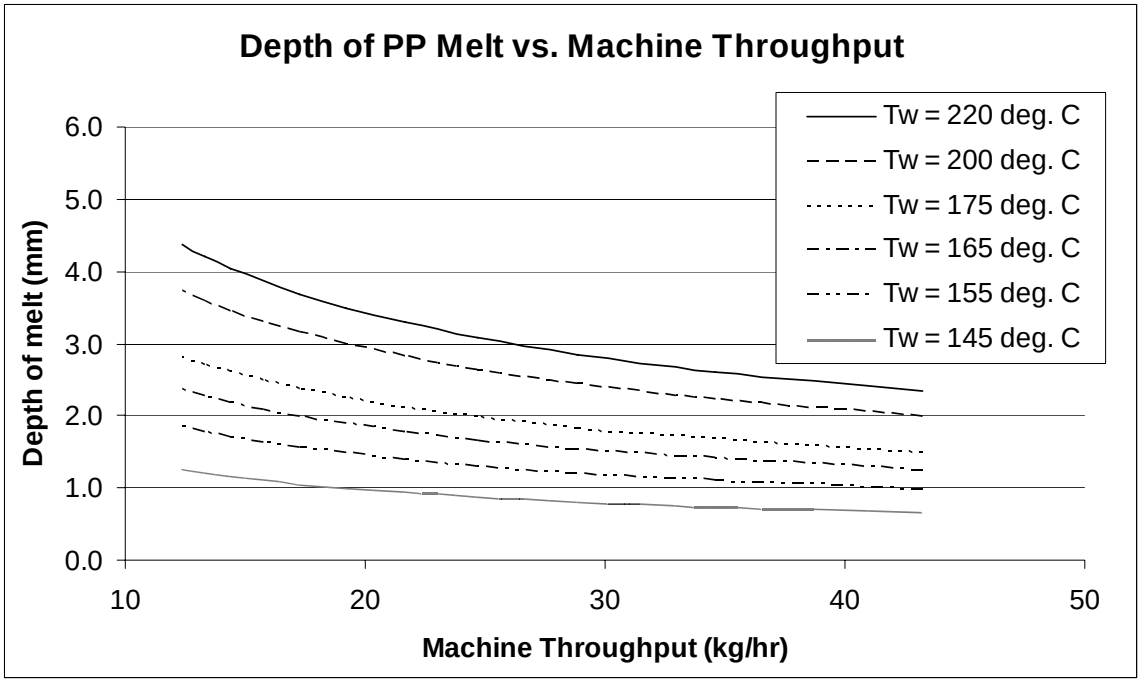

Figure 15: Melt Depth Prediction for Polypropylene

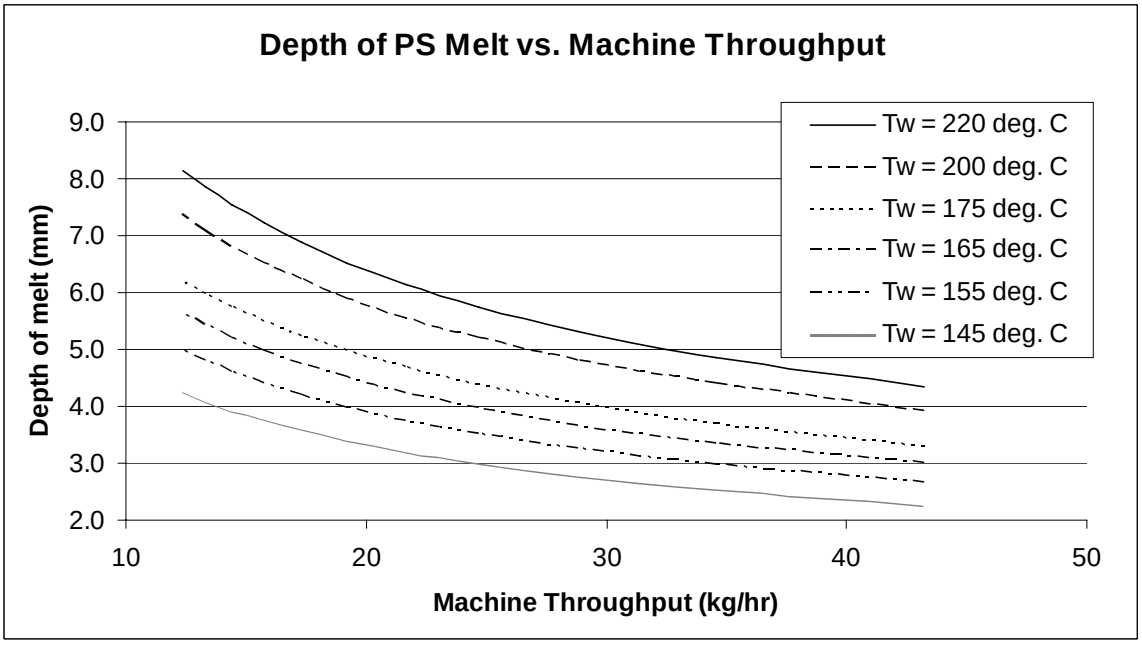

Figure 16: Melt Depth Prediction for Polystyrene

Trend lines were fit to all wall temperature relationships in Figure 13, Figure 14, Figure 15, and Figure 16. Melt depth could then be calculated for any plastic type and

throughput rate at a given die temperature using the trend line equations. The trend line equations and R^2 values for each plastic type and die temperature are listed in Table 5.

Table 5: Trend Line Equations from Melt Depth to Throughput Rate Relationships for Different Plastic Types

Die Temp (ºC)	HDPE Equation (R^2 Value)	LDPE Equation (R^2 Value)	PP Equation (R^2 Value)	PS Equation (R^2 Value)
145	$y = 2.87x^{-0.5}$ ($R^2 = 1$)	$y = 9.92x^{-0.5}$ ($R^2 = 1$)	$y = 4.42x^{-0.5}$ ($R^2 = 1$)	$y = 14.92x^{-0.5}$ ($R^2 = 1$)
155	$y = 5.20x^{-0.5}$ ($R^2 = 1$)	$y = 11.72x^{-0.5}$ ($R^2 = 1$)	$y = 6.56x^{-0.5}$ ($R^2 = 1$)	$y = 17.57x^{-0.5}$ ($R^2 = 1$)
165	$y = 7.20x^{-0.5}$ ($R^2 = 1$)	$y = 13.32x^{-0.5}$ ($R^2 = 1$)	$y = 8.37x^{-0.5}$ ($R^2 = 1$)	$y = 19.86x^{-0.5}$ ($R^2 = 1$)
175	$y = 8.97x^{-0.5}$ ($R^2 = 1$)	$y = 14.77x^{-0.5}$ ($R^2 = 1$)	$y = 9.94x^{-0.5}$ ($R^2 = 1$)	$y = 21.86x^{-0.5}$ ($R^2 = 1$)
200	$y = 12.70x^{-0.5}$ ($R^2 = 1$)	$y = 17.89x^{-0.5}$ ($R^2 = 1$)	$y = 13.20x^{-0.5}$ ($R^2 = 1$)	$y = 25.97x^{-0.5}$ ($R^2 = 1$)
220	$y = 15.19x^{-0.5}$ ($R^2 = 1$)	$y = 20.02x^{-0.5}$ ($R^2 = 1$)	$y = 15.34x^{-0.5}$ ($R^2 = 1$)	$y = 28.618x^{-0.5}$ ($R^2 = 1$)

All regression coefficients in Table 5 are equal to 1 because Equation 2 was used to establish the relationship between melt depth and throughput rate. In Equation 2, melt depth is a function of the square root of residence time, and residence time is inversely proportional to throughput rate.

Melt depth was predicted for Plastofuel™ by first assuming a feedstock type. Polystyrene is a common agricultural plastic; however, there were only trace amounts of PS in the feedstock used in this research. After a visual inspection, the feedstock used for this research was assumed to contain equal parts by weight HDPE, LDPE, and PP only. Predicting melt depth for Plastofuel™ again used the Stefan-Neumann equation (Equation 1) but with weighted averages from the HDPE, LDPE, and PP properties found in Table 4. The thermal property values for Plastofuel™ used in the equation to solve for the K-value in the Stefan-Neumann equation are listed in Table 6.

Table 6: Plastofuel™ Properties used in Stefan-Neumann Equation*

Material	Density (kg/m^3)	Thermal Conductivity (W/m-°K)	Heat Capacity (J/°K-kg)	Heat of Fusion (J/kg)	Melt Temp. (°K)
Liquid Plastofuel™	854	0.22	2280	--	--
Solid Plastofuel™	927	0.26	2220	256000	393

* Weighted averages of properties assuming a feedstock consisting of equal parts HDPE, LDPE, and PP.

The Stefan-Neumann equation (Equation 1) cannot be solved algebraically for the K-value. Predicted melt depth was determined by first solving for the "K" term in Equation 1 for die temperatures ranging from 125ºC to 305ºC using the same spreadsheet solution found in Appendix G incorporating the properties for Plastofuel™ found in Table 6. The Plastofuel™ K-values for the die temperature range are listed in Table 7.

Table 7: Solutions for "K" Value for Several Different Die Temperatures

Die Temp (ºC)	K Value (m/√s)
125	2.5E-05
135	6.5E-05
145	9.7E-05
155	1.2E-04
165	1.5E-04
175	1.7E-04
185	1.9E-04
195	2.1E-04
205	2.2E-04
215	2.4E-04
225	2.5E-04
235	2.6E-04
245	2.8E-04
255	2.9E-04
265	3.0E-04
275	3.1E-04
285	3.2E-04
295	3.3E-04
305	3.4E-04

A plot of K versus die temperature (Figure 17) illustrates a relatively simple empirical relationship.

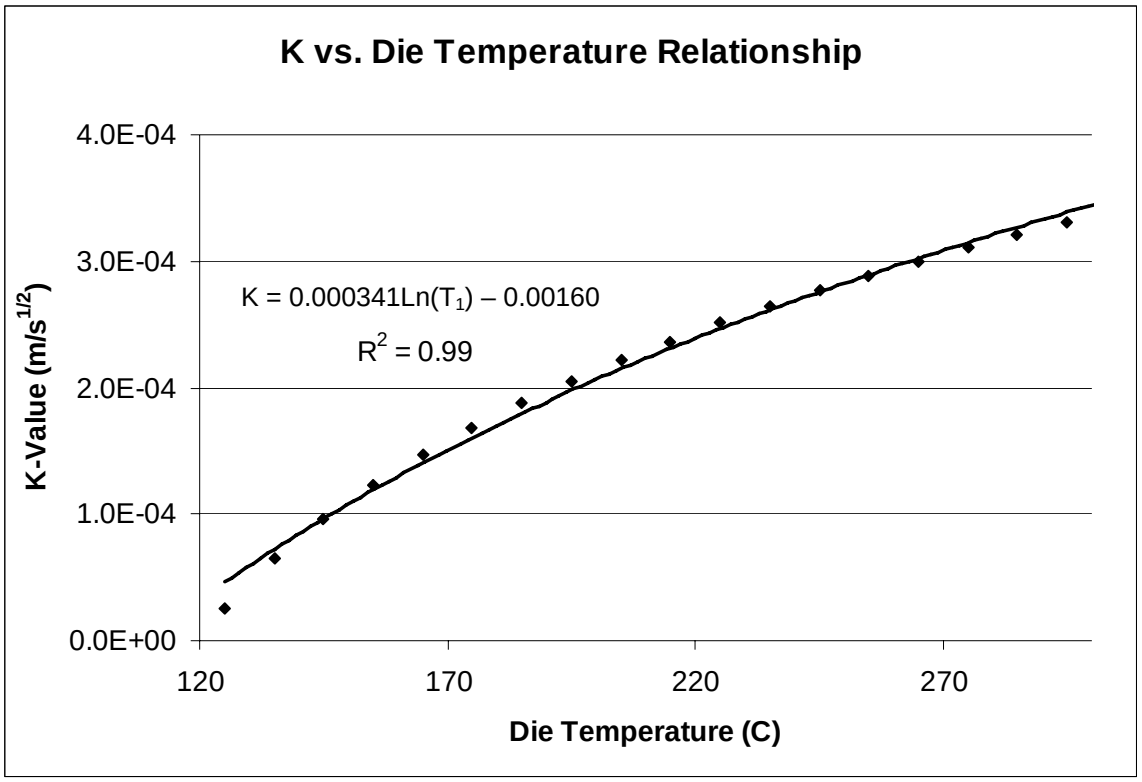

Figure 17: K-Value and Die Temperature Relationship for Plastofuel™

Residence time of Plastofuel™ in the heated zone ("t" term in Equation 2) is a function of die length, Plastofuel™ density, die cross-sectional area, and production rate. The relationship between these variables and residence time is shown in Equation 5.

Equation 5: Residence Time in Die as a Function of Die Length, Plastofuel™ Density, Die Opening Area, and Production Rate

$$t = \frac{L\rho A}{P}$$

where

t = residence time in die (s)

L = length of die (m)

ρ = Plastofuel™ density (kg/m^3)

A = area of die exit openings (m^2)

P = production rate (kg/s)

Combining this relationship for residence time and the empirical model for K (Figure 17) leads to the following model for predicting melt depth with the Plastofuel™ machine.

Equation 6: Predictive Equation for Melt Depth in the Machine

$$X = (.000341 \ln T_1 - .00160)\left(\frac{L\rho A}{P}\right)^{1/2}$$

where

X = melt depth (m)

T_1 = die temperature (ºC)

4.1.5 Machine Component Design

This discussion of machine design includes each major system component as well as a more detailed look at the major Plastofuel™ machine components. Detailed, to-scale drawings of all Plastofuel™ machine components manufactured during this phase were created using AutoCAD© 2006. These files are available on a compact disk accompanying this thesis. When applicable, actual photographs of the machine are used in this section. Internal parts, however, are sometimes shown using representations from the computer files generated for the machining operations.

Major System Components

The major system components were an engine-generator, a hydraulic power unit, the Plastofuel™ machine, and a trailer that housed all components.

Figure 18: The Plastofuel™ Trailer

Figure 18 shows the trailer being towed by a heavy-duty vehicle. The trailer artwork was added for educational purposes. Similarly, the awning-type doors can be seen in this picture. The five doors could be opened for demonstration and presentation.

Figure 19: A View Inside the Plastofuel™ Trailer

The major components inside the trailer can be seen in Figure 19. The engine generator (orange) was diesel powered and the exhaust stack was ported outside the trailer. The engine-generator was rated to produce 28 kW (38 hp) of continuous power at 2900 rpm. The Kubota model number was SQ-3350, and the unit was equipped with a sound attenuation system to lessen background noise during demonstration. The engine-generator had a 68 liter (18 gal) fuel tank capable of running for nine hours at rated output.

Output from the engine-generator produced three types of electrical power used for this research. Single phase, 120V power was used to run Plastofuel™ machine instrumentation and electrical accessories (laptop and datalogger). Single phase, 220V power was used to power the heating elements surrounding the die assembly on the machine. Finally, three phase, 220V was used to run the hydraulic power unit.

The hydraulic power unit in Figure 19 (blue) was assembled and purchased from Beiler Hydraulics located in Leola, PA. The unit was powered by an 11 kW (15 hp) electric motor directly coupled to a load-sensing hydraulic pump. The 76 lpm (20 gpm) pump was rated to 31 MPa (4500 psi). The pump model number was K3VL45 and manufactured by Kawasaki. The unit was equipped with a 227 liter (60 gallon) reservoir, and filled with John Deere HyGuard bio-based hydraulic oil. The hydraulic power unit was protected with a load center located directly above the hydraulic power unit. The purpose of the load center was to absorb power surges and gradually start and stop the electric motor.

Finally, the Plastofuel^{TM} machine can be seen in the foreground of Figure 19 (grey). Specific machine components are discussed in detail later in this section. The machine could either be run inside the trailer or wheeled out of the trailer using a winch-powered ramp system.

Major Plastofuel^{TM} Machine Components

As discussed in section 4.1.2, the machine was designed to perform three major operations using hydraulic power: feedstock compaction, extrusion, and nugget cut-off. The machine also melted the exterior of the plastic as it was forced through the die assembly. Additionally, all consumption of hydraulic and electric power was recorded to perform an energy balance. This section will include a discussion of machine components that made these operations possible.

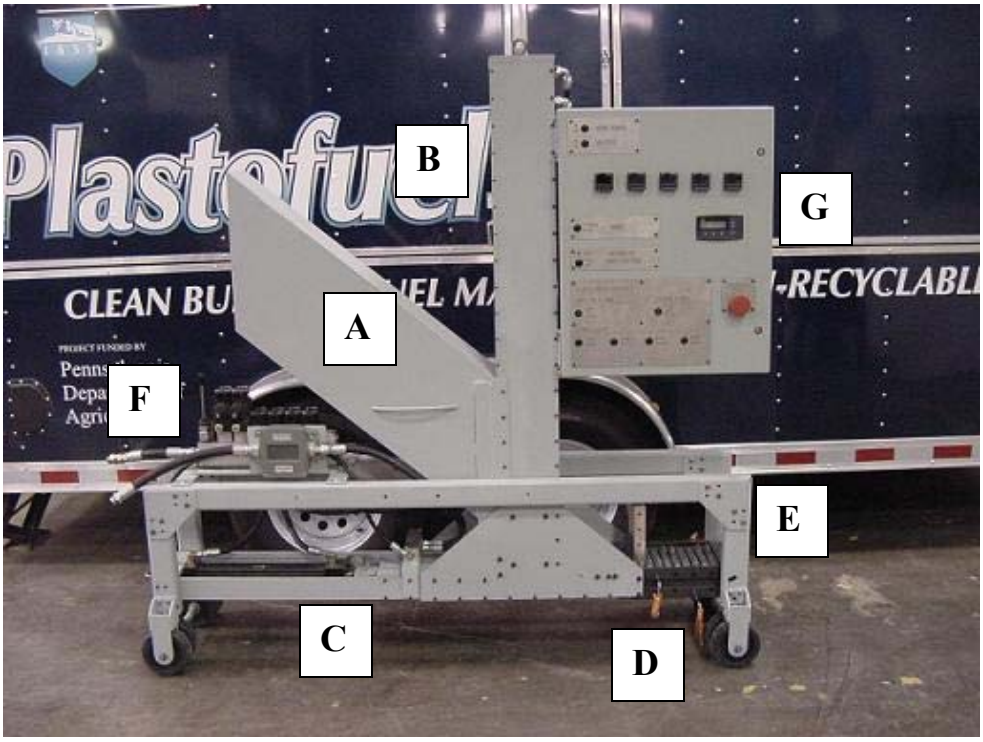

Figure 20: Plastofuel™ Machine (A. Feed Chute, B. Compaction Chamber, C. Extrusion Chamber, D. Die Assembly, E. Nugget Cut-Off, F. Valve Manifold, G. Control Box)

Figure 20 shows a side view of the machine. This was the side facing an operator when the machine was in use. Each major component is listed below with a brief description and a label corresponding to its location in Figure 20 for clarification.

A. The machine was initially loaded with non-recyclable, plastic feedstock through the feed chute. During testing, the feed chute was removed to get a better view of the internal processes.
B. The compaction chamber housed a hydraulic cylinder and compaction plunger in a vertical orientation. The plunger was supposed to reduce the size of large items loaded into the machine and compact the feedstock.

C. The extrusion chamber housed a horizontally oriented hydraulic cylinder and extrusion plunger. The plunger drove the compacted plastic into the die assembly.

D. The die assembly was heated using heating strips mounted to the exterior surface. At the die assembly entrance, the plastic was forced through a linear knife grid and into one of four chambers. The Plastofuel^{TM} exterior was melted as it passed through the die assembly. The die assembly was insulated from the frame using fiberglass board to reduce heat loss due to conduction.

E. As the Plastofuel^{TM} exited the die, it was cut to length using four, vertically oriented hydraulic cylinders.

F. Each of the six hydraulic cylinders was controlled by its own directional control valve located on a valve manifold. Quick couplings were also located here to connect the machine to the hydraulic power unit.

G. The machine electronics and wiring were centrally located in a control box. It housed the machine logic microprocessors, fuses, terminal strips, two data loggers, and several solid-state electrical relays.

The Compaction Chamber

The addition of the capability to pre-compact feedstock before the extrusion process was a major change from the prototype design. This fundamental change was driven by the goal of an increased throughput; if a large volume of loose feedstock was quickly compressed to the required nugget density before extrusion, the extrusion cylinder would extrude a higher volume with each cycle.

The compaction chamber contained two major components: a hydraulic cylinder and a compaction plunger. The 5 cm (2 in) bore 53 cm (21 in) stroke hydraulic cylinder had a standard 2.5 cm (1 in) rod which was threaded into a compaction plunger. The hydraulic cylinder was equipped with an externally mounted 64cm (25in) string potentiometer (model SP-1) from Celesco Transducer Products, Inc. The potentiometer voltage signal acted as an input to the machine logic device so plunger location could be determined. The compaction hydraulic cylinder and compaction plunger can be seen in Figure 21.

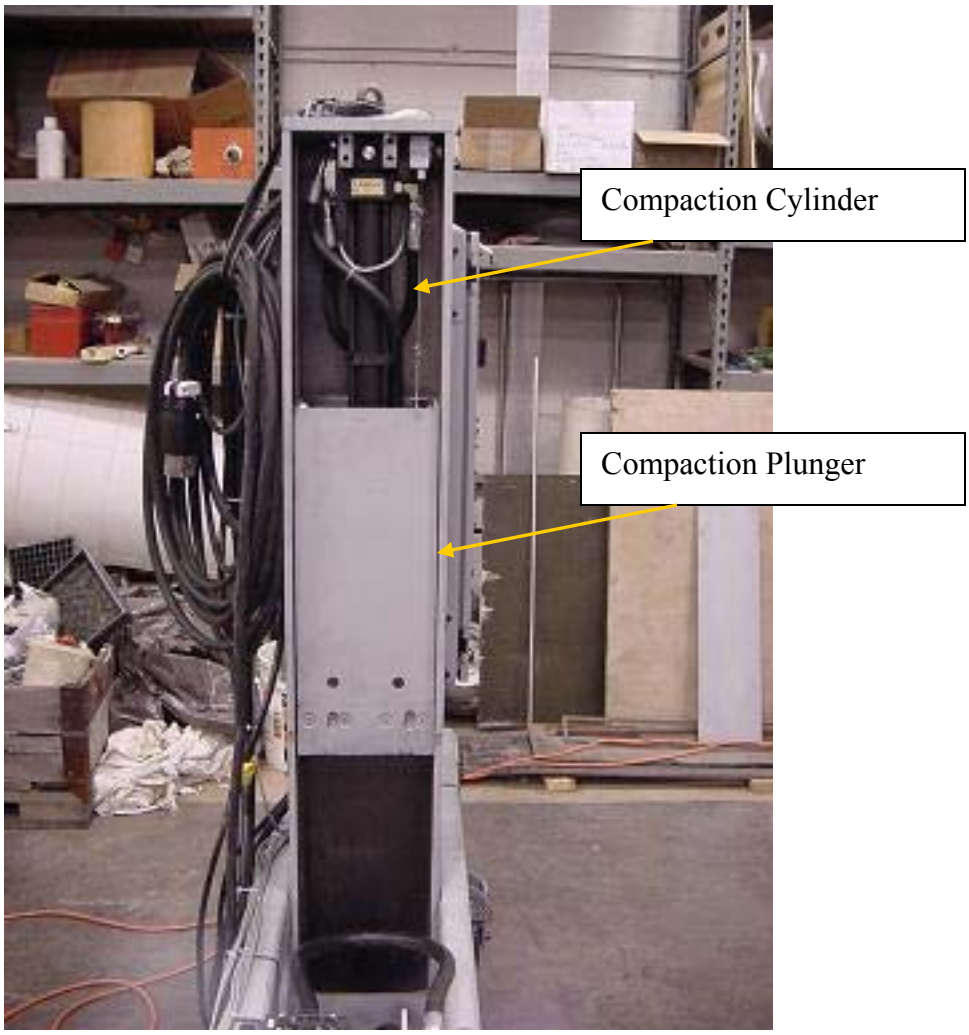

Figure 21: Inside the Compaction Chamber (One Panel Removed)

The compaction plunger was to reduce the size of large feedstocks by shearing off sections of oversized feedstock as the machine was loaded. To adequately shear oversized feedstock, the plunger had to completely close the feedstock opening of the machine at full extension. To minimize machine height and maximize feedstock opening, one end of the compaction plunger body was left open to receive the hydraulic cylinder body at full retraction with the rod end of the hydraulic cylinder mounted to the inside of the compaction plunger face. Half of the hydraulic cylinder was inside the compaction plunger at full retraction.

As with all machine components manufactured for this research the compaction plunger was designed with computer assisted drawings. In Figure 22 the compaction plunger is shown along with the associated AutoCAD© drawing.

Figure 22: Compaction Plunger and CAD Drawing

Knives mounted to the plunger face (red in Figure 22) were put on the compaction plunger so it could be removed, rotated, and reinserted to expose a new knife when one

became dull. The inside of the compaction housing contained a mating shear bar mounted on a bias to complete the knife/shear bar cutting system.

The plunger had two brass guides on each side which slid in grooves cut into the compaction chamber housing interior (Figure 22). The guides kept the knife mounted to the compaction plunger the proper distance from the shear bar and also acted as a replaceable wear surface.

The Extrusion Chamber

The extrusion chamber had many similarities to the compaction chamber. The major components were a 5 cm (2 in) bore 38 cm (15 in) stroke hydraulic cylinder with a standard 2.5 cm (1 in) rod and an extrusion plunger. This hydraulic cylinder was also equipped with an externally mounted 64 cm (25 in) string potentiometer (model SP-1) from Celesco Transducer Products, Inc. The potentiometer voltage signal acted as an input to the machine logic device so plunger location could be determined.

The extrusion cylinder stroke length allowed ample room for the hydraulic cylinder to be attached to the rear of the extrusion plunger. The CAD drawing of the extrusion plunger can be seen in Figure 24. The hydraulic cylinder attached to the plunger can be seen in Figure 23.

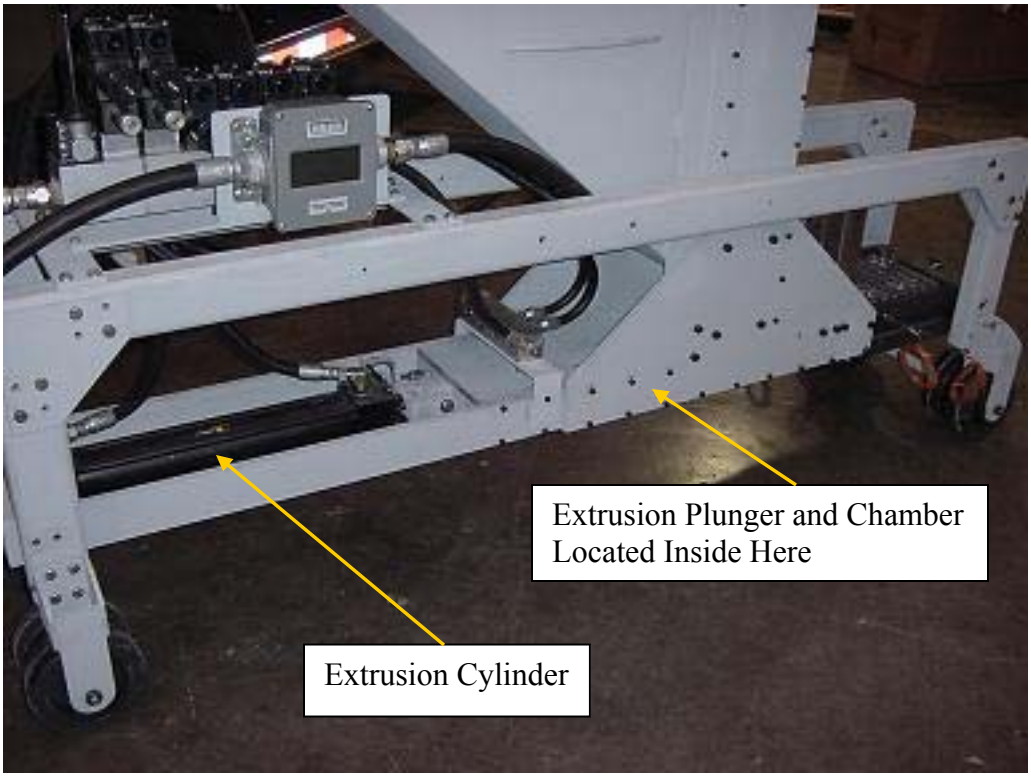

Figure 23: Extrusion Hydraulic Cylinder

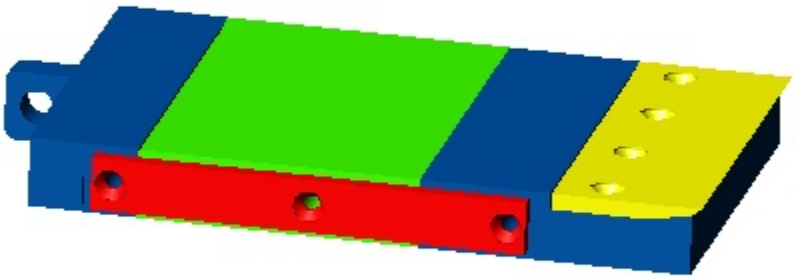

Figure 24: Extrusion Plunger

With a similar design as the compaction plunger, the extrusion plunger was equipped with brass guides (shown in red in Figure 24) to maintain the plunger in a specified path and act as a wear surface. Also, the extrusion plunger was designed to cut a portion of the compacted plastic from the compaction chamber while in extension, so a knife/shear bar system identical to the one located in the compaction chamber was added (yellow in Figure 24).

Die Assembly

The die assembly was the most complicated portion to design and machine for many reasons. The die assembly consisted of two identical halves – a top and bottom. This was because of the difficulties associated with machining four large channels through the length of a one-piece die. The two die halves were fastened together so that the five fins separating the four internal channels were the only contact points between the halves. The two die pieces can be seen in Figure 25.

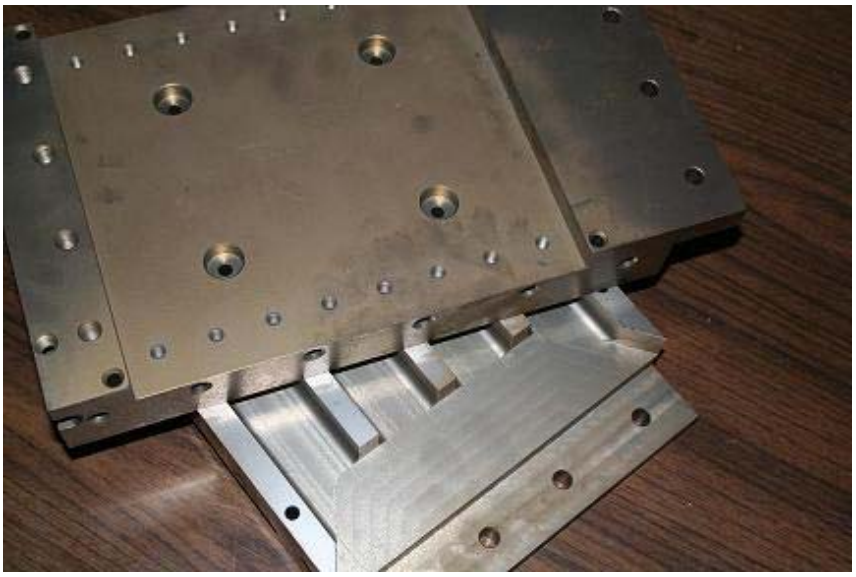

Figure 25: Die Halves Prior to Assembly

The complexity of the die machining was not only due to the formation of the die channels but also the sheer number of holes, both clearance and tapped, that needed to be placed in each die half. Each die half contained 42 holes. The breakdown of number and types of holes in each die half is listed below:

- 9 – ¼" tapped NPT to receive thermocouples
- 4 – 3/8"-24 tapped to mount die to frame assembly
- 8 – ¼" through clearance holes to hold die halves together
- 4 – 3/8"-24 tapped unused holes on top of die – initially designed to mount cut-off cylinders but ultimately unused
- 16 – ¼"-28 tapped to hold eight strip heaters
- 1 – ½" through clearance hole to receive cartridge heater

Because Plastofuel^{TM} feedstock may be abrasive, the die was made from D-2 tool steel and then hardened. After the majority of the machining was completed, the halves were hardened to a Rockwell Hardness of 62. Next, the mating fins were surface ground for a perfect fit. The cutouts to receive the vertical knives at the die entrance (not shown in Figure 25) were added last using an electro-discharge machine (EDM) to ensure a slip-fit for the knives. The assembly was fastened together, mounted to the machine frame, and the heaters and knives were added (Figure 26).

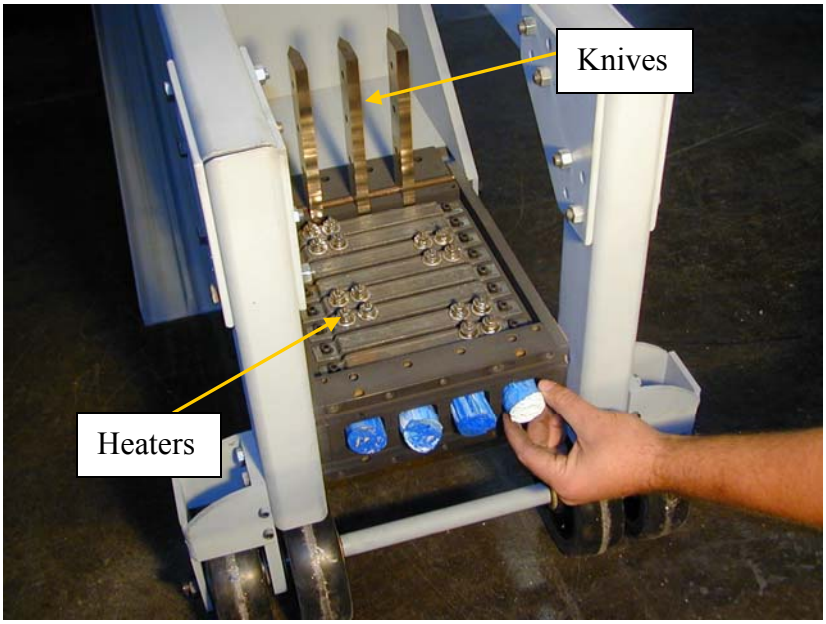

Figure 26: Die Assembly Mounted to Machine with Heaters and Knives

To ease the machining process, the shape of the die channels was changed during die fabrication. On the prototype machine, the Plastofuel™ was forced through a 3.8 cm (1.5 in) diameter water pipe. On the new machine, the four die channels were 3.8 cm (1.5 in) square with 0.63 cm (.25 in) fillets at each corner.

The die was surrounded with a total of 18 strip heaters located on the top, bottom, and sides. The strip heaters were purchased from Omega Engineering (model SNH-08/120) and each had a 250W rating. One cartridge heater was placed at the rear of the die to heat the cut-off knives while they were in a retracted position. The cartridge heater was manufactured by Omega Engineering (model CIR-5082/240) and had a 2000W rating. All heaters could achieve temperatures up to 650ºC, a value far larger than the intended die temperature range of 135 ºC to 250 ºC.

The die assembly also housed five K-type thermocouples that provided an input to the temperature controllers. The thermocouples could be placed in any of eight holes

along the die body. One thermocouple was used for each of the four heating strip banks, and a fifth thermocouple monitored the temperature of the cartridge heater at the rear of the die. The heater strip wiring diagram can be found in Appendix I.

The temperature controllers were set such that the heaters in a heating zone were activated if the temperature detected by the heating zone thermocouple fell 5ºC below the set temperature. They deactivated if the temperature raised 5ºC above the set temperature. If the temperature in any zone fell below 10ºC of the set temperature, an alarm signal was sent to the IQAN algorithm and automatic machine operation ceased.

Cut-Off Cylinders

At the die exit, two plates were mounted and machined to receive four guillotine-style knives. The knives were affixed to the rod clevises of four 3.8 cm (1.5 in) bore and 1.9 cm (0.75 in) rod cut-off cylinders. The cylinders had a four inch stroke (the minimum available) but were assembled with a stop-tube to limit stroke to 6.4 cm (2.5 in). Each cut-off cylinder could be activated manually using the control panel or automatically with limit switches manufactured by Honeywell (model SZL-VL-F) that were activated upon nugget contact. The limit switches were placed 5 cm (2 in) from the die exit. The assembly can be seen in Figure 27, but the limit switches have been removed to make the assembly more visible.

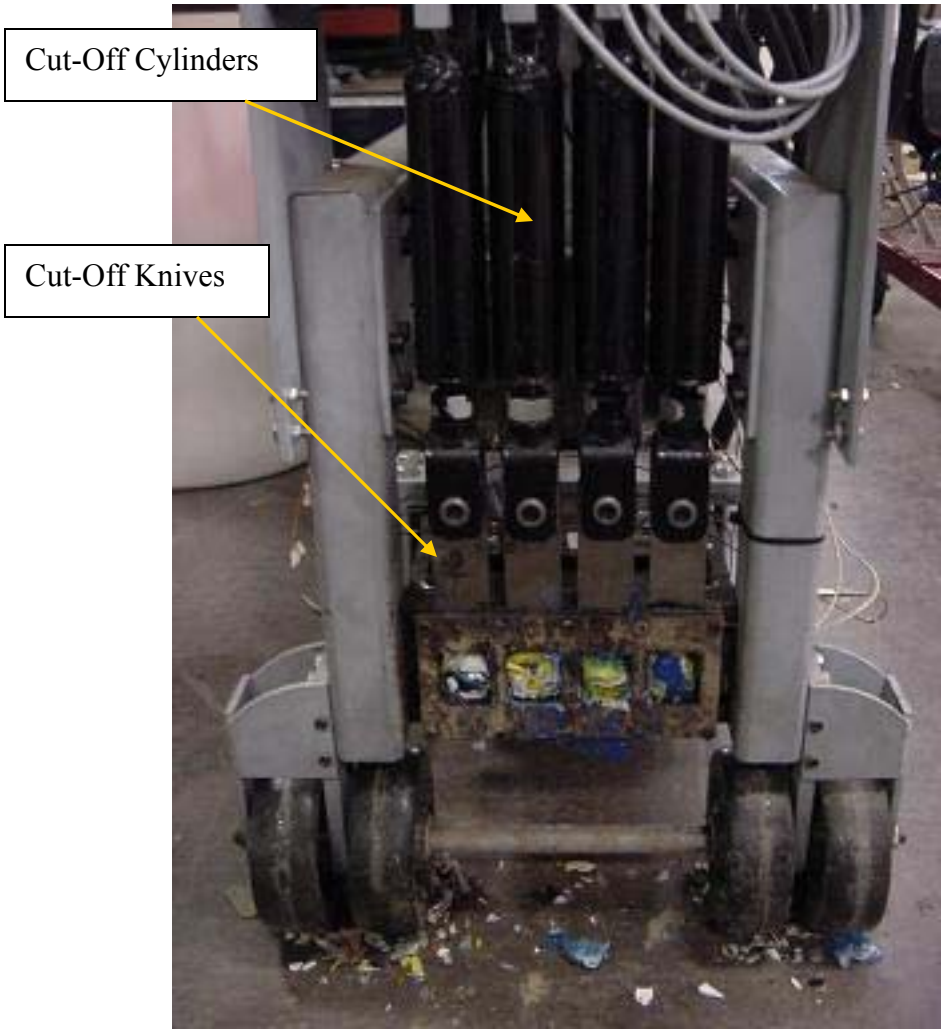

Figure 27: Cut-off Cylinders and Knives at Die Exit

Hydraulic System

The hydraulic system used a load-sensing pump and power unit previously described. A load sensing pump was selected, since this machine was expected to have widely varying flow and pressure requirements. Load-sensing hydraulic circuits maximize system efficiency by providing only the flow and pressure required by the circuit components (Cundiff, 2002). With a research goal to maximize the machine energy balance, minimizing hydraulic power was critical. The hydraulic schematic

(Figure 28) was designed such that the maximum system pressure required by any of the six hydraulic cylinders was transmitted to the pump via a load-sense line.

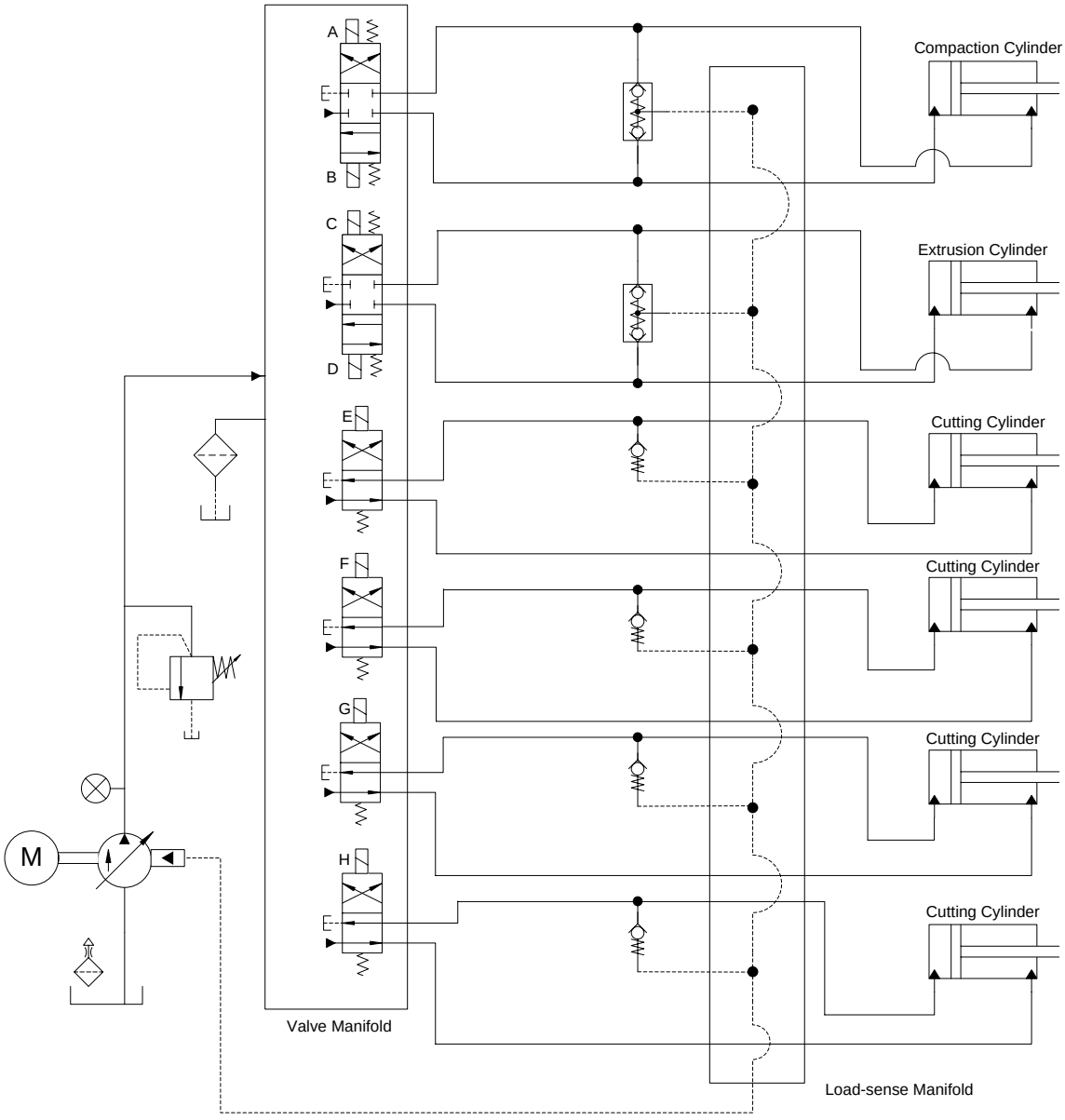

Figure 28: Hydraulic System Schematic

Obtaining the maximum instantaneous pressure demand was accomplished using a series of check valves and a manifold block. All cylinder working lines were plumbed to a central manifold. The flow to this manifold was rendered unidirectional from the

cylinders with check valves. A single line, the load-sense line, was plumbed back to the pump from the manifold.

The compaction and extrusion cylinders were electronically controlled and capable of stopping mid-stroke, so three position, spring centered, closed center, double solenoid valves were selected. The speed of the compaction and extrusion cylinders could be controlled by sandwich-style flow controls mounted between the valve and the valve manifold. The cutting cylinders were also electronically controlled but only required to fully extend and fully retract; for this reason, two position, spring return, single solenoid were selected. The valves selected were made by NACHI and conformed to the industry standard, D03 mounting style. All valves were mounted on an aluminum manifold (Figure 29).

The hydraulic system was outfitted with two sensors: a hydraulic pressure transducer and a hydraulic flow meter. The pressure transducer was manufactured by Omega Engineering (model number PX603) and threaded directly into a gauge port on the hydraulic manifold. The transducer had a best fit straight line accuracy specification of ±0.4%. The transducer was powered with 12VDC and provided a 1-5V output signal which corresponded to hydraulic pressures from 0-34 MPa (5000 psi). This output was directly connected to the control system as a system input.

The hydraulic flow meter, in the foreground of Figure 29, was manufactured by Hedland (model number H700A-020-MR) and was also powered with 12VDC. The flow meter provided an input to the control system that varied from 0-5VDC. This signal corresponded to hydraulic flows from 0-76 lpm (20 gpm). The flow meter was plumbed

such that all flow from the pump to the manifold was directed first through the flow meter.

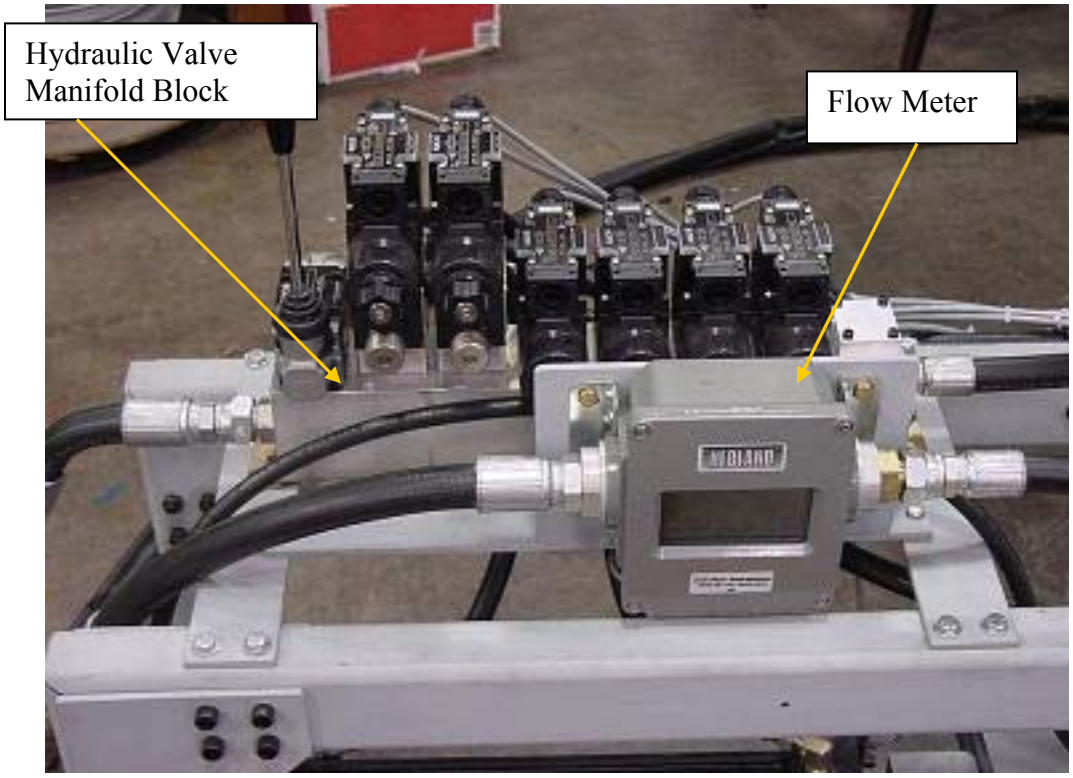

Figure 29: Hydraulic Manifold and Flow Meter

Control System

The Plastofuel™ machine had a sophisticated control system monitoring all system input signals and providing system output signals based on a control algorithm. The control system was governed by an onboard microprocessor. Three different algorithms were used during the machine testing. The channel information and block diagrams for each algorithm can be found in Appendix H.

At the heart of the control system was a Parker Hannifin IQAN© controller area network (CAN). A CAN system uses a modular approach to collect system inputs and provide outputs using a master module and a single serial communication line between

system components. For this research, a Master Display Module (MDM), XP expansion module, and XS expansion module were used.

Figure 30: Outside of Control Box

The control box (Figure 30) had numerous switches to enable machine operation. The switches and their function are listed in Table 8.

Table 8: Control Box Switches and Their Function

Switch Label	Position	Function
Main Power	On	Enable cylinder operation
	Off	Disable cylinder operation
Heaters	On	Turn on all heaters
	Off	Turn off all heaters
Mode	Manual	Switch machine to manual operation
	Automatic	Switch machine to automatic operation
Automatic Mode Control	Start	Start automatic operation
	Stop	Stop automatic operation
Compaction Cylinder	Extend	Manually extend compaction cylinder
	Stop	Manually stop compaction cylinder at current location
	Retract	Manually retract compaction cylinder
Extrusion Cylinder	Extend	Manually extend extrusion cylinder
	Stop	Manually stop extrusion cylinder at current location
	Retract	Manually retract extrusion cylinder
Cutting Cylinder 1	Extend	Manually extend cutting cylinder 1
	Retract	Manually retract cutting cylinder 1
Cutting Cylinder 2	Extend	Manually extend cutting cylinder 2
	Retract	Manually retract cutting cylinder 2
Cutting Cylinder 3	Extend	Manually extend cutting cylinder 3
	Retract	Manually retract cutting cylinder 3
Cutting Cylinder 4	Extend	Manually extend cutting cylinder 4
	Retract	Manually retract cutting cylinder 4
Emergency Stop	On	Disable power to MDM
	Off	Enable power to MDM

The control panel also included six displays. Five displays were located on the temperature controllers. Each of the five temperature controllers were made by Omega Engineering (model number CN77R343) and controlled one of five heating zones on the die assembly. The MDM component of the CAN system was also visible on the control panel. The MDM was capable of displaying any system variable, but was set to automatically display the location of both the compaction and extrusion plungers.

The control box housed the IQAN XP and XS expansion modules, terminal strips for all AC and DC voltages, a terminal strip for IQAN inputs, several solid-state relays, and a 12VDC power supply. Two electrical supply lines entered the control box: a single phase, 220VAC line, and a 115VAC line. The 220V line was only used for the die heaters. The 115V line provided power for the electrical power consumption data logger, the temperature controllers, and an attached laptop computer (which interfaced with the IQAN system to datalog hydraulic system information). The 115V line also connected to a 12VDC power supply to run CAN components and all sensors and switches. A view inside the control box is shown in Figure 31.

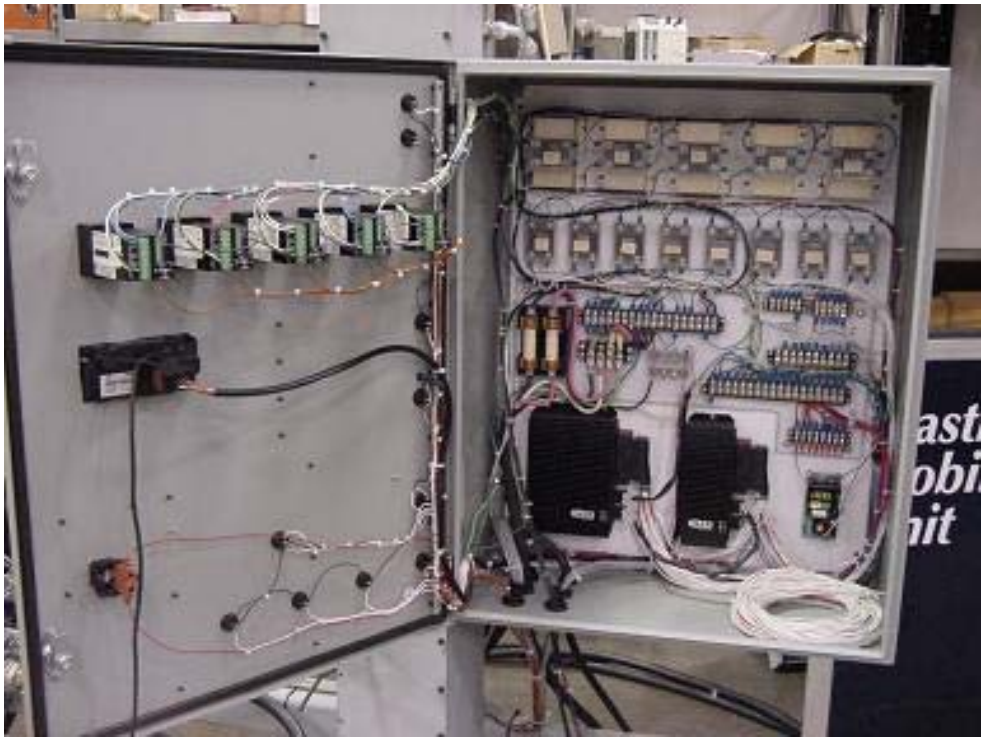

Figure 31: Components and Wiring Inside the Control Box

The wiring diagrams for the control box components are detailed in Appendix I.

4.2 Data Collection and Analysis

One goal of this research was to perform an energy balance of the Plastofuel™ machine. This required both an analysis of the energy used to form the nuggets and the energy content of the Plastofuel™ produced.

4.2.1 Electrical Energy Consumption

An accurate account of the electric energy used by the machine during nugget formation required the use of a specialized data logger. The data logger that recorded machine electrical usage was an ElitePro Recording Polyphase Power Meter made by DENT Instruments. Jumpers were connected to both the incoming 220V and 115V lines from the generator to measure voltage readings. Current transformers were also affixed around both lines to measure current readings. These readings were communicated to a laptop running the ELOG 2002b software via a serial connection (ELOG, 2002). The software converted the voltage and current readings to average power consumption over a three second interval. Sample output from the ELOG 2002b software can be found in Appendix J.

Power readings from the collected data were converted to energy consumed during each three second interval. These energy usage statistics were summed over the test duration for a total electrical energy consumption value. An excerpt from a data analysis spreadsheet is also included in Appendix J.

4.2.2 Hydraulic Energy Consumption

The MDM component of the CAN system was used to log hydraulic system information. The MDM can display and record up to ten system variables during

operation. It recorded values of selected variables every 50 ms. The following variables, required to calculate total hydraulic power, were recorded during each test run:

1. Hydraulic system pressure
2. Compaction cylinder location
3. Extrusion cylinder location
4. Hydraulic flow
5. Valve solenoid activation for cutting cylinder 1
6. Valve solenoid activation for cutting cylinder 2
7. Valve solenoid activation for cutting cylinder 3
8. Valve solenoid activation for cutting cylinder 4
9. Heaters "ready light"

Sample data collected from the MDM data logger can be found in Appendix K.

Power is a function of hydraulic pressure and flow. The Hedland flow meter had a significant lag time (1.5 s) when reporting current flow back to the data logger. For this reason, although the flow meter reading was recorded, it was not used to determine hydraulic system flow. As a much more accurate alternative, the location change of each cylinder over each 50 ms time step was recorded, and the flow required to produce that cylinder motion was calculated. Leakage internal to the hydraulic system was considered to be negligible.

The compaction and extrusion cylinders were equipped with potentiometers that provided feedback about each cylinder location throughout the cylinder stroke. The cutting cylinders, however, did not have instrumentation for position sensing. Calculating the flow to each cutting cylinder was accomplished by recording the time for

cylinder actuation during both extension and retraction, and then adding this flow to a spreadsheet each time a cutting cylinder valve solenoid switched from “on” to “off” or “off” to “on”.

Total hydraulic flow was calculated for each 50 ms time step during the test run by determining the change in volume of the hydraulic fluid in the compaction, extrusion, and cutting cylinders. This total flow was multiplied by the hydraulic system pressure recorded during the same time step and an instantaneous hydraulic power was calculated. The power used in each time step was multiplied by the time step duration resulting in energy consumed. The total energy consumption by the hydraulic system was determined by summing all energy values for each time step in the test run. A sample data analysis spreadsheet can be found in Appendix K.

Total energy consumed by the Plastofuel^{TM} machine was electrical energy plus hydraulic energy.

4.2.3 Plastofuel^{TM} Energy Content Analysis

Energy content of the Plastofuel^{TM} nuggets was evaluated at the Penn State Combustion Laboratory. The combustion lab technician provided sample preparation recommendations and tested the nugget samples in a model 1241 adiabatic oxygen bomb calorimeter manufactured by Parr Instrument Company (Figure 32).

Figure 32: Bomb Calorimeter Used for Plastofuel™ Energy Content Analysis

Two types of feedstocks were tested for a high heat value – (type 1) a mixture of clean waste agricultural plastic film and clean household plastic waste, and (type 2) a mixture of dirty agricultural pots and film. A total of ten sample nuggets were randomly selected from four different tests using the first type of feedstock. Similarly, a total of ten sample nuggets were randomly selected from four different tests using the second type of feedstock.

Testing in the bomb calorimeter required a sample size of 1 gram. A typical nugget weight was 60 grams. The nuggets had to be finely shredded for sampling, because calorimetry testing required the sample to be pulverized to nearly powder form. The shredding procedure was done using a drill press, a course "sanding disk", a clamp,

and a collection tray (Figure 33). The sanding disk had metal teeth permanently affixed to the face such that none of the teeth fell off during shredding.

Figure 33: Plastofuel™ Sample Preparation for Calorimetry Testing

Sample preparation began by cleaning the disk, tray, and clamp with denatured alcohol to remove foreign matter. Each of the ten nuggets of the same variety was then clamped below the sanding disk, and the drill press was slowly lowered onto the nugget. A low drill press speed was selected to reduce the possibility of melting the plastic. The fine particles removed from the nugget were collected from the tray and placed in a plastic sandwich bag. This process was repeated for each of the ten nuggets until the nuggets were unable to be effectively clamped. Before switching to the second feedstock variety, all components were again cleaned. A sample size of approximately 100 grams

was collected from each feedstock variety. These samples were delivered to the combustion lab for analysis.

Bomb calorimetry testing was completed by a lab technician according to American Society for Testing and Materials (ASTM) method 5865-04 for coal. Four test replications were required with each feedstock type in order to satisfy a minimum variability between samples of 0.17 MJ/kg (50 BTU/lb) dictated by ASTM 5865-04.

4.3 Machine Testing

Machine testing took place over a seven-day period in March, April, and May of 2007. All testing took place with the machine in automatic mode to minimize operator effort. Twenty-two test runs were completed to determine maximum production rate. For this research, a maximum production rate was defined as a 90% probability that one of the test run production rates was in the top 10% of the sample population. Melt depth, nugget density, and energy consumption data were also collected during these test runs. The test run duration was initially 20 minutes, and nine test runs of this duration were completed. All subsequent test runs were of 10 minute duration.

At least one production rate test run was completed with die temperatures of 125ºC, 135 ºC, 145ºC, 155 ºC, 165 ºC, 175 ºC, 200 ºC and 220 ºC. Multiple test runs were completed at die temperatures of 155 ºC and 175 ºC because these temperatures appeared to produce optimal conditions – high throughput rates without compromising the quality of the Plastofuel^{TM} nuggets formed.

Twelve additional test runs were completed to allow further analysis of the effects of temperature and throughput rate on melt depth. Energy consumption and nugget

density were also collected for these test runs. The melt depth test runs occurred at two different temperatures: 155ºC and 175 ºC.

Each test began by placing ample feedstock near the machine. Then, all five die heating zones were pre-heated to the test run temperature. After the die reached test temperature, the machine was operated in manual mode to force out the plastic which was in the die during pre-heating. Melt depth prediction using a mathematical model was a function of time in contact with the die surface, so plastic that had been in the die during pre-heating, rather than machine steady-state operation, was discarded.

Just prior to machine start-up, both electrical and hydraulic data loggers were activated. Testing then started by turning the main switch "on" the mode switch to "automatic" and the automatic mode control switch to "start".

After the test duration, the data loggers were disabled, and the raw data was copied to a laptop computer. The Plastofuel^{TM} nuggets formed were collected, measured, photographed, and placed in a labeled bag. The melt depth, length, and mass of 25 nuggets from each test were recorded. The melt depth was measured with vernier calipers. The maximum melt for each nugget was located by inspecting the nugget end and measured to the nearest 0.1 mm (0.004 in). The nugget length was measured to the nearest 0.1 cm (0.04 in) along the centerline of each nugget using a ruler. The individual nugget mass was measured to the nearest 1 g (0.002 lb) using a model PE6 scale manufactured by Mettler Instrument Corporation. The scale was calibrated using calibration weights prior to use.

5.0 Results

Data collected during machine testing was analyzed to evaluate machine performance and capacity, the system energy balance, Plastofuel™ nugget characteristics, and the effectiveness of the melt depth model. Each of these topics is discussed in this section.

5.1 Machine Performance and Capacity

A series of preliminary tests were run to verify machine logic and basic functionality, and many subsequent machine modifications were made. Machine performance and was quantified by collecting data over the course of 34 production test runs. In 22 of these runs, a maximum capacity was pursued; in all 34, melt depth and energy balance were evaluated.

5.1.1 Preliminary Testing and Modifications

The first preliminary machine test was performed on November 30, 2006 and was carried out with the machine in manual mode only and a die temperature of 135ºC. Clean, dry rigid and film household plastics (type 1 feedstock) were loaded into the compaction chamber, compressed, and forced against the linear knife grid at the face of the die by the extrusion plunger. The machine immediately plugged. The compressed feedstock would not pass through the "cutting" vertical knives at the front of the die assembly and into the die channels. The machine was disassembled, and the plug was carefully removed for analysis (Figure 34). It was clear that plastic had begun to enter the die assembly, and the leading edge of the plug was cut under the force exerted from

the extrusion cylinder. This cutting behavior had been predicted in experiments 1 and 2; however, it appeared that after the plastic reached a certain density the cutting stopped.

Figure 34: Plug Removed from Machine During Initial Testing

Sole reliance upon results from experiment 1 (knife temperature required to cut plastic at a given density) revealed a flaw in machine design. Although the plastic feedstock did, in fact, begin to cut as predicted, the fact that it required much more force to continue to cut was not considered when sizing cylinders. Experiment 1 would have been much more applicable if data were collected which more closely modeled the confined space of the extrusion chamber and the three, vertical "cutting" knives at the die entrance. The design of experiment 1 (Figure 6) offered a relief to the plastic displaced by the heated knife. As plastic was compacted by the knife and began to cut, the plastic displaced by the knife was able to retreat into the less dense volume of uncompacted plastic in the PVC tube. In the extrusion chamber, all entrapped plastic was first

compacted to the cutting density before cutting began. When cutting began, the entrapped plastic had reached its maximum density, and there was no relief volume available for the plastic displaced by the three, vertical knives. The result was an example of Hooke's Law, and it prevented operation – as the feedstock materials were placed under stress from the extrusion cylinder and the restricted die opening, they began to deform. This deformation forced the plastic against the extrusion housing and increased internal friction to a point that the cylinder could not force the plastic through the die.

Six possible solutions to machine plugging and their impact on the research budget and timeline were considered and are listed below. Four of these solutions were applied to the machine prior to capacity testing.

1. Increasing Extrusion Cylinder Force

If hydraulic system pressure remained the same, increasing the bore size of the extrusion plunger would increase the force on the plastic, and could result in overcoming the hydrostatic lock. This would require a redesign and remanufacture of the extrusion cap which held the cylinder clevis and the mating frame assembly that bolted to the cap. Also, increasing the size of the extrusion cylinder bore would result in a high separation force in the machine frame. Frame bolt shear calculations indicated that any cylinder bore larger than 12.2 cm (4.8 in) would result in frame failure. Even if machine modifications were made to accept a 10.1 cm (4 in) bore cylinder, hydraulic cylinder suppliers followed National Fluid Power Association standards, and the smallest cylinder rod that was available on a standard 10.1 cm (4 in) bore cylinder was 4.4 cm (1.75 in) in diameter. The extrusion chamber was 4.1 cm (1.625 in) high meaning that the standard

rod would not fit in the chamber and a special, small rod cylinder would have to be ordered. This was cost and time prohibitive and not pursued.

2. Matching Extrusion Chamber and Die Opening Cross-Sectional Area

A second option to eliminate plugging focused on the extrusion chamber to die opening transition area inside the machine. In this transition zone, the compacted plastic was being forced from the open extrusion chamber with a cross-sectional area of 97 cm^2 (15 in^2) to the four die channels with a combined cross sectional area of 57 cm^2 (8.8 in^2). A cross sectional view of the extrusion chamber housing (red) and die (blue) is shown in Figure 35.

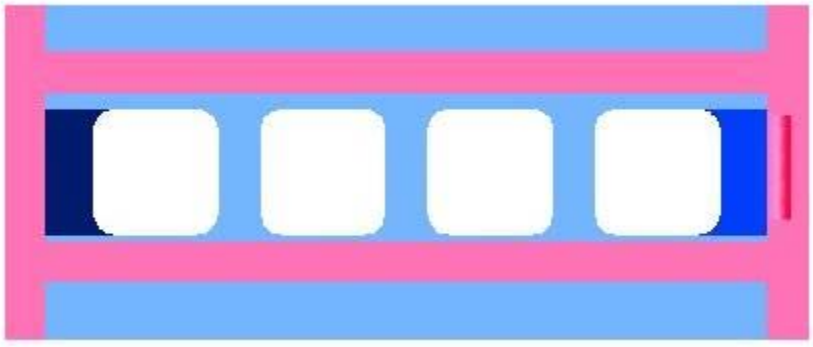

Figure 35: Cross-sectional view of Extrusion Housing and Die Openings

Changing the extrusion housing and/or die configuration was both cost and time prohibitive. Reducing the size of the extrusion chamber required a redesign and remanufacture of the extrusion chamber walls as well as the extrusion plunger. Increasing the size of the die would require alteration of the die assembly, cut-off cylinders, cut-off knives, and machine frame. This solution was not pursued.

3. Concentrating Existing Extrusion Cylinder Force

The third alternative was to alter the existing extrusion plunger (Figure 24) to concentrate the extrusion cylinder force at the die openings. Four solid rod sections, termed "disruptors", were added to the face of the extrusion plunger. These disruptors were made from mild steel and measured 5 cm (2 in) long and 2.9 cm (1.125 in) in diameter. The disruptors were fixed to the plunger face using 4.4 cm (1.75 in) long, 3/8"-24 socket head cap screws which were countersunk into the disruptor face and threaded into the extrusion plunger body. The new extrusion plunger with the disruptors (purple) added can be seen in Figure 36.

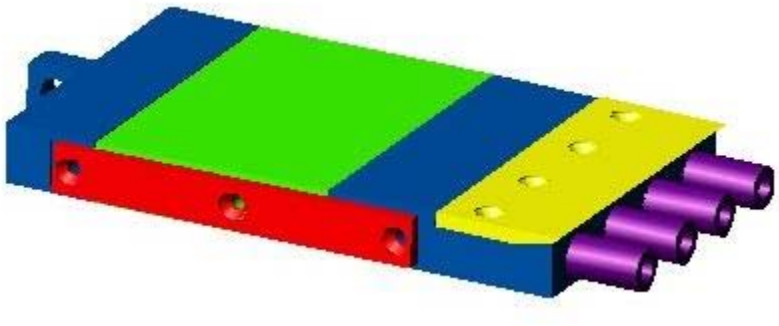

Figure 36: Extrusion Plunger with Purple Disruptors

The machine was originally designed to achieve its production goal under the assumption that extrusion plunger would extrude a charge of compacted plastic measuring 1500 cm^3 (91 in^3) each extrusion cylinder stroke. However, with the addition of the disruptors the volume extruded each cylinder cycle was closer to the volume of the four disruptors: 115 cm^3 (7 in^3), because the plastic was only extruded during the portion of cylinder stroke in which the disruptors were at or beyond the die knife edge. Attempting to force a wad of compacted plastic from the extrusion chamber into the die

openings which was longer in length than the disruptor length mimicked the conditions that caused initial plugging.

4. Increasing Knife Temperature

There were two parameters analyzed during preliminary experiment 1: knife temperature and plastic density at cutting. Increasing the knife temperature decreased the cutting resistance for plastic. In the original design, the knives were heated by conduction from the die only – the heater strips mounted to the die warmed the die which was in contact with the knives. The knives were likely cooler than the die during operation due to heat loss from feedstock plastic contact. To maintain the knife temperature at the die temperature, four strip heaters were removed from the rear of the die and clamped directly to the sides of the three knives to provide more effective knife heating (Figure 37).

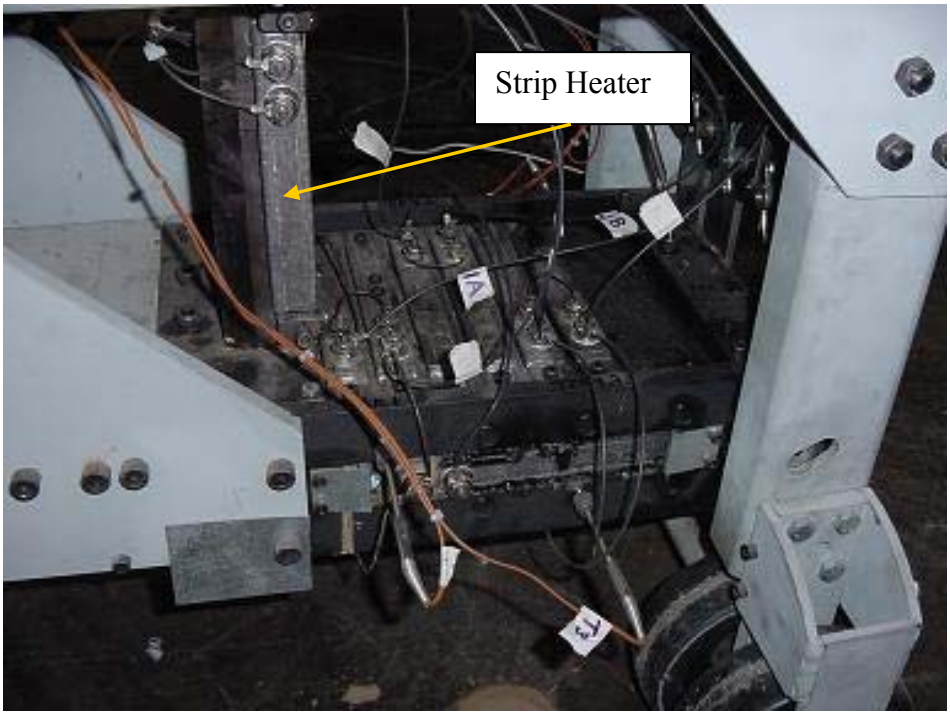

Figure 37: Strip Heater Mounted to Die Knife

The thermocouple providing temperature feedback to the temperature controllers from the circuit with the four strip heaters clamped to the die knives remained in the die. The intent was to maintain the knives at the die temperature after the thermocouple was warmed by the remaining strip heaters on the die.

After this extrusion plunger alteration and the addition of strip heaters to the die knives, preliminary testing resumed with improved results. The first "successful" preliminary test using the disruptor-enhanced extrusion plunger and heated knives took place January 10, 2007, resulting in 14 kg (31 lbs) of high quality Plastofuel^{TM} in 45 minutes of machine operation. However, the throughput rate was far short of the 227 kg/hr (500 lb/hr) goal.

5. Shredding Feedstock

Improving machine throughput by feedstock alteration was also pursued. The machine bottleneck was at the die entrance. Even with the increased die temperature and the addition of the disruptors to the extrusion plunger, the machine plugged if too much feedstock was placed in the extrusion chamber. Shredding of material prior to placement in the chamber would reduce the size of the size of the feedstock and could reduce required cutting at the die entrance.

Approximately 1000 kg (2200 lb) of waste agricultural plastics were transported to Ultra-Poly Corporation in East Stroudsburg, PA on March 23rd, 2007. Ultra-Poly is an industrial shredding facility specializing in shredding and pelletizing clean, industrial waste plastics. The pellets are then sold back to industry for secondary recycling. Ultra-Poly provided the use of a single-shaft shredder (model ZTLL 1000x1200) manufactured by Zeno (Figure 38).

Figure 38: Zeno ZTL 1000x1200 Shredder Used to Shred Plastic Film and Rigids

The waste agricultural plastics shredded included 470 kg (1000 lb) of film plastics (dirty, wet LDPE mulch film and drip tape) and 520 kg (1100 lb) of rigid plastics (dirty HDPE and PP buckets, pots, and trays). The shredder was powered by a 37 kW (50 hp) electric motor manufactured by Lincoln Electric (S/N U3960904392). The motor had a power factor of 0.80 when drawing 45 amps. During shredding, the machine consumed an average of 45 amps of current from a 480VAC circuit over the course of 2.5 hours. This resulted in an average energy consumption rate of 0.08 kW·h per kilogram of plastic for the shredding process. The shredder was equipped with a 5 cm (2 in) screen resulting in shredded particles about the size of a credit card (Figure 39).

The shredding process consumed an average of 26% of the total energy required to form Plastofuel™ nuggets with a minimum contribution of 20%, and a maximum of 31%. This average equated to less than 1% of the energy in the nuggets formed.

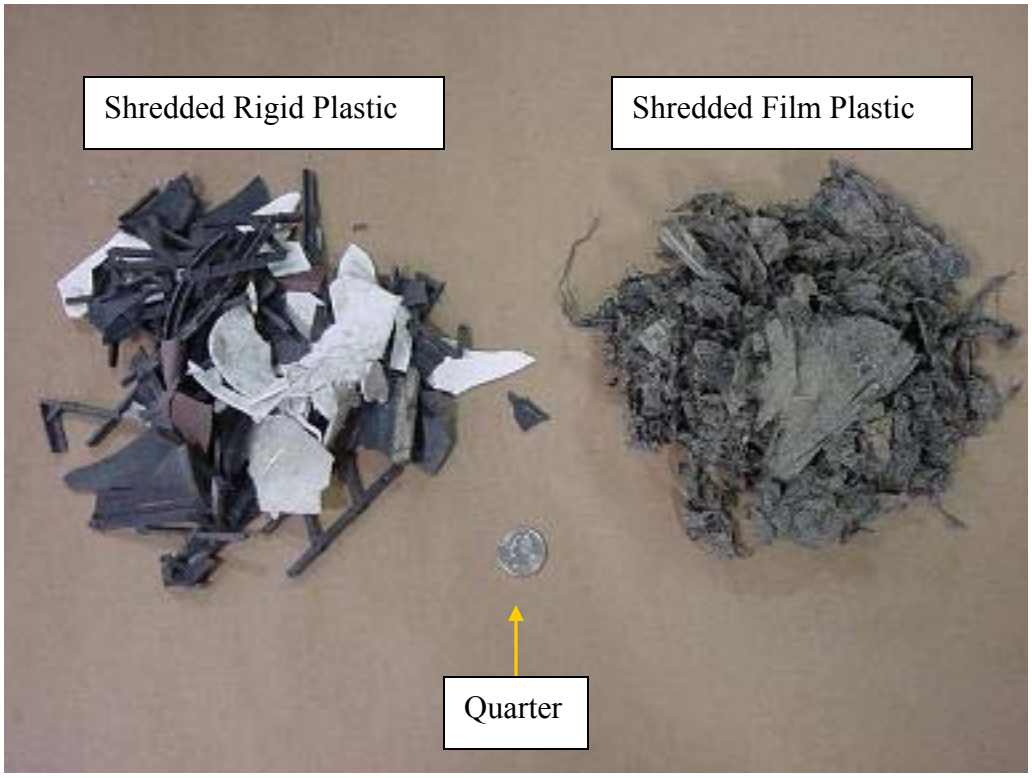

Figure 39: Shredded Rigid and Film Plastic

The shredded feedstock (type 2 feedstock) did not result in an increased machine throughput. The machine continued to plug if the volume of plastic placed in the extrusion chamber exceeded the volume of the disruptors.

6. Alternate Machine Logic

The final machine modification to reduce machine plugging focused on altering machine logic based of feedstock type. It was no longer possible to pre-compact feedstock using several cycles of the compaction cylinder prior to a single extrusion cylinder cycle (Control Algorithm 1, Appendix H). For non-shredded feedstocks (type 1), a second machine algorithm (Control Algorithm 2, Appendix H) was written to perform a single extrusion cycle each time the compaction plunger extended. With this new logic, the compaction cylinder would reach full extension and hold position trapping

a limited amount of plastic in the extrusion chamber. This allowed initial size reduction with the compaction plunger knife/shear bar system. The extrusion cylinder then fully extended forcing the trapped plastic into the die. Finally, both compaction and extrusion cylinders would retract simultaneously and the cycle was repeated. The logic modification affected the compaction and extrusion cylinders only; the cutting cylinder and control box logic were unchanged.

If the effect of die temperature was disregarded and a volume of compacted feedstock equal to that of all disruptors is forced into the die each extrusion cylinder stroke, a theoretical machine production rate could be calculated for control algorithm 2. Assuming an average type 1 feedstock density of 69 kg/m^3 (4.3 lb/ft^3) (determined in experiment 2) and a typical cycle rate of 15 cycles per minute for the extrusion cylinder, the theoretical production rate was 7 kg/hr (16 lb/hr).

A third machine algorithm (Control Algorithm 3, Appendix H) was written for processing shredded feedstock (type 2). The type 2 feedstock needed no initial size reduction in the machine, so the operation of the compaction cylinder was eliminated. The compaction cylinder and plunger was locked in the retracted position. The third algorithm consisted of continuous extension and retraction of the extrusion cylinder. The machine operator loaded the extrusion chamber directly and avoided machine plugging by limiting the plastic feed rate.

If the effect of die temperature was disregarded and a volume of compacted feedstock equal to that of all disruptors is forced into the die each extrusion cylinder stroke, a theoretical machine production rate could be calculated for control algorithm 3. Assuming an average type 2 feedstock density of 107 kg/m^3 (determined experimentally)

and a typical cycle rate of 30 cycles per minute for the extrusion cylinder, the theoretical production rate was 11 kg/hr (24.4 lb/hr).

Other Modifications

During preliminary testing, the pressure exerted on the die halves by the extruding plastic sheared the ¼”-28, grade 2 bolts that held the die halves together (Figure 40). Eight of these through-bolts were used to hold the die halves together – two at the leading edge of the die, four in the center of the die, and two at the die exit. The two bolts sheared at the leading edge of the die near the knives.

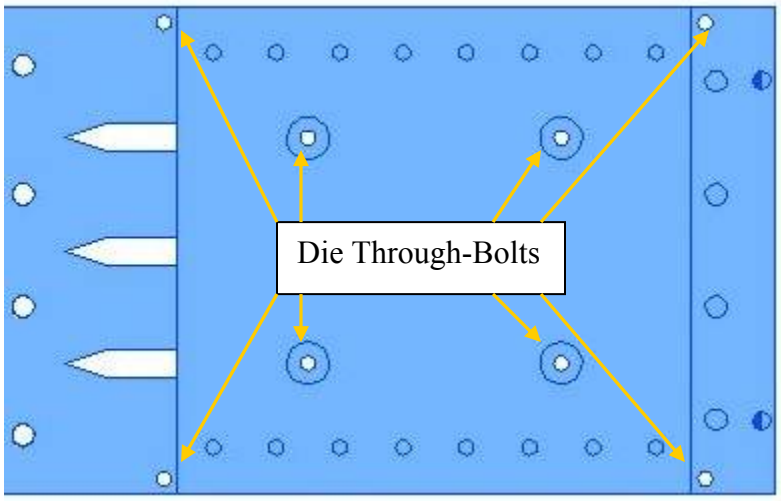

Figure 40: Die Through-Bolt Location

The shearing stress on the leading edge bolts was estimated to be 1740 MPa (252,000 psi) - a value much larger than the 1240 MPa (180,000 psi) rating of grade 8, 14”-28 bolts readily available. To reduce the shearing stress on the through-bolts, an external clamp (Figure 41) was fabricated and placed on the die and between the heating strips on the die surface. This clamp was fastened using four, ¾”-16 bolts. All eight grade 2 through-bolts were also replaced with grade 8, ¼”-28 bolts.

Figure 41: Die Assembly with External Clamp

Preliminary Testing Observations

Prior to data collection and after machine modification, more preliminary testing was performed to determine minimum and maximum die temperatures. If die temperature was less than 125ºC the Plastofuel™ perimeter would not melt and the machine plugged (Figure 34), because plastic could not be cut by the knives at the die entrance. If the die temperature exceeded 220ºC the nuggets would not be properly formed, and the plastic feedstock would thermally degrade in the die resulting in smoke and odor. Further discussion of nugget quality at different die temperatures is included in section 5.4.2.

The hydraulic pump was observed during preliminary testing to have a slower response time slower than expected. The load-sense pump did vary flow and pressure

based on system demand, so remedial action was not taken during the testing period. Discussion with the pump supplier regarding this concern was raised during testing, and focused on hydraulic system design and pump installation guidelines with no result. It was not until after testing that further analysis was performed involving the pump manufacturer and a method to decrease pump response time became apparent. A detailed discussion of the hydraulic pump performance during testing and its impact on the overall system energy ratio is included in section 7.1.1.

5.1.2 Maximum Production Rate

The maximum machine production rate was 27.6 kg/hr (60.8 lb/hr). This test used type 2 feedstock, control algorithm 3, and a die temperature of 220ºC. Determining this rate required that twenty-two test runs be completed with all test run production rates following a normal distribution. If a normal distribution was not achieved, a statistically significant conclusion regarding maximum production rate could not be stated with confidence. Twenty-two test runs ensured with 90% confidence that the maximum production rate achieved fell within the top 10% of the population. Throughout maximum production rate testing, the temperature of the die was adjusted at the discretion of the operator before each test to optimize both production rate and nugget formation. Production rates achieved at different die temperatures are listed in Table 9.

Table 9: Production Rate Test Run Results

Test Run	Die Temperature* (ºC)	Test Duration (min)	Feedstock	Production Rate (kg/hr)
1	135	20	type 1	17.4
2	145	20	type 1	16.2
3	125	21	type 1	16.9
4	155	20	type 1	20.4
5	155	20	type 2	15.3
6	145	20	type 2	18.6
7	155	20	type 2	15.9
8	155	20	type 2	19.5
9	155	11	type 2	22.9
10	165	20	type 2	20.1
11	220	10	type 2	27.6
12	200	10	type 2	27.0
13	175	10	type 2	27.0
14	175	10	type 2	24.0
15	155	10	type 2	24.0
16	155	10	type 2	22.8
17	155	10	type 2	23.4
18	175	10	type 2	21.6
19	175	10	type 2	21.0
20	175	10	type 2	20.4
21	175	10	type 2	21.6
22	175	10	type 2	20.4

* Type 1 – Household plastics and unused agricultural film
Type 2 – Dirty, shredded agricultural rigids and film
** Die temperature setting. Actual die temperature could be as much as 10ºC lower during operation.

After maximum production rate test run data collection, an analysis of the production rates for normality was performed (Figure 42). All production rates fell within the 95% confidence interval of a probability plot and the collected data followed a normal distribution.

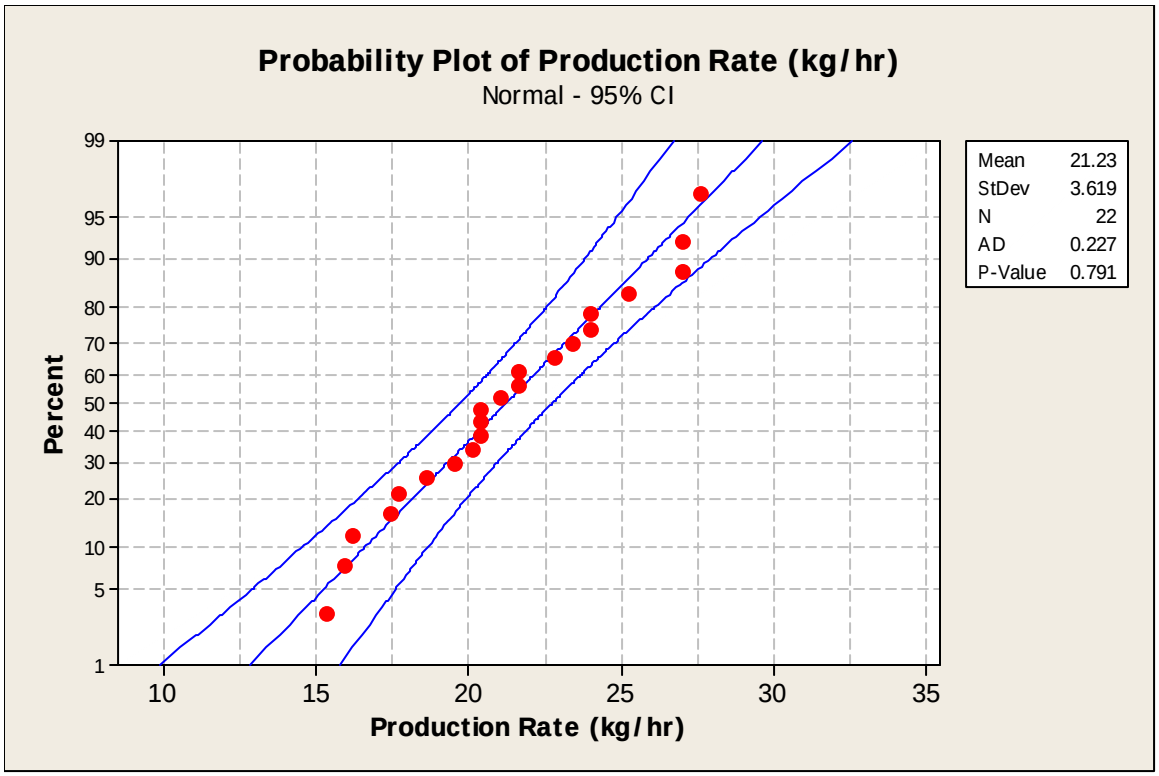

Figure 42: Normality Test for Production Rate Test Runs

There is sufficient statistical evidence ($P < .05$) to conclude that there is a linear association between die temperature and Plastofuel™ production rates. Furthermore, there is sufficient statistical evidence ($P < .05$) to conclude that the relationship is an increase in production rate with an increase in die temperature. The Minitab© regression is shown in Figure 43. The intercept was insignificant ($P > 0.9$).

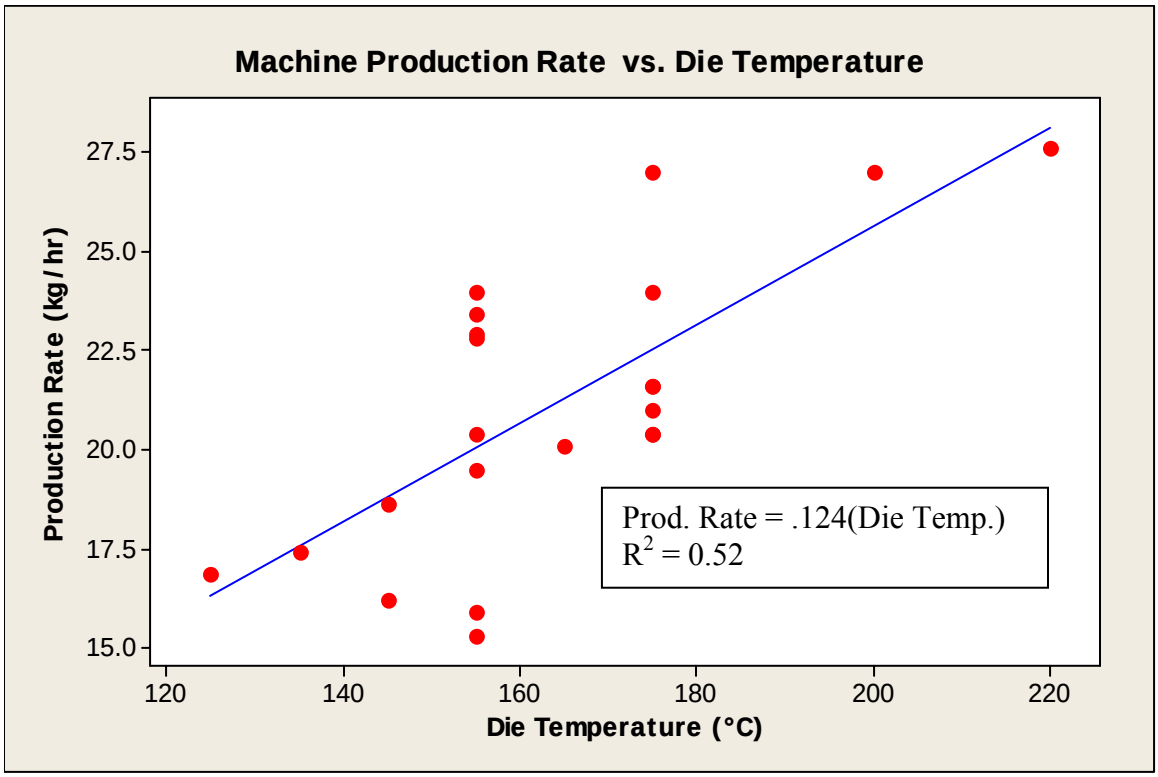

Figure 43: Regression Plot for Production Rate and die Temperature

Over the course of the twenty-two production rate tests, it became apparent that tests run with a die temperature of either 155ºC or 175ºC produced the best results – high quality nuggets at reasonable rates. Production rates at these temperature settings were compared. All test runs performed at each temperature were first tested for normality then a 2 sample t-test was performed to compare the production rates achieved. The Minitab© normality tests for the 155ºC (Figure 44) and 175ºC (Figure 45) die temperature test runs are included The production rates averaged 21.3 kg/hr (47 lb/hr) and were no different ($P < 0.05$) for these conditions.

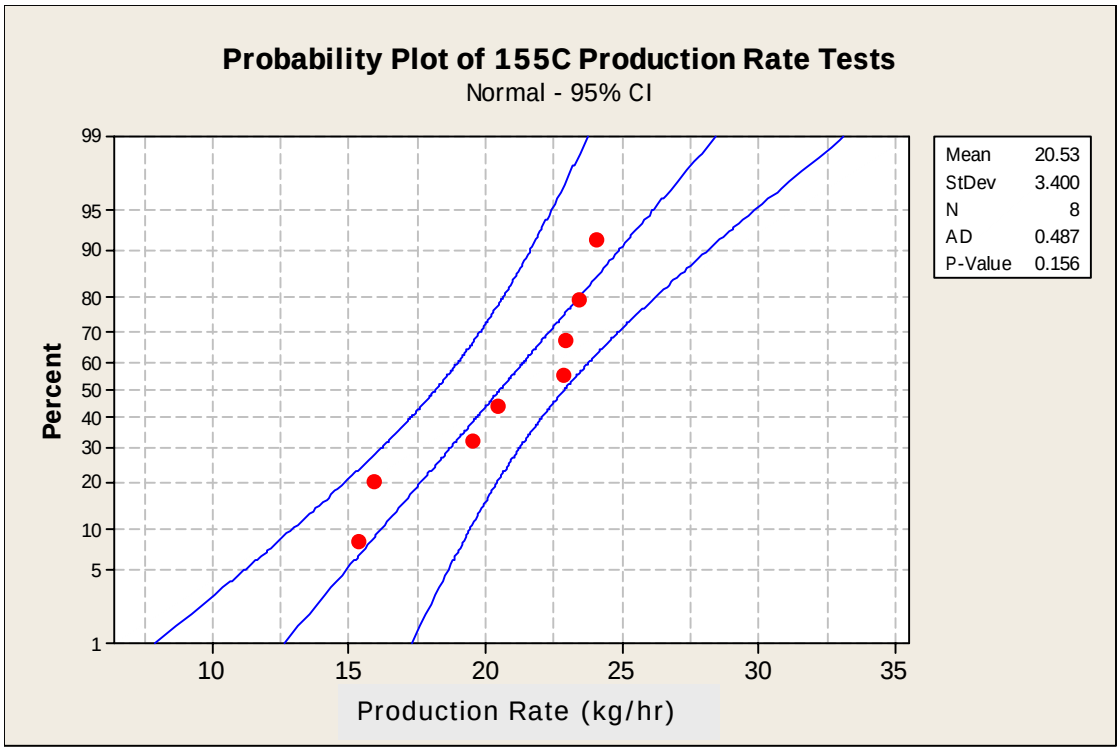

Figure 44: Normality Test for 155ºC Test Runs

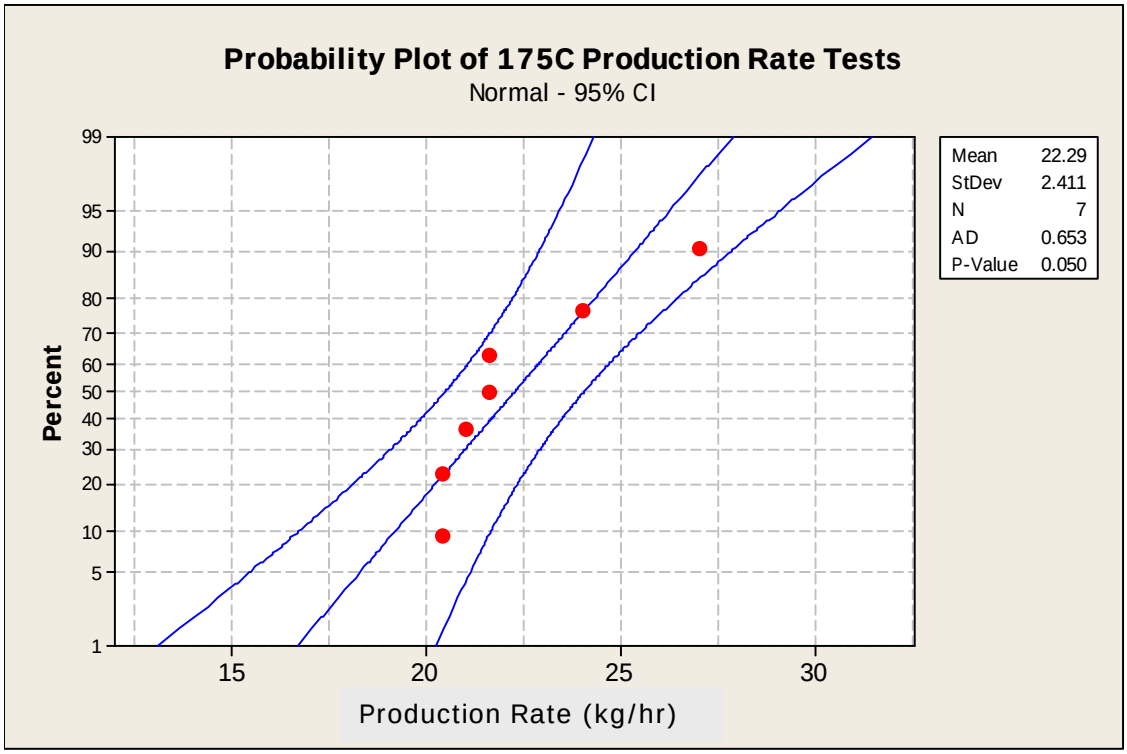

Figure 45: Normality Test for 175ºC Test Runs

5.2 System Energy Balance

Analysis of the system energy balance required a comparison of energy consumed by the machine to potential thermal energy stored in the Plastofuel™ nuggets formed. Data collected during all 34 test runs were used for this analysis.

5.2.1 Plastofuel™ Energy Content

The Plastofuel™ energy content was determined using ASTM method 5865-04 for each feedstock type. The results are listed in Table 10.

Table 10: Heating Value of Two Plastofuel™ Feedstock Types Used in All Test Runs

Plastofuel™ Feedstock Type	Heating Value MJ/kg (BTU/lb)
Type 1 (Clean households and unused agricultural film)	45.5 (19500)
Type 2 (Used agricultural rigids and films)	38.8 (16700)

Both type 1 and type 2 feedstock contained what appeared to be equal parts of HDPE, LDPE, and PS. A weighted average for a mixture of this type should have a heating value of 45.4 MJ/kg (19500 BTU/lb) using the values from Table 2. The results from the calorimetry tests are expected. Type 1 feedstock was clean plastic with minimal contaminants present to reduce the energy content. Type 2 feedstock was used agricultural plastic with visible contaminants throughout. These contaminants reduced the energy content as shown in Table 10.

5.2.2 System Energy Ratio

The system energy ratio was determined for each test run by dividing the total energy consumption during processing feedstock into the total energy content of the

Plastofuel™ nuggets formed. To compare these two values, the total energy consumption data collected during a test run by the hydraulic system and electrical system data loggers were added to the energy consumption during the shredding process, if applicable. The total energy consumed was compared to the energy content of the Plastofuel™ nuggets formed using a heating value from Table 10.

The energy ratios ranged from 22 to 47 with a mean of 33. The maximum ratio occurred with a die temperature of 155ºC and type 1 feedstock. Energy data for each test run and the associated energy ratio can be found in the following table -

Table 11: Energy Usage and Ratio for Each Test Run

Table 11: Energy Usage and Ratio for Each Test Run

Test Number	Feedstock	Electrical Energy For Shredding (kw·hr)	Machine Electrical Energy Use (kw·hr)	Hydraulic Energy Use (kw·hr)	Energy in Plastofuel Formed (kw·h)	Energy Ratio (Energy Out/Energy In)
1	type 1	0.00	0.54	1.1	73	45
2	type 1	0.00	0.54	1.2	68	38
3	type 1	0.00	0.47	1.8	74	33
4	type 1	0.00	0.55	1.3	86	47
5	type 2	0.41	0.51	1.1	55	27
6	type 2	0.50	0.56	1.3	67	29
7	type 2	0.42	0.58	1.0	57	28
8	type 2	0.52	0.61	1.5	70	27
9	type 2	0.34	0.34	0.8	45	31
10	type 2	0.54	0.62	1.1	72	32
11	type 2	0.37	0.37	0.5	50	39
12	type 2	0.36	0.32	0.6	48	38
13	type 2	0.36	0.3	0.5	48	42
14	type 2	0.32	0.33	0.5	43	37
15	type 2	0.32	0.32	0.6	43	34
16	type 2	0.30	0.3	0.6	41	35
17	type 2	0.31	0.27	0.7	42	34
18	type 2	0.29	0.32	0.4	39	38
19	type 2	0.28	0.33	0.4	38	39
20	type 2	0.27	0.33	0.4	37	38
21	type 2	0.29	0.31	0.5	39	37
22	type 2	0.27	0.33	0.4	37	37
23	type 2	0.24	0.31	0.5	32	31
24	type 2	0.19	0.30	0.5	26	26
25	type 2	0.24	0.31	0.5	32	30
26	type 2	0.19	0.31	0.6	26	25
27	type 2	0.24	0.31	0.6	32	28
28	type 2	0.19	0.31	0.7	26	22
29	type 2	0.24	0.29	0.6	32	28
30	type 2	0.19	0.30	0.7	26	22
31	type 2	0.24	0.29	0.5	32	33
32	type 2	0.19	0.29	0.5	26	26
33	type 2	0.24	0.29	0.7	32	26
34	type 2	0.19	0.27	0.6	26	25

5.3 Thermal Model and Melt Depth Analysis

This section begins with an analysis of the applicability of this model to the machine by comparing the relationship between actual and predicted melt depths for the twenty-two production rate tests. It also includes an analysis of the effect of throughput rate and die temperature on melt depth using data collected during the twelve melt depth test runs.

5.3.1 Actual and Predicted Melt Depths

The melt depth was predicted for a range of die temperatures and throughput rates prior to testing using Equation 6. Twenty of the twenty-two production rate test runs (Table 12) were used to compare predicted melt depth to actual melt depth. Test runs 1 and 3 were not considered because the die temperature was below the HDPE melt temperature. Melt depth around the Plastofuel^{TM} nugget perimeter was measured and recorded for 25 randomly selected nuggets from each test run, and a mean melt depth was recorded for each run. Feedstocks type 1 and type 2 included no noticeable polystyrene, so that plastic type is not included in this analysis. The Plastofuel^{TM} components were assumed to be equal parts HDPE, LDPE, and PP. The actual mean melt depth in the Plastofuel^{TM} samples from each test run and the predicted melt depth using Equation 6 are shown in Table 12.

Table 12: Actual Melt Depths and Melt Depths Predicted Using Equation 6

Test Run	Actual	Predicted
	Mean Melt Depth (mm)	Melt Depth (mm)
1	1.3	*
2	1.3	1.4
3	1.5	*
4	1.6	1.6
5	1.5	2.0
6	1.1	1.4
7	1.4	1.9
8	1.2	1.7
9	1.2	1.6
10	1.8	2.0
11	2.3	2.7
12	2.2	2.4
13	1.7	1.9
14	1.8	2.0
15	1.3	1.5
16	1.2	1.6
17	1.1	1.6
18	2.0	2.2
19	1.9	2.2
20	1.9	2.1
21	1.8	2.1
22	1.9	2.3

* Test runs 1 and 3 were not analyzed because die temperatures of 135ºC or below were below the HDPE melting temperature.

A plot of actual versus predicted melt depth (Figure 46) shows that actual melt depth was 15% less than predicted (the slope of the best fit, linear model was 0.85). The differences between the Stefan-Neumann model assumptions and the actual machine conditions were discussed in detail in section 3.3.5 and are likely the cause of the 15% difference. The presence in air pockets in the Plastofuel^{TM} resulting in reduced conduction is probably the single largest contributor to a low actual melt depth.

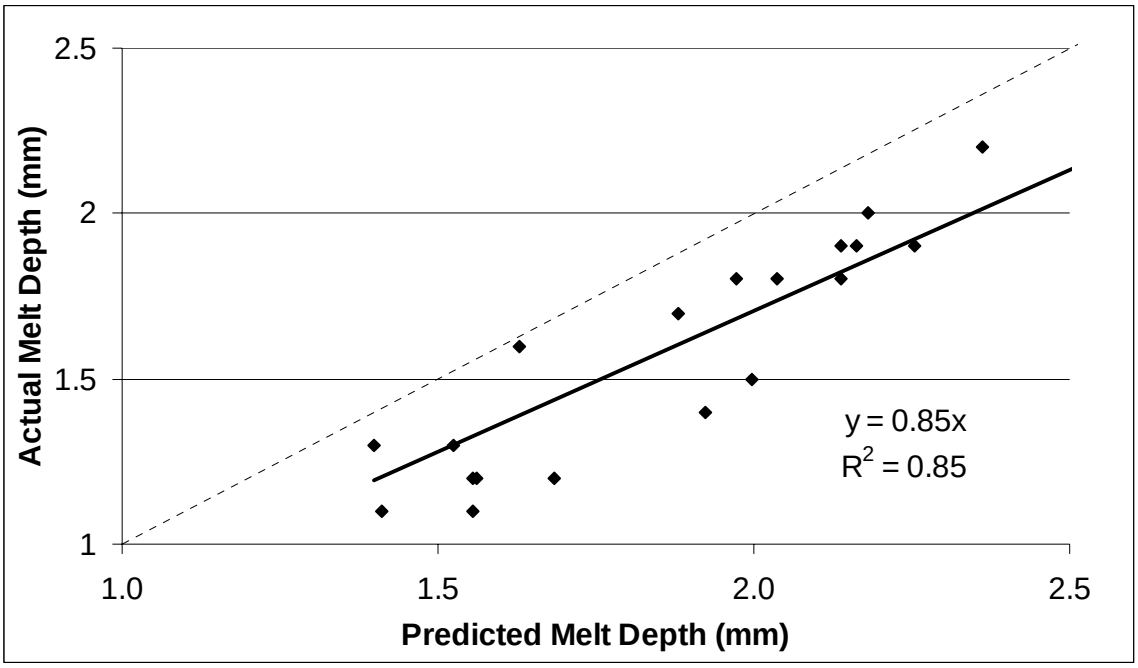

Figure 46: Scatter Plot of Actual Melt Depth and Melt Depth Predicted Using Equation 6

Incorporating a 0.85 adjustment factor into Equation 6 leads to a better melt depth prediction model (Equation 7).

Equation 7: Adjusted Equation to Predict Melt Depth in Plastofuel™ Machine

$$X = 0.85\left[(.000341\ln T_1 - .00160)\left(\frac{L\rho A}{P}\right)^{1/2}\right]$$

where

X = melt depth (m)

T_1 = die temperature (ºC)

L = length of die (m)

ρ = Plastofuel™ density (kg/m^3)

A = area of die exit openings (m^2)

P = production rate (kg/s)

This equation can be rewritten to solve for die temperature in terms of melt depth (Equation 8).

Equation 8: Adjusted Equation Solved for Die Temperature in Terms of Melt Depth

$$T_1 = e^{\left[\frac{3450X}{\left(\frac{L\rho A}{P}\right)^{1/2}} + 4.7\right]}$$

Using Equation 7, the 99% confidence interval on the mean difference between actual and predicted melt depth was -0.08 mm (-0.003 in) to 0.1 mm (0.004 in) (P = 0.8).

5.3.2 The Effect of Throughput Rate and Die Temperature on Melt Depth

Twelve test runs were completed to analyze the effect of both throughput rate and die temperature on melt depth (Table 13). All test runs used type 2 feedstock. Six test runs were performed at a die temperature of 155ºC and six test runs were performed at a die temperature of 175ºC. These temperatures were selected because they were observed to produce the highest quality nuggets. For these runs, production rates were fixed to either 18 kg/hr (40 lb/hr) or 14.4 kg/hr (32 lb/hr) for three tests at each of the two temperatures. Again, 25 nuggets were randomly selected from those formed during each test, and the melt depths were recorded. The test runs, die temperatures, production rates, and mean melt depths are listed in Table 13.

Table 13: Test Runs to Analyze Effect of Die Temperature and Production Rate on Melt Depth*

Test Number	Die Temperature (°C)	Production Rate (kg/hr)	Mean Melt Depth (mm)	Standard Deviation (mm)
23	175	18	2.0	0.35
24	175	14	2.2	0.33
25	175	18	1.9	0.44
26	175	14	2.2	0.40
27	175	18	1.9	0.44
28	175	14	2.2	0.36
29	155	18	1.3	0.32
30	155	14	1.6	0.35
31	155	18	1.4	0.37
32	155	14	1.9	0.27
33	155	18	1.4	0.37
34	155	14	1.8	0.29

* All melt depth test runs used type 2 feedstock.

A balanced ANOVA test was performed in Minitab© to determine if die temperature or production rate had an effect on the mean melt depth. There is sufficient evidence ($P < .01$) to conclude that both die temperature and production rate had an effect on melt depth.

This effect was further analyzed using the melt depth means from Table 13. The means were first tabulated in Minitab© to show the mean melt for both temperature and throughput rate combinations. Trends for the effects of die temperature and residence time were identified by generating a Minitab© Main Effects Plot (Figure 47) from the tabular data.

The results of the main effects plot are logical. As die temperature increased, the melt depth increased for a fixed throughput rate. Throughput rate is directly associated with residence time in the die. Given equal residence times, higher melt depths were expected at higher temperatures.

Conversely, as throughput rate increased melt depth decreased. At a fixed temperature, higher throughput rates decreased Plastofuel™ residence time in the die which resulted in a lower melt depth.

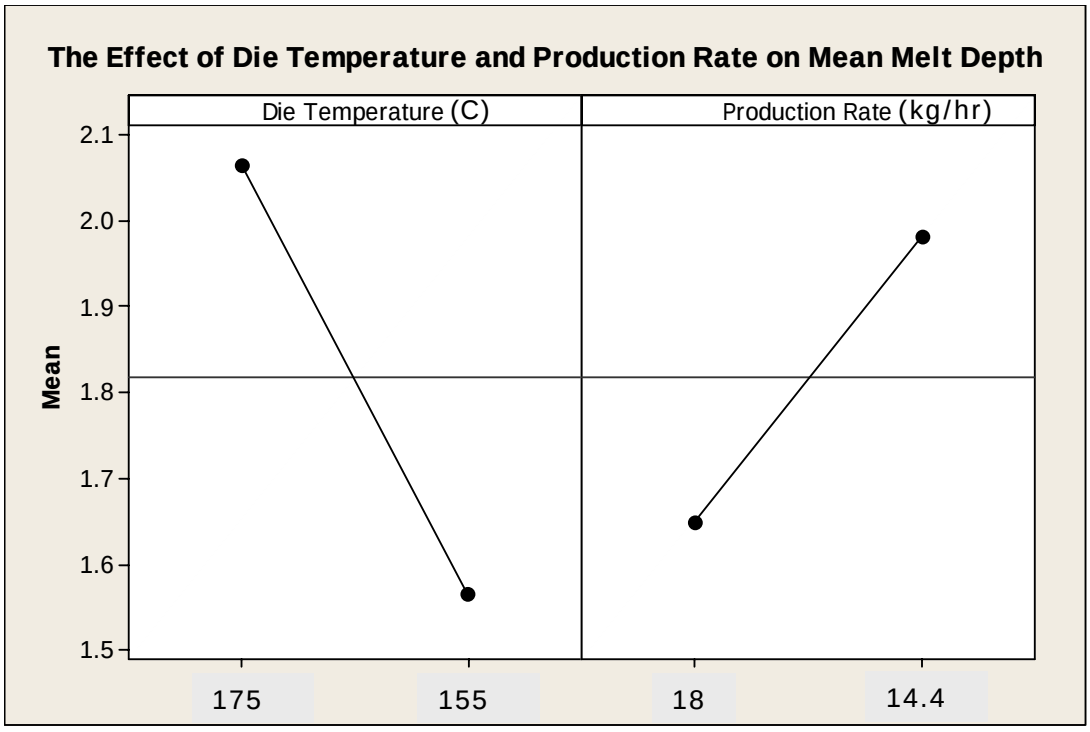

Figure 47: The Effect of Die Temperature and Production Rate on Mean Melt Depth

5.3.3 Energy Lost To Heat Internal Plastofuel™ Components

Only the exterior of each Plastofuel™ nugget was melted. The internal nugget components were left unmelted to minimize the energy required during formation. However, the temperature of the unmelted, interior Plastofuel™ components did increase as the feedstock traveled through the die. It was impossible to eliminate the heating of internal nugget components for the machine developed for this research, but minimizing internal temperatures would reduce energy consumption. This section will show the relationship between internal nugget temperature and distance from the heated die for typical machine operation. This analysis was an approximation and is included for reference purposes only; the actual temperature of internal components was not measured.

Equation 3 and Equation 4 were used to determine the temperature distribution in melted and solid plastic, respectively. These equations were derivations of the Stefan-Neumann model and the same differences between the model and the actual research conditions discussed in section 3.3.5 apply. This analysis was performed for Plastofuel™ rather than a single type of plastic, so the thermal properties found in Table 6 were used.

Reaching the Plastofuel™ melt temperature at a depth of 2 mm (0.08 in) around the nugget perimeter was only possible if the die temperature was above the melt temperature. The energy required to elevate the temperature of the volume of plastic between the melt/solid transition point and the die surface was required to drive the temperature at the transition to the melt temperature. The temperature distribution in the melt zone can be calculated for any die temperature and residence time using Equation 3. For this analysis, a typical operating condition was used – a 175ºC die temperature and a throughput rate of 19 kg/hr (42 lb/hr).

The temperature distribution in the melt zone is shown in Figure 48. The spreadsheet solution used to generate the distribution can be found in Appendix L.

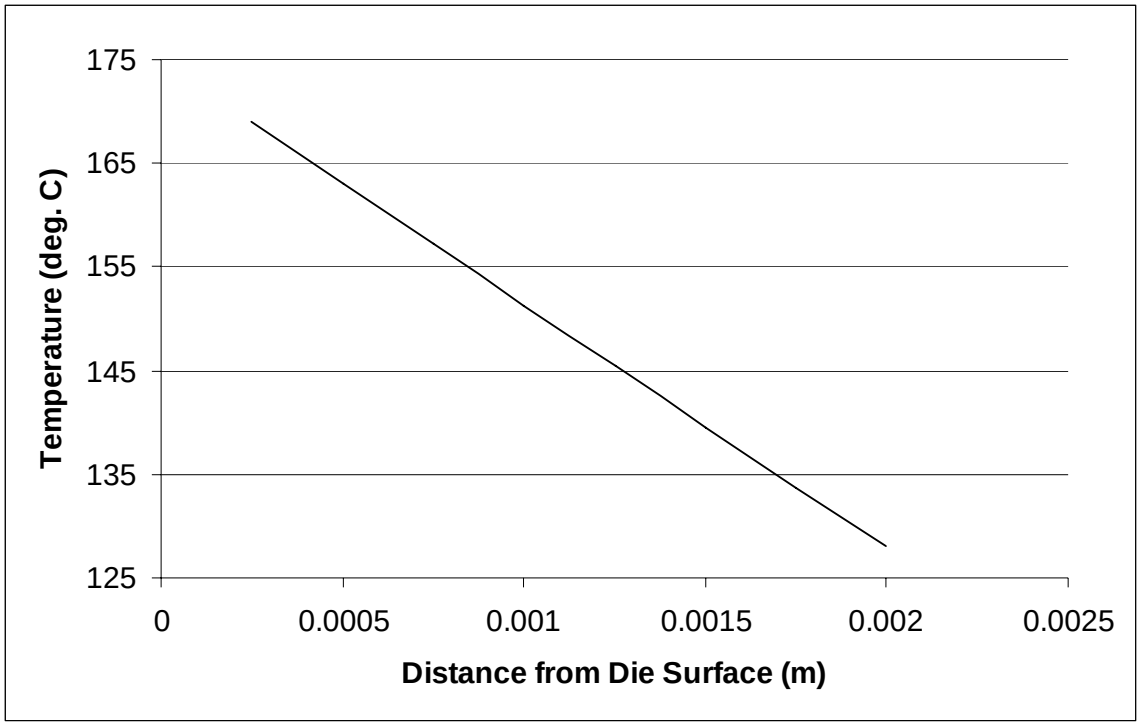

Figure 48: Predicted Temperature Profile of Plastofuel™ Melt Zone with a 175ºC Die and a Production Rate of 19 kg/hr

Significant temperature increases due to heat transfer by conduction did occur beyond the melt/solid transition in the nugget interior. The energy required for this heat transfer was wasted energy, because it did not contribute to nugget formation. However, some heat transfer into the unmelted zone of the Plastofuel™ nuggets was unavoidable with the existing machine design. The temperature gradient in the unmelted zone of the Plastofuel™ nugget was calculated using the spreadsheet in Appendix M and is graphically represented in Figure 49.

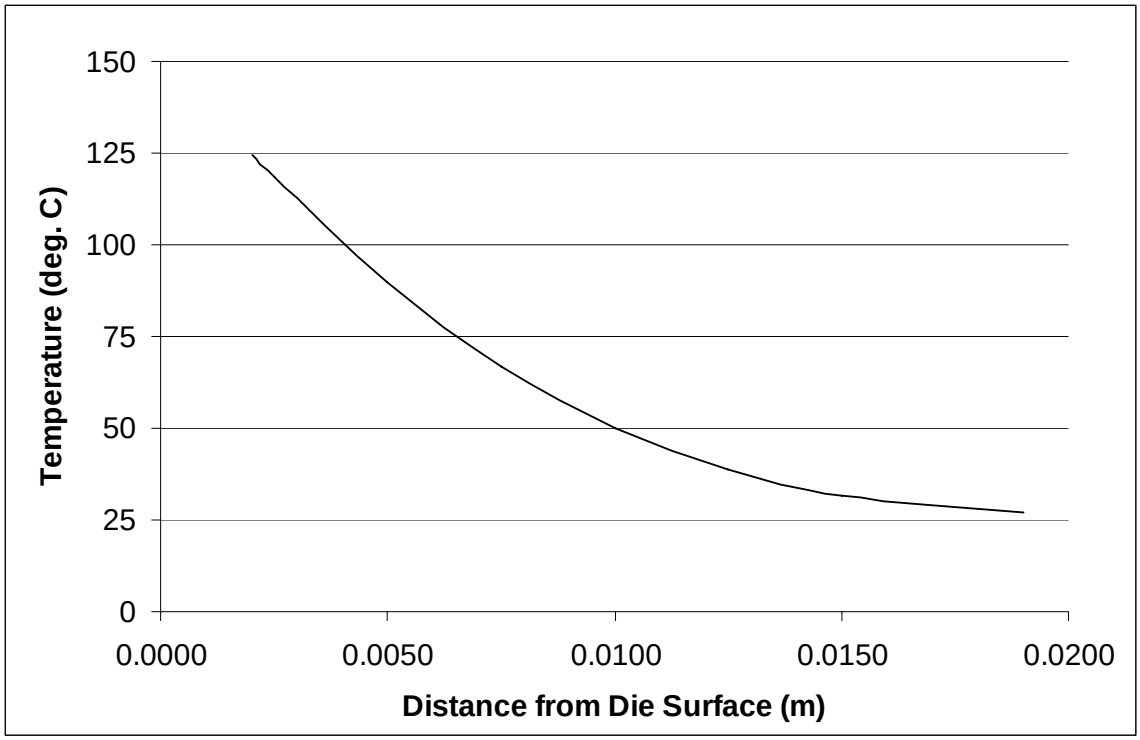

Figure 49: Predicted Temperature Profile of Plastofuel™ Solid Zone with a 175ºC Die and a Production Rate of 19 kg/hr

The energy required to drive the heat transferred to the unmelted interior was approximated using a triple integral and assumed a cylindrical nugget. The solution was an application of the steady-state conduction heat transfer equation (Equation 9).

Equation 9: Steady-State Heat Transfer due to Conduction Equation Applied to Plastofuel™ Nugget

$$dE = dV\rho c_p (T_{(r)} - T_0)$$

where

dE = energy required to heat internal element (J)

dV = volume of internal element (m^3)

ρ = density of Plastofuel™ (kg/m^3)

c_p = specific heat of Plastofuel™ (J/°K-kg)

$T_{(r)}$ = final temperature of internal element (°K)

$T_{(0)}$ = initial temperature of internal element (°K)

The integral of Equation 9 used polar coordinates to reflect the cylindrical shape of a nugget and is shown in Equation 10.

Equation 10: Triple Integral to Determine Energy Required to Heat Unmelted Plastofuel™ Interior

$$dE = \int_0^{2\pi}\int_0^{L}\int_0^{R} dV\rho c_p (T_{(r)} - T_0) r\,dr\,dz\,d\theta$$

where

L = nugget length (m)

R = radius of unmelted nugget interior (m)

Equation 10 was simplified by expressing the unmelted interior's temperature distribution in terms of the distance from the melt/solid transition using a polynomial function fitted to Figure 49. The polynomial and the associated R^2 value are shown in Figure 50.

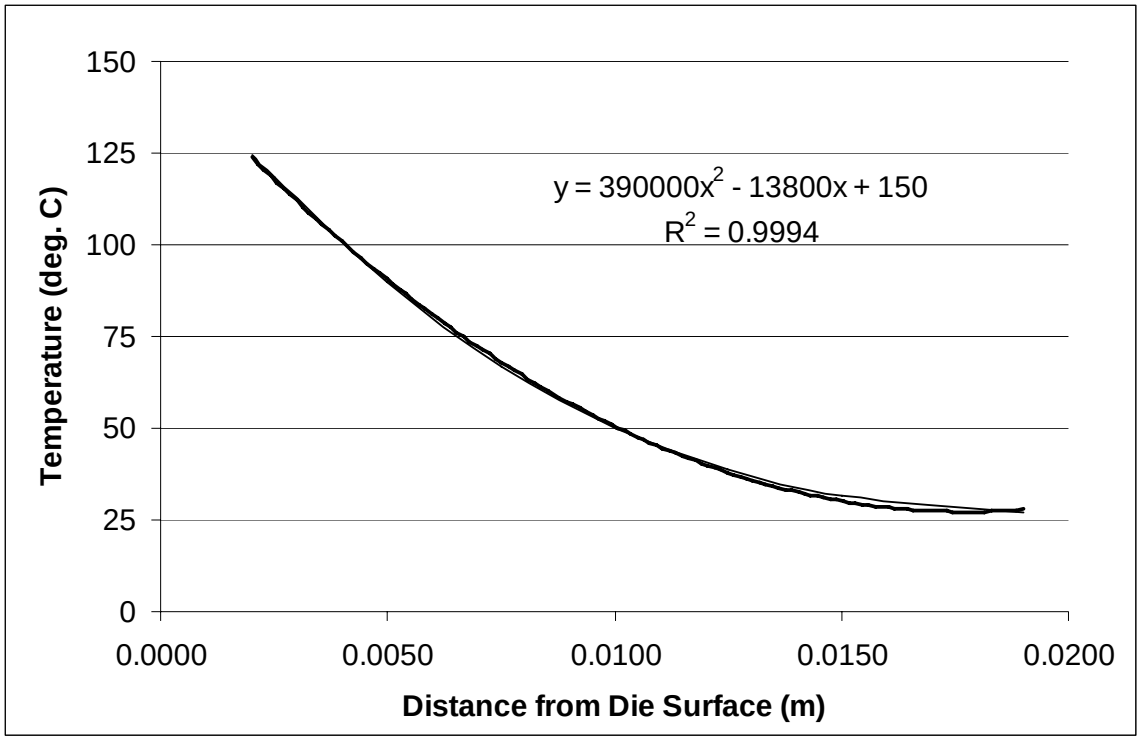

Figure 50: Polynomial Function Fitted to Temperature Distribution Profile of Unmelted Plastofuel™ Interior

Finally, the energy required to produce the conditions shown in Figure 50 for a single Plastofuel™ nugget could be written in terms of nugget length, density, specific heat, and radius of unmelted contents (Equation 11).

Equation 11: Energy Required to Raise Internal Temperature of a Plastofuel™ Nugget

$$E = 2\pi L\rho c_p\left(97500R^4 - 4600R^3 + 75R^2\right)$$

The conditions of production rate test run 22 (Table 9) were similar to the conditions for this analysis. Test 22 had a die temperature of 175ºC and a production rate of 20.4 kg/hr (45 lb/hr). The total electrical energy consumption for the machine for this test run was 0.33 kW·h. This analysis indicated that total electrical energy consumed by

the heating strips during the test run could have been reduced by 0.06 kW·h to 0.27 kW·h if no heat was transferred to the nugget interior. This would have equated in an increase in the total energy ratio for the test run from 37 to 39. The calculations for this analysis can be found in Appendix N.

5.4 Plastofuel™ Nugget Characteristics

The research focus was the determination of the system energy ratio, but data was also collected to provide benchmark information about Plastofuel™ nugget characteristics. This section includes discussion regarding Plastofuel™ density and quality as they related to die temperature.

5.4.1 Plastofuel™ Density

At the conclusion of each test run, 25 nuggets were randomly selected from the total produced. These nuggets were measured for total length and weighed. These metrics were used in conjunction with the die opening area to determine average nugget density. The average density of all Plastofuel™ nuggets produced during testing was 708 kg/m^3 (44.1 lb/ft^3). The average density of Plastofuel™ nuggets formed from type 1 feedstock, used household plastics and unused agricultural film, was 677 kg/m^3 (42.2 lb/ft^3). The average density of Plastofuel™ nuggets formed from type 2 feedstock, shredded, used agricultural rigid and film plastics, was 712 kg/m^3 (44.4 lb/ft^3). The bulk density of Plastofuel™ nuggets was measured by filling and weighing a 0.028 m^3 (1 ft^3) box with nuggets formed during twelve randomly selected test runs. The average bulk density of Plastofuel™, including air pockets, was 378 kg/m^3 (23.6 lb/ft^3).

5.4.2 Plastofuel™ Quality

Plastofuel™ quality was subjectively assessed. A high quality nugget was compact, dense, and not only held the shape of the die opening but also retained the unmelted interior contents during handling. An initial test completed with die temperature set to 250ºC produced no recognizable nuggets. The die extrudate was melted on the outside, but upon exit from the die it expanded and the unmelted interior separated from the melted mass. Furthermore, the melted plastic exiting the die was so hot that upon contact, it melted the nylon limit switches that activated nugget cut-off. The result was an accumulation of melted plastic interspersed with unmelted plastic which ultimately hardened into a single pile (Figure 51).

Figure 51: 250ºC Test Result - Solid Mass of Melted and Unmelted Plastic

The resulting mass from the 250ºC die temperature was due to insufficient cooling of the nugget exterior prior to nugget cut-off. Upon cut-off the exterior was still melted and did not hold the nugget shape. The nuggets expanded after cut-off releasing the unmelted interior and the melted exterior adhered to other melted nuggets under the die.

The highest temperature test to produce a recognizable nugget form occurred with the die temperature set to 220ºC. The nuggets formed had a tendency to stick together as they accumulated after cut-off, but the nugget form was intact (Figure 52). However, overall nugget quality was poor due to expanding at the ends and a tendency for the unmelted contents to fall out of the ends while they were being handled. Again, insufficient cooling of the nugget exterior prior to cut-off allowed the compacted interior of the nugget to expand when the nugget was cut to length.

Figure 52: Four Nuggets Produced with Die Temperature of 220ºC

Similarly, Plastofuel™ formed during a test at 200ºC were misshapen, lost unmelted interior components during handling, and had expanded ends (Figure 53).

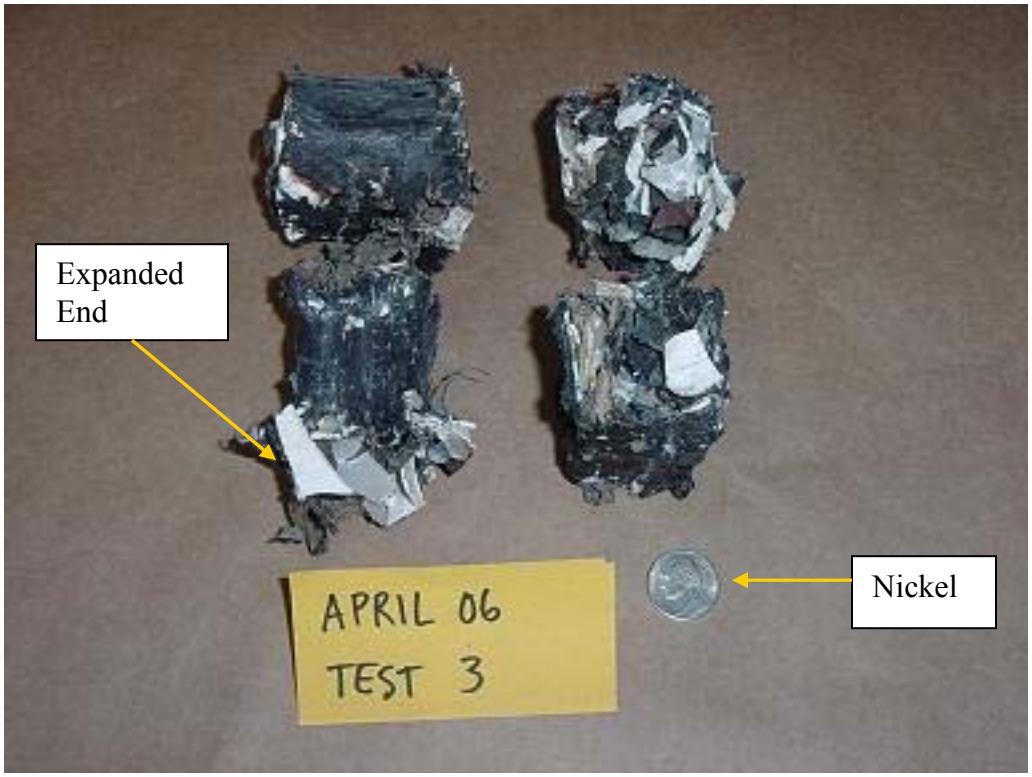

Figure 53: Four Nuggets Produced with Die Temperature of 200ºC

Tests could not be run at temperatures below 125ºC due to machine plugging caused by insufficient cutting at the die entrance. Nuggets were formed at test temperatures of 125ºC and 135 ºC, temperatures below the melting point of HDPE, but they were only possible with type 1 feedstock, and therefore testing at these temperatures was abandoned. The fact that nuggets could be formed at this temperature may be explained that the wall friction and pressure within the die slightly elevated the temperature of the nugget exterior to melt the HDPE. An alternative and more likely explanation is that the other components of the nuggets (LDPE and PP) would melt at these temperatures and may have encapsulated the HDPE components. Nuggets formed with type 1 feedstock and a die temperature of 125 ºC are shown in Figure 54.

Figure 54: Four Nuggets Produced with Die Temperature of 125ºC

With type 2 feedstock the increased contaminants, as evidenced by the lower energy content values, were sufficient to reduce the heat transfer due to conduction to a point that did not allow the exterior of the nugget to melt at these lower temperatures. No successful tests were run using type 2 feedstock at temperatures at or below 135 ºC.

The Plastofuel™ formed during tests where die temperatures ranged from 155ºC to 175º had a high quality. Die temperature could not be estimated with a visual inspection of sample nuggets produced in this range. They held the shape of the die after cut-off and retained the unmelted, internal components.

Sample, high quality Plastofuel™ randomly selected from test runs with die temperatures of 155ºC and 175ºC are shown in Figure 55, and Figure 56, respectively.

Figure 55: Four Nuggets Produced with Die Temperature of 155ºC

Figure 56: Four Nuggets Produced with Die Temperature of 175ºC

6.0 Conclusions

This research provided scientific evidence for a viable solution for the problem of non-recyclable agricultural plastics. It represents the first attempt to automate Plastofuel™ production, quantify an energy balance analysis for the process, and provide benchmark Plastofuel™ physical and melt characteristics.

The research hypothesis indicated that a system energy ratio of 100 could be achieved with this machine. The hypothesis was not supported by the machine; the maximum system energy ratio attained during this research was 47 – a three-fold increase over the prototype machine. This, however, does not preclude a next-generation machine, using advances and observations made possible with this research, from reaching an energy ratio of 100 or more. Regardless of system energy ratio, this machine and the accompanying trailer, generator, and hydraulic power unit do provide an effective tool to educate the public on the topic of energy reclamation from an environmental and economic liability.

The conclusions as they relate to the research objectives are discussed in this section.

6.1 Thermal Model (Objective 1)

The Stefan-Neumann equation was used to determine a range of die temperatures sufficient to jacket the exterior of each nugget in melted plastic. An analysis of Plastofuel™ formed with a prototype machine indicated that a maximum melt depth of 2 mm (0.08 in) was sufficient to hold unmelted, interior nugget components in place while at the same time minimize plastic melt. Equation 6 was solved for a number of expected

throughput rates and die temperatures to determine a melt depth of 2 mm (0.08 in). With throughput rates from 15 kg/hr (33 lb/hr) to 35 kg/hr (77 lb/hr), proper melt depth should be achieved with die temperatures from 156ºC to 190ºC. With the exception of test runs to determine operating limits, a majority (16 of 22) of production rate test runs were performed at these temperatures based on the prediction. After data analysis, actual melt depths for the tests performed at 155ºC - 175ºC ranged from 1.1 mm (0.04 in) to 2 mm (0.08 in) with an average value of 1.6 mm (0.06). This melt depth was sufficient for high quality Plastofuel™ nuggets.

The Stefan-Neumann model for melt prediction was adjusted to better fit the data collected during the twenty-two production rate test runs. The result, Equation 7, was used to calculate a predicted melt depth for each test run using actual test conditions. The 99% confidence interval on the mean difference between actual and predicted melt depth was -0.08 mm (-0.003 in) to 0.1 mm (0.004 in) (P = 0.8).

6.2 System Design and Fabrication (Objective 2)

After final assembly and minor machine modifications, acceptable Plastofuel™ nuggets were produced from waste agricultural plastics using a novel machine completely developed during the research timeframe. The final system had all major components as specified in the original research proposal: a compaction chamber, an extrusion chamber, and a cut-off assembly. The machine was mobile, required no energy source outside that which was housed in the trailer, and the operation of the machine was fully automated.

The total research timeline spanned thirty months. The first twenty-seven of these months were dedicated exclusively to system design and fabrication. Design processes

included preliminary experiments with plastic feedstock, spreadsheet modeling of machine hydraulic and electrical components, and determination of overall machine geometry. Fabrication was an ongoing process. Throughout the process, budgetary and time restrictions dictated that parts were specified and machined before other components could be designed. Part fabrication occurred in the Agricultural and Biological Fabrication Laboratory, the Penn State Learning Factory, and the Penn State Engineering Services facility.

6.3 Maximum Production Rate (Objective 3)

Twenty-two steady-state test runs with durations of either 10 or 20 minutes were performed to determine maximum Plastofuel^{TM} production rate. Two different types of plastic feedstock were used: (1) clean household plastic and unused plastic mulch and (2) shredded, dirty plastic pots, trays, and mulch film. Die temperatures ranged from 125ºC to 220ºC. Production rates ranged from 15.3 kg/hr (33.7 lb/hr) to 27.7 kg/hr (61 lb/hr) and were found to follow a normal distribution (Figure 42). The maximum rate was determined to be one which had a 90% chance of being in the top 10% of the entire population. The maximum machine production rate achieved was 27.6 kg/hr (61 lb/hr). This test used type 2 feedstock and a die temperature of 220ºC.

The original design parameter of producing 227 kg/hr (500 lb/hr) was not realized. Production rate was limited by extrusion cylinder force and the design of the extrusion chamber/die opening transition zone. Attempts to meet this design goal were pursued with little result. These included adding the disruptors to the extrusion plunger face, shredding feedstock, changing the machine control algorithm, and applying more heat to the die knives. Research budget and time restrictions excluded a major design

change, but reliable data regarding the final system energy ratio was collected at the production rates achieved.

6.4 Optimization through Machine Feedback (Objective 4)

The system energy ratio was optimized by minimizing energy used to form the Plastofuel™ nuggets and maximizing the amount of Plastofuel™ formed. Automation contributes to both. Automation of the compaction, extrusion, and cutting processes nearly eliminated operator effort. The operator was only required to load the machine with feedstock – a task requiring very little effort given the production rates.

Automation required machine feedback in the form of compaction and extrusion cylinder locations. Production was maximized and steady state operation, which produces consistent nugget formation, was more likely with automation because the cylinders operated in a steady, predictable manner.

Machine feedback in the form of a load-sensing hydraulic signal was also critical to reduce hydraulic energy consumption. Decreasing hydraulic energy consumption during operation increased the system energy ratio. When the hydraulic cylinders encountered high resistance hydraulic pressure increased and flow decreased. Conversely, supply line pressure decreased and flow increased as the hydraulic cylinders encountered little resistance during their stroke. A change to the hydraulic system design that would increase hydraulic pump response times to decrease the total system energy ratio is detailed in section 7.1.1.

Finally, electrical energy consumption by the die assembly heaters was minimized using feedback from five, independently operated temperature controllers. Each controller was set to the same die temperature during a test run, but it reacted to its own

thermocouple placed in one of five heating zones within the die assembly. This design minimized electrical energy consumption by only providing power to the die heaters in the zone that fell below a set temperature.

6.5 System Energy Balance (Objective 5)

Energy used to form the Plastofuel^{TM} nuggets was quantified for each test run (Table 11) in three categories: (1) hydraulic energy used to compact, extrude, and cut Plastofuel^{TM}, (2) electrical energy used by the machine to automate the system, log data, and melt the nugget perimeter, and (3) electrical energy used to shred feedstock (when applicable). Potential energy stored in the Plastofuel^{TM} nuggets formed was determined by multiplying gross energy content upon the complete combustion of Plastofuel^{TM} feedstock (Table 10) to the total mass of nuggets formed. The maximum energy ratio (E_{out}/E_{in}) was determined to be 47. This test used 1.28 kW·h of hydraulic energy, 0 kW·h of electrical energy for shredding, and 0.55 kW·h of electrical energy for the machine operation and perimeter melting. This was a total of 1.83 kW·h for nugget formation. The test produced 6.8 kg (15 lb) of Plastofuel^{TM} from type 1 feedstock representing 85.9 kW·h of potential thermal energy.

7.0 Recommendations

This section details recommendations for further research regarding the reclamation of energy from waste agricultural plastics. It includes information specific to the machine developed for this research and addresses research possibilities that would provide a more thorough understanding of industrial Plastofuel™ production and incineration.

7.1 Machine Improvements

The machine designed and fabricated for this research has the possibility of an increased system energy ratio if either the machine throughput increases with no increase in energy consumption or a decrease in energy consumption with no decrease in machine throughput. An alteration to the hydraulic system would provide decreased hydraulic energy consumption but would not affect machine throughput.

7.1.1 Increasing Hydraulic Pump Response Time

The response time for a load-sensing pump is the time that elapses between the pump's reception of a feedback signal from the hydraulic circuit and its subsequent reaction to that signal. This reaction can be an increase or decrease of both flow and pressure to the hydraulic system.

Slow response times when the pump is "signaled" to move from high pressure to low pressure result in higher system hydraulic pressure than actually required by the actuator -- and therefore higher energy consumption. Increasing pump response time would increase the efficiency of the hydraulic system and lower energy consumption.

According the specification sheet of the pump used in this research, the response time is 20 ms when moving from low to high pressure and 115 ms when moving from high to low pressure. However, these are values from a lab environment and response times are largely a function of hydraulic system design.

The pump response times observed during this research were much higher than that specification. Going from standby pressure (2 MPa (300 psi)) to maximum system pressure (19.3 MPa (2800 psi)), the response time was about 400 ms. Going from maximum system pressure to standby pressure took about 7100 ms.

These slower response times are, as indicated in the pump specification sheet, a function of hydraulic system design. These response times are graphically depicted in Figure 57 with actual system output during a controlled test. The times required going from minimum to maximum pressure and maximum to minimum pressure are delineated in red and the blue, respectively.

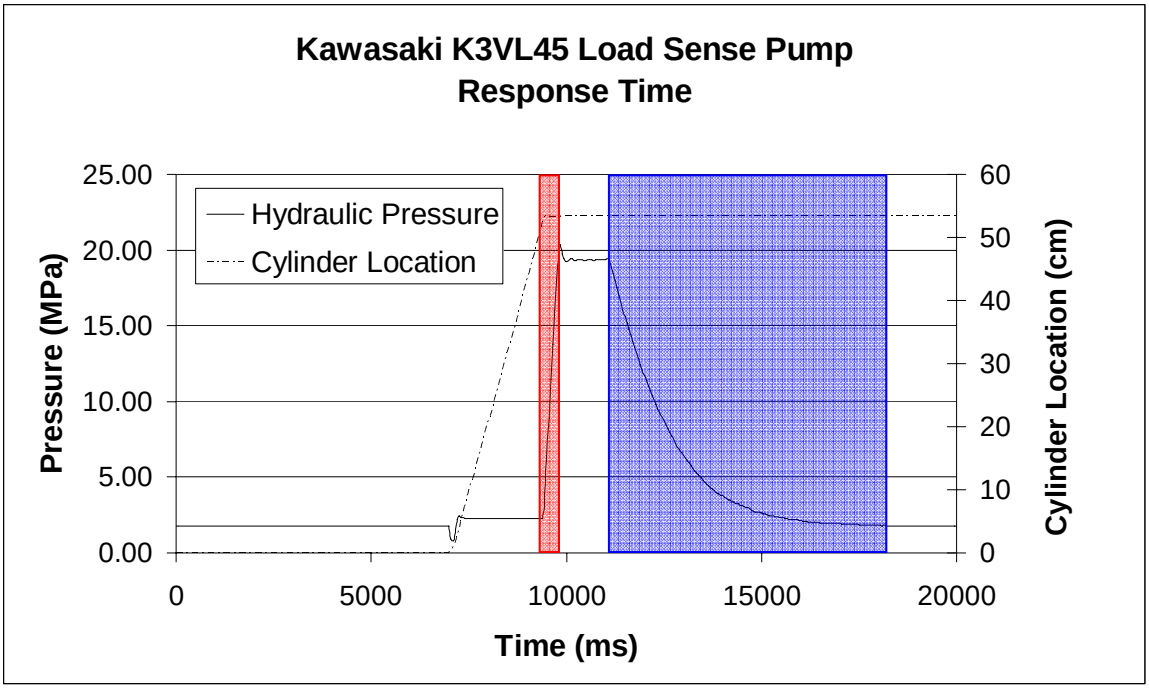

Figure 57: Pump Response Times from Low to High (Red) and High to Low (Blue) Pressure

According to the pump manufacturer, load-sensing pumps work most efficiently when the volume of oil in the load sensing line is minimized (M. Boll, personal communication, 24 May 2007). The load-sense signal originates on the machine, and, when in operation, the machine is about 7.6 m (25 ft) from the hydraulic pump located in the front of the trailer. Considering the pressurized oil inside the cylinder, the cylinder hydraulic lines, and the load-sense line, there are approximately 1700 cm^3 (104 in^3) of hydraulic fluid between the machine and the pump. The load-sense pump is equipped with a 0.4 mm (0.016 in) orifice that receives the load-sense signal. Pressurized flow through this orifice changes the flow and pressure compensator settings on the pump.

The volume of oil between the machine and the pump, the compressibility of the fluid, and the flow through this restricted orifice account for the decreased response times. When the hydraulic system on the machine operates at low pressure and requires

high pressure, the volume of oil between the machine and the pump simultaneously compresses as the load-sense signal travels through the load-sense orifice. When the hydraulic system on the machine operates at high pressure and requires low pressure, the volume of high-pressure oil between the machine and the pump must first find relief through the load-sense orifice before the actual signal is realized by the pump.

Changing the volume of oil between the machine and the pump and changing the fluid compressibility are not viable options. The machine must be located outside the trailer during operation for safety and demonstration reasons. The volume of oil in the hydraulic cylinders is fixed, and hose size (6.4 mm (0.25 in) diameter for the load-sense line and 13 mm (0.5 in) diameter for the cylinder lines) was already minimized during system design. The compressibility of the fluid is also a fluid property and cannot be dramatically changed.

Adding a "bleed-off" valve to the hydraulic system would increase pump response times by allowing the compressed fluid to find relief through an orifice other than the load-sense orifice. Doing so would allow the actual signal to be realized sooner by the pump, because the trapped fluid would not have find relief through the load-sense orifice. This would only decrease pump response times for switching from a high pressure demand to a low pressure demand (delineated in blue in Figure 57). The pump response time from low pressure to high pressure (delineated in red in Figure 57) would remain the same unless the volume of oil between the machine and the pump is changed. Introducing an always open bleed-off valve between the load-sense line and the pump would result in a slight increase in system inefficiency, but its impact would be negligible to the system as a whole.

Adding an additional bleed-off orifice to the system would require the addition of a flow control valve in the volume of oil trapped between the machine and the pump and the hydraulic system reservoir. This flow control valve would be opened slightly to limit the flow of oil through it. Limiting this flow (to a rate < 1 cm^3/min) would allow the hydraulic cylinders to function as they currently do while at the same time provide an alternative path for the load-sense signal to find relief at the low pressure tank. The addition of a bleed-off orifice to the current hydraulic schematic is shown in the red box in Figure 58.

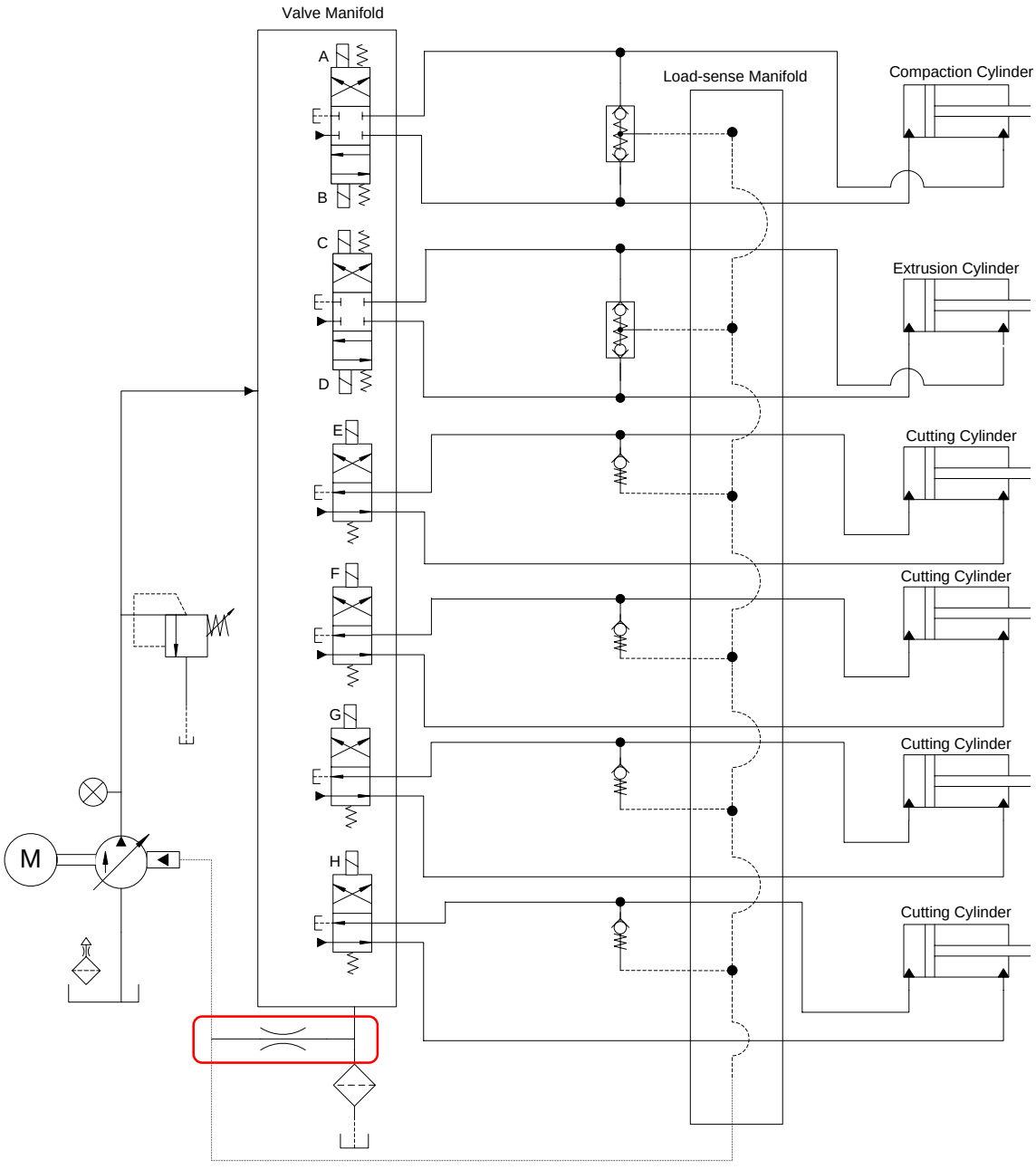

Figure 58: Hydraulic Schematic with Bleed-Off Orifice Added (Red Box)

The impact of such an addition to the hydraulic system can be estimated. According to pump specifications, the response time to move from high pressure to low pressure is approximately six times the time required to move from low pressure to high

pressure. In its current form, the hydraulic system on the machine requires 400 ms to move from low pressure to high pressure. Maintaining the same proportion as indicated by the pump specifications, the new expected response time moving from high pressure to low pressure would be approximately 2400 ms. Simulated response times to reflect this change are shown in Figure 59.

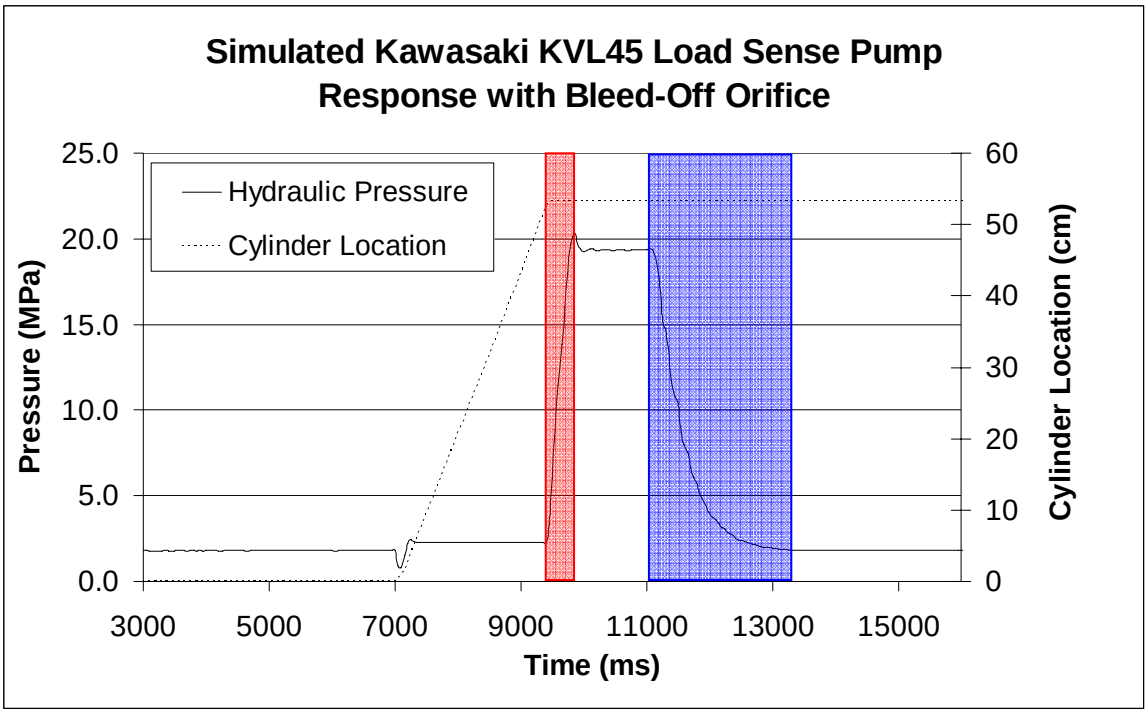

Figure 59: Simulated Pump Response Times from Low to High (Red) and High to Low (Blue) Pressure with Bleed-Off Orifice Added to System

Applying this change would affect the energy used to cycle the hydraulic cylinders and therefore the overall energy ratio. Assuming control algorithm 3 is used, the extrusion cylinder consumes approximately nearly all of the hydraulic energy. In this algorithm, the compaction cylinder was not used and the cut-off cylinders consumed only about 2% of the total hydraulic energy so the effect of the bleed-off orifice on their energy consumption is neglected for this analysis.

With the bleed-off orifice, the energy consumption by the extrusion cylinder would be reduced to approximately 42% per cylinder stroke. This decrease in hydraulic energy consumption would reduce the total energy consumption by an average of 20%. This could increase the energy ratio for the system by an average of 25% resulting in a maximum system energy ratio of 58 rather than 47 as noted in Table 11.

7.1.2 Production Rate Improvements

Throughout testing, the production rate was below the original design goal of 227 kg/hr (500 lb/hr). During preliminary testing, alterations were made to the machine algorithm, the feedstock, and the machine itself to increase production rate to this goal with little success. Additional changes to the machine which would require significant monetary and time investment could greatly increase production. Both recommendations in this section target the machine bottleneck – the extrusion chamber to die transition area. Each recommended change represents a method to achieve the original production goal.

Increasing Extrusion Force

When plastic moved from the extrusion chamber to the die entrance it failed to enter the die due to increased resistance on the extrusion chamber walls. An increase of the extrusion cylinder bore area could produce sufficient force to push the plastic from the chamber into the die and out the die exit.

If the extrusion chamber were filled with compacted plastic using the compaction cylinder and the extrusion cylinder could force all entrapped plastic out of the extrusion chamber with each stroke, the production goal would be achieved. Pursuing this option

would require system experimentation and verification that ample force could be generated with a larger extrusion cylinder. Experimentation could involve removing the die assembly and vertical knives from the machine to perform tests with different sized cylinders using actual system components. Increasing the extrusion cylinder bore size would require a redesign and remanufacture of the machine frame to not only accommodate the larger cylinder dimensions, but also increase frame strength.

Plastofuel™ Bricks

Production rate could also be greatly increased if the extrusion chamber to die transition area were removed entirely. This would require no change to the extrusion cylinder assembly, only the die itself. If this recommendation were applied, the machine would no longer produce Plastofuel™ nuggets, but rather Plastofuel™ "bricks".

To produce Plastofuel™ bricks, the die assembly would have to be removed and the die channels cut out of the die half interiors. The knives at the die entrance would no longer be used. When reassembled, the die interior would be an extension of the cross-sectional area of the extrusion chamber thus eliminating the troublesome transition zone. The four cut-off cylinders at the rear of the die would no longer be used, but rather replaced with a solid gate blocking the exit of plastic from the die. The gate would be hinged at the top of the die and opened with a small hydraulic cylinder.

The machine algorithm would be very similar to that of control algorithm 1. The feedstock could be compacted by the compaction cylinder and then further compacted and forced into the heated die using the extrusion cylinder. When the system pressure achieved a predetermined threshold during the extrusion stroke, all cylinders would hold their position for an ample amount of time for the exterior of the brick to melt. The gate

at the die exit would then open and the extrusion cylinder would force the brick out of the die.

Such a change is relatively simple from a manufacturing and machine alteration standpoint, but the fundamental change in the end product may be unacceptable to incineration facilities.

7.1.3 Machine Use

If no alterations are made to the current machine, recommendations can be made based on this research for continued use. The optimum die temperature for maximum production should be held within the 155ºC to 175ºC range. This produces the highest quality nuggets at reasonable rates. To prevent machine plugging at the die entrance, feedstock should not be added at a rate greater than 25 kg/hr (55 lb/hr). Control algorithm 2 should be used for un-shredded feedstock to make use of the size reduction capability of the compaction plunger. Control algorithm 3 should be used when shredded feedstock is available to exclude the compaction plunger operation.

The nugget cut-off procedure was acceptable for this research, but could be improved if the limit switch location was slightly raised. This would prevent the cut nuggets from being trapped between the limit switch and the die exit. This sometimes resulted in nuggets not falling away from the die during testing.

The feed chute was removed during testing to better see inside the machine. For safety reasons, this chute should be attached during demonstration.

7.2 Further Research

7.2.1 Industrial Use

Plastofuel™ production has great potential and realizes an untapped energy source from a current liability. This research proves that its production is a very high net energy gain at the machine level, but did not prove that it is a net energy gain at an industrial level.

Over the course of this research, an estimated 250 kg (550 lb) was produced using the machine and is currently in storage. Unfortunately, it will probably end up in the very place it was produced to avoid: a landfill. The reason for this is that production levels achieved with this machine make large scale incineration testing impossible. There has been an interest from an energy generation plant in Venango County, PA, to test the addition of Plastofuel™ to their current fuel source of coal. However, at their current coal consumption rate of 1640 Mg ($3.6(10^6)$ lbs) per day, it would require 82 Mg ($1.8(10^5)$ lbs) of Plastofuel™ for a single day of stack testing if the Plastofuel™ were added at a rate of 5% by weight.

Smaller scale emission testing is possible, but ultimately it is the large scale incineration facilities that represent the last stop for Plastofuel™; until the fuel is tested in such an environment, it is unlikely it would be accepted by the industry. These facilities provide not only the elevated temperatures required for clean incineration, but also have in place the logistical means to move fuel from a source to the destination.

There are several considerations that require further research before Plastofuel™ is accepted on an industrial level that go beyond emission testing. Plastic collection, beginning with a re-education of the public, is a major hurdle. Getting the plastic from

the point of use to the incineration facility would likely require transportation of raw feedstock to a central location for nugget formation. This would most likely be followed by transportation of the Plastofuel™ nuggets to an incineration facility. Both require energy input and must be considered in the final energy balance. Furthermore, certainly an industrial scale Plastofuel™ machine may have a different energy ratio than that determined during this research.

The economic viability of a large scale Plastofuel™ collection, production and incineration system could be approximated with several key assumptions regarding collection costs, processing costs with a larger machine, and transportation costs. However, such a study would be incomplete without considering the environmental impact associated with the current disposal methods.

Exploring research partnerships with companies that are developing similar fuel cube technologies would make logical sense for both cost and information sharing. Balcones Recycling and Ore-Cal RC&D have partnered to produce fuel cubes using waste plastics. They are currently looking to market a fuel cube similar to Plastofuel™ and may share information on methods to increase production rates.

7.2.2 Feedstock Analysis

There was limited documentation regarding the quantity and quality of agricultural wastes that accumulate annually. Contamination levels can reasonably vary from 0% by weight for unused, waste plastic to over 100% to dirty, wet mulch film. Unfortunately, this variability has a great impact on the system energy balance and must be carefully quantified for reliable, predictable results – an absolute requirement for large-scale incineration.

Further research may include quantification of accumulation rates for different agricultural plastic types and their contamination levels. If reliable feedstock statistics can be obtained for an agricultural plastic type from a typical application (i.e. mulch film recovered from sandy soil, etc) then energy content of the Plastofuel™ can be estimated without a calorimetry test.

Reliable statistics regarding accumulation rates and current disposal methods of waste plastics at a state, nation, or worldwide level would highlight the energy held within the waste product. Such attention could encourage funding for further Plastofuel™ development.

Epilogue

The demand for energy in our society is continually growing and the search for energy sources is endlessly expanding. The energy held in Plastofuel™ feedstocks accumulates daily in every country around the world. This research represents the next step in bringing the two together and provides scientific evidence that we are literally throwing away an energy source that can be transformed to a usable form with a significant energy return.

Bibliography

ACRC. 2005. Recycled Products. Washington, D.C.: Ag Container Recycling Council. Available at: www.acrecycle.org. Accessed 12 August 2005.

Amidon, A. 2005. Personal communication.12 August.

APC. 1994. Use and disposal of plastics in agriculture. Washington, D.C.: American Plastics Council.

Autocar, 2005. Alka Zadgaonkar Gets Cheap Fuel Out of Waste Plastic – Will It One Day Power Our Cars?. Available at: www.indiacar.com/infobank/Plastic_fuel.asp.

Balcones Resources, 2006. Balcones Fuel Technology. Available at: www.balconesresources.com/pages/fuel_tech.html.

Boll, M. 2007. Personal communication. 24 May.

Brandrup, J., E. H. Immergut, and E. A. Grulke. 1999. *Polymer Handbook.* 4th ed. New York, N.Y.: John Wiley and Sons.

Brooks, T. W. 1997. Apparatus for recycling previously used agricultural plastic film mulch. U.S. Patent No. 5635224.

Campbell, P.E., R.H. Evans, J.T. McMullan and B.C. Williams. 2001. The Potential for Adding Plastic Waste Fuel at a Coal Gasification Power Plant. Available at: wmr.sagepub.com/cgi/reprint/19/6/526.pdf.

Clarke, S. P. 1995. Recycling Farm Plastic Films. Available at: www.omafra.gov.on.ca/english/livestock/dairy/facts/95-019.htm.

Corr, B. E. 1992. What to do about plastic waste. *American Vegetable Grower* 40: 42-46.

Cundiff, J. S. 2002. *Fluid Power Circuits and Controls Fundamentals and Applications.* Boca Raton, F.L.: CRC Press.

Ehrig, R. J. 1992. *Plastics Recycling*. New York, N.Y.: Oxford University Press.

ELOG. 2002. *ELITEpro and DATApro User's Manual.* Ver. 2002b. Bend, Ore.: Dent Instruments, Inc.

Fisher, M. M. 2003. Chapter 14: Plastics recycling. In *Plastics and the Environment*, 563-627. A.L. Andrady, ed. Hoboken, NJ.: John Wiley and Sons.

Garthe, J. W., and P.D. Kowal. 1993. Resource recovery: turning waste into energy. University Park, PA.: Penn State Agricultural Sciences Cooperative Extension.

Garthe, J. W. 2004. Managing used agricultural plastics. In *Production of Vegetables, Strawberries, and Cut Flowers Using Plasticulture,* 116-122. Ithaca, N.Y.: NRAES.

Garthe, J. W., B. G. Miller, W. J. Lamont, Jr., and M. D. Orzolek. 2006. Air emissions from fuel made from used agricultural plastics. In *Proc. 33rd National Agricultural Plastics Congress*, CD-ROM. W. H. Tietjen, ed. San Antonio, Tx.: ASP.

Good News India Magazine. 2006. Alka Zadgaonkar Wrings Plastic Waste for Profit. Available at: www.goodnewsindia.com/index.php/Magazine/story/alkaZ/.

Gupta, A. K. and D. G. Lilly. 2003. Chapter 15: Thermal destruction of wastes and plastics. In *Plastics and the Environment*, 629-696. A.L. Andrady, ed. Hoboken, NJ.: John Wiley and Sons.

Harper, C. A. 1992. *Handbook of Plastics, Elastomers, and Composites.* 2nd ed. New York, N.Y.: McGraw-Hill.

Harper, C. A. 2002. *Handbook of Plastics, Elastomers, and Composites.* 4th ed. New York, N.Y.: McGraw-Hill.

Hochmuth, G. 1990. Plastic mulch disposal options. *American Vegetable Grower* 38: 50-51.

Hochmuth, G. 1998. What to do with all that mulch? *American Vegetable Grower* 46(4): 45.

Hussain, I. and H. Hamid. 2003. Chapter 5: Plastics in agriculture. In *Plastics and the Environment*, 185-206. A.L. Andrady, ed. Hoboken, NJ.: John Wiley and Sons.

Moore, G. R., and D. E. Kline. 1984. *Properties and Processing of Polymers for Engineers.* Englewood Cliffs, N.J.: Prentice-Hall, Inc.

Muccio, E. A. 1994. *Plastics Processing Technology*. Materials Park, O.H.: ASM International.

Ore-Cal RC&D. 2006. Agricultural Plastics and Western Juniper Fuel Cubes. Available at: www.orecalrcandd.org/ag-plastic_recovery.htm.

Osswald, T. A. and G. Menges. 2003. *Material Science of Polymers for Engineers.* 2nd ed. Cincinnati, OH.: Hanser Gardner Publications, Inc.

Ozmotech. 2007. New Thermofuel System Produces the Goods. Available at: www.ozmotech.com.au/ThermofuelJan07.pdf.

Parish, R. L., R. P. Bracy, and J. E. McCoy. 2000. Evaluation of field incineration of plastic mulch. *Journal of Vegetable Crop Production* 6(1): 17-23.

Rathje, W. and C. Murphy. 1992. *Rubbish! The Archaeology of Garbage*. New York, N.Y.: Harper Collins Publishers.

Rao, N. S. and K. O'Brien. 1998. *Design Data for Plastics Engineers.* Cincinnatti, O.H.: Hanser Gardner Publications, Inc.

Rao, N. S. and G. Schumacher. 2004. *Design Formulas for Plastics Engineers.* Cincinnatti, O.H.: Hanser Gardner Publications, Inc.

South, L. 1992. Turning plastic waste into energy. *American Vegetable Grower* 40: 26-27.

Tadmor, Z. and C. G. Gogos. 1979. *Principles of Polymer Processing.* New York, N.Y.: John Wiley and Sons.

USDOE. 2003. Electric power annual 2003. Washington, D.C.: Energy Information Administration.

Warner, J. 2005. Films of the future. *American Vegetable Grower* 53: 16.

Wittwer, S. H. 1993. World-wide use of plastics in horticultural production. *HortTechnology* 3(1): 6-19.

Zook, D. 2005. Personal communication. 20 September.

Appendices

Appendix A – Knife Temperature and Plastic Density when Cutting Begins

Tare Weight (lb)= 3.97
Inside Diameter(in)= 5.875

Temperature of knife (Celsius)	Compressed Depth (In)	Total weight (lb)	Weight of Plastic (lb)	Plastic Volume (in^3)	Density at Cutting (lb/in^3)	Density at Cutting (g/cm^3)
100	4	5.32	1.35	108	0.012	0.34
105	5.625	5.35	1.38	152	0.009	0.25
110	5.75	5.58	1.61	156	0.010	0.29
115	3.625	4.996	1.026	98	0.010	0.29
120	4.625	5.2	1.23	125	0.010	0.27
125	2.5	4.57	0.6	68	0.009	0.25
130	5.5	5.39	1.42	149	0.010	0.26
135	4.875	5.18	1.21	132	0.009	0.25

Data from experiment 1

Appendix B – Compaction Calculations and Data for Different Agricultural Plastics

INPUTS

PVC_Dia	diameter of PVC cylinder	28.26	cm	measured
PVC_Ht	height of PVC cylinder	43.18	cm	measured
Stamp_Dia	diameter of stamp	25.4	cm	measured
Stamp_Depth	distance of stamp travel after compaction	34.93	cm	measured
P_hyd	hydraulic system pressure	1379	kPa	measured
cyl_bore	hydraulic cylinder bore diameter	5.08	cm	measured
cyl_stroke	hydraulic cylinder stroke	45.72	cm	measured
Wt_sample	weight of sample	2948	g	measured

INTERMEDIATE CALCULATIONS

PVC_vol_initial	initial volume of PVC cylinder	27079	cm^3	(PI()*((PVC_Dia)/2)^2)*PVC_Ht
PVC_vol_final	final volume of PVC cylinder	5177	cm^3	(PI()*((PVC_Dia)/2)^2)*(PVC_Ht-Stamp_Depth)
cyl_area	area of cylinder bore	20.27	cm^2	PI()*(cyl_bore/2)^2
Compacted_Ht	height of plastic within PVC cylinder	8.255	cm	PVC_Ht-Stamp_Depth

OUTPUTS

cyl_Force	cylinder force	2795	kN	P_hyd*cyl_area*1000/(10000)
Density	density of sample	0.569	g/cm^3	Wt_sample/PVC_vol_final
P_plastic	pressure exerted on plastic	55158	kPa	(cyl_Force/(PI()*(Stamp_Dia/2)^2))*10000

Example calculations and raw data from experiment 2

Cut Up Plastic Film and Unused Plastic Mulch
Run 1

Sample Weight (lb)= 6.4 Sample Weight (g)= 2903

Hydraulic Pressure (psi)	Hydraulic Pressure (kPa)	Pressure on Plastic (psi)	Pressure on Plastic (kPa)	Stamp Depth (in)	Stamp Depth (cm)	Compacted Height (in)	Compacted Height (cm)	Density (lbs/in^3)	Density (g/cm^3)
0	0	0	0	0	0.00	17	43.18	0.003873	0.107
200	1379	25	173	13.75	34.93	3.25	8.26	0.020	0.561
250	1724	31	217	13.875	35.24	3.125	7.94	0.021	0.583
300	2068	38	260	13.9375	35.40	3.0625	7.78	0.021	0.595
400	2758	50	347	14	35.56	3	7.62	0.022	0.607
500	3447	63	433	14.125	35.88	2.875	7.30	0.023	0.634
600	4137	75	520	14.1875	36.04	2.8125	7.14	0.023	0.648
700	4826	88	607	14.25	36.20	2.75	6.99	0.024	0.663
800	5516	100	693	14.3125	36.35	2.6875	6.83	0.024	0.678
900	6205	113	780	14.3125	36.35	2.6875	6.83	0.024	0.678
1000	6895	126	866	14.375	36.51	2.625	6.67	0.025	0.694
1250	8618	157	1083	14.4375	36.67	2.5625	6.51	0.026	0.711
1500	10342	188	1300	14.5	36.83	2.5	6.35	0.026	0.729
1800	12411	226	1560	14.625	37.15	2.375	6.03	0.028	0.767

Cut Up Plastic Film and Unused Plastic Mulch
Run 2

Sample Weight (lb)= 6.4 Sample Weight (g)= 2903

Hydraulic Pressure (psi)	Hydraulic Pressure (kPa)	Pressure on Plastic (psi)	Pressure on Plastic (kPa)	Stamp Depth (in)	Stamp Depth (cm)	Compacted Height (in)	Compacted Height (cm)	Density (lbs/in^3)	Density (g/cm^3)
0	0	0	0	0	0.00	17	43.18	0.004	0.107
200	1379	25	173	13.875	35.24	3.125	7.94	0.021	0.583
250	1724	31	217	13.9375	35.40	3.0625	7.78	0.021	0.595
300	2068	38	260	14	35.56	3	7.62	0.022	0.607
400	2758	50	347	14.125	35.88	2.875	7.30	0.023	0.634
500	3447	63	433	14.125	35.88	2.875	7.30	0.023	0.634
600	4137	75	520	14.1875	36.04	2.8125	7.14	0.023	0.648
700	4826	88	607	14.25	36.20	2.75	6.99	0.024	0.663
800	5516	100	693	14.3125	36.35	2.6875	6.83	0.024	0.678
900	6205	113	780	14.375	36.51	2.625	6.67	0.025	0.694
1000	6895	126	866	14.375	36.51	2.625	6.67	0.025	0.694
1250	8618	157	1083	14.4375	36.67	2.5625	6.51	0.026	0.711
1500	10342	188	1300	14.5625	36.99	2.4375	6.19	0.027	0.748
1800	12411	226	1560	14.75	37.47	2.25	5.72	0.029	0.810

Cut Up Trays and Pots
Run 1

Sample Weight (lb)= 2.9 Sample Weight (g)= 1315

Hydraulic Pressure (psi)	Hydraulic Pressure (kPa)	Pressure on Plastic (psi)	Pressure on Plastic (kPa)	Stamp Depth (in)	Stamp Depth (cm)	Compacted Height (in)	Compacted Height (cm)	Density (lbs/in^3)	Density (g/cm^3)
0	0	0	0	0	0.00	17	43.18	0.002	0.049
200	1379	25	173	11.75	29.85	5.25	13.34	0.006	0.157
250	1724	31	217	12	30.48	5	12.70	0.006	0.165
300	2068	38	260	12.375	31.43	4.625	11.75	0.006	0.178
400	2758	50	347	12.8125	32.54	4.1875	10.64	0.007	0.197
500	3447	63	433	13.375	33.97	3.625	9.21	0.008	0.228
600	4137	75	520	13.75	34.93	3.25	8.26	0.009	0.254
700	4826	88	607	13.9375	35.40	3.0625	7.78	0.010	0.270
800	5516	100	693	14.125	35.88	2.875	7.30	0.010	0.287
900	6205	113	780	14.375	36.51	2.625	6.67	0.011	0.314
1000	6895	126	866	14.5625	36.99	2.4375	6.19	0.012	0.339
1250	8618	157	1083	14.875	37.78	2.125	5.40	0.014	0.388
1500	10342	188	1300	15.0625	38.26	1.9375	4.92	0.015	0.426
1800	12411	226	1560	15.25	38.74	1.75	4.45	0.017	0.472

Cut Up Trays and Pots
Run 2

Sample Weight (lb)= 2.9 Sample Weight (g)= 1315

Hydraulic Pressure (psi)	Hydraulic Pressure (kPa)	Pressure on Plastic (psi)	Pressure on Plastic (kPa)	Stamp Depth (in)	Stamp Depth (cm)	Compacted Height (in)	Compacted Height (cm)	Density (lbs/in^3)	Density (g/cm^3)
0	0	0	0	0	0.00	17	43.18	0.002	0.049
200	1379	25	173	13	33.02	4	10.16	0.007	0.206
250	1724	31	217	13.125	33.34	3.875	9.84	0.008	0.213
300	2068	38	260	13.3125	33.81	3.6875	9.37	0.008	0.224
400	2758	50	347	13.625	34.61	3.375	8.57	0.009	0.245
500	3447	63	433	13.9375	35.40	3.0625	7.78	0.010	0.270
600	4137	75	520	14.1875	36.04	2.8125	7.14	0.011	0.293
700	4826	88	607	14.375	36.51	2.625	6.67	0.011	0.314
800	5516	100	693	14.625	37.15	2.375	6.03	0.013	0.348
900	6205	113	780	14.8125	37.62	2.1875	5.56	0.014	0.377
1000	6895	126	866	14.875	37.78	2.125	5.40	0.014	0.388
1250	8618	157	1083	15.125	38.42	1.875	4.76	0.016	0.440
1500	10342	188	1300	15.3125	38.89	1.6875	4.29	0.018	0.489
1800	12411	226	1560	15.5	39.37	1.5	3.81	0.020	0.550

Cut Up Drip Tape
Run 1

Sample Weight (lb)= 2.2 Sample Weight (g)= 998

Hydraulic Pressure (psi)	Hydraulic Pressure (kPa)	Pressure on Plastic (psi)	Pressure on Plastic (kPa)	Stamp Depth (in)	Stamp Depth (cm)	Compacted Height (in)	Compacted Height (cm)	Density (lbs/in^3)	Density (g/cm^3)
0	0	0	0	0	0.00	17	43.18	0.001	0.037
200	1379	25	173	15	38.10	2	5.08	0.011	0.313
250	1724	31	217	15.125	38.42	1.875	4.76	0.012	0.334
300	2068	38	260	15.1875	38.58	1.8125	4.60	0.012	0.346
400	2758	50	347	15.25	38.74	1.75	4.45	0.013	0.358
500	3447	63	433	15.375	39.05	1.625	4.13	0.014	0.385
600	4137	75	520	15.375	39.05	1.625	4.13	0.014	0.385
700	4826	88	607	15.5	39.37	1.5	3.81	0.015	0.418
800	5516	100	693	15.5625	39.53	1.4375	3.65	0.016	0.436
900	6205	113	780	15.625	39.69	1.375	3.49	0.016	0.456
1000	6895	126	866	15.625	39.69	1.375	3.49	0.016	0.456
1250	8618	157	1083	15.875	40.32	1.125	2.86	0.020	0.557
1500	10342	188	1300	16	40.64	1	2.54	0.023	0.626
1800	12411	226	1560	16.0625	40.80	0.9375	2.38	0.024	0.668

Cut Up Drip Tape
Run 2

Sample Weight (lb)= 2.2 Sample Weight (g)= 998

Hydraulic Pressure (psi)	Hydraulic Pressure (kPa)	Pressure on Plastic (psi)	Pressure on Plastic (kPa)	Stamp Depth (in)	Stamp Depth (cm)	Compacted Height (in)	Compacted Height (cm)	Density (lbs/in^3)	Density (g/cm^3)
0	0	0	0	0	0.00	17	43.18	0.001	0.037
200	1379	25	173	15.625	39.69	1.375	3.49	0.016	0.456
250	1724	31	217	15.625	39.69	1.375	3.49	0.016	0.456
300	2068	38	260	15.625	39.69	1.375	3.49	0.016	0.456
400	2758	50	347	15.75	40.01	1.25	3.18	0.018	0.501
500	3447	63	433	15.75	40.01	1.25	3.18	0.018	0.501
600	4137	75	520	15.8125	40.16	1.1875	3.02	0.019	0.528
700	4826	88	607	15.8125	40.16	1.1875	3.02	0.019	0.528
800	5516	100	693	15.875	40.32	1.125	2.86	0.020	0.557
900	6205	113	780	15.9375	40.48	1.0625	2.70	0.021	0.590
1000	6895	126	866	15.9375	40.48	1.0625	2.70	0.021	0.590
1250	8618	157	1083	16	40.64	1	2.54	0.023	0.626
1500	10342	188	1300	16	40.64	1	2.54	0.023	0.626
1800	12411	226	1560	16.375	41.59	0.625	1.59	0.036	1.002

Bound, Used Mulch and Drip Tape (Dirty, Wet)
Run 1

Sample Weight (lb)= 5.64 Sample Weight (g)= 2558

Hydraulic Pressure (psi)	Hydraulic Pressure (kPa)	Pressure on Plastic (psi)	Pressure on Plastic (kPa)	Stamp Depth (in)	Stamp Depth (cm)	Compacted Height (in)	Compacted Height (cm)	Density (lbs/in^3)	Density (g/cm^3)
0	0	0	0	0	0.00	17	43.18	0.003	0.094
200	1379	25	173	14.625	37.15	2.375	6.03	0.024	0.676
250	1724	31	217	14.875	37.78	2.125	5.40	0.027	0.756
300	2068	38	260	14.9375	37.94	2.0625	5.24	0.028	0.778
400	2758	50	347	15.125	38.42	1.875	4.76	0.031	0.856
500	3447	63	433	15.25	38.74	1.75	4.45	0.033	0.917
600	4137	75	520	15.375	39.05	1.625	4.13	0.036	0.988
700	4826	88	607	15.4375	39.21	1.5625	3.97	0.037	1.028
800	5516	100	693	15.4375	39.21	1.5625	3.97	0.037	1.028
900	6205	113	780	15.625	39.69	1.375	3.49	0.042	1.168
1000	6895	126	866	15.6875	39.85	1.3125	3.33	0.044	1.223
1250	8618	157	1083	15.75	40.01	1.25	3.18	0.046	1.284
1500	10342	188	1300	15.875	40.32	1.125	2.86	0.052	1.427
1800	12411	226	1560	15.9375	40.48	1.0625	2.70	0.055	1.511

Bound, Used Mulch and Drip Tape (Dirty, Wet)
Run 2

Sample Weight (lb)= 5.64 Sample Weight (g)= 2558

Hydraulic Pressure (psi)	Hydraulic Pressure (kPa)	Pressure on Plastic (psi)	Pressure on Plastic (kPa)	Stamp Depth (in)	Stamp Depth (cm)	Compacted Height (in)	Compacted Height (cm)	Density (lbs/in^3)	Density (g/cm^3)
0	0	0	0	0	0.00	17	43.18	0.003	0.094
200	1379	25	173	15.1875	38.58	1.8125	4.60	0.032	0.886
250	1724	31	217	15.25	38.74	1.75	4.45	0.033	0.917
300	2068	38	260	15.3125	38.89	1.6875	4.29	0.034	0.951
400	2758	50	347	15.4375	39.21	1.5625	3.97	0.037	1.028
500	3447	63	433	15.5	39.37	1.5	3.81	0.039	1.070
600	4137	75	520	15.5	39.37	1.5	3.81	0.039	1.070
700	4826	88	607	15.5625	39.53	1.4375	3.65	0.040	1.117
800	5516	100	693	15.625	39.69	1.375	3.49	0.042	1.168
900	6205	113	780	15.6875	39.85	1.3125	3.33	0.044	1.223
1000	6895	126	866	15.75	40.01	1.25	3.18	0.046	1.284
1250	8618	157	1083	15.8125	40.16	1.1875	3.02	0.049	1.352
1500	10342	188	1300	15.875	40.32	1.125	2.86	0.052	1.427
1800	12411	226	1560	15.9375	40.48	1.0625	2.70	0.055	1.511

Appendix C – Compaction Cylinder Sizing Calculation

INPUTS				
sample_wt	weight of first charge of material	2	lb	assumed
p_width	plunger width	8.375	in	assumed
p_height	plunger height	5.75	in	assumed
p_location	plunger location	18	in	measured- variable (0-20in)
stroke_max	plunger cylinder stroke	20	in	measured
d_film	density of film at 0 psi	0.004	lb/in^3	measured
d_trays	density of trays and pots at 0 psi	0.002	lb/in^3	measured
d_used_film	density of used film at 0 psi	0.003	lb/in^3	measured
d_drip	density of drip tape at 0 psi	0.001	lb/in^3	measured
INTERMEDIATE CALCULATIONS				
p_area	area of plunger face	48.16	in^2	p_width*p_height
d_avg	average density of all materials at 0 psi	0.0025	lb/in^3	(d_film+d_trays+d_used_film+d_drip)/4
OUTPUTS				
sample_d	density of sample	0.021	lb/in^3	sample_wt/(p_area*(stroke_max-p_location))
		0.018	lb/ cu in target density	
	Hydraulic Operating Pressure (psi) =		3000	
	Density (lb/in^3) Table			

Plunger Travel Distance (in)	Initial weight (lb)	Cut Up Trays and Pots		
0.021	2.000	Pressure (psi)	Force (lb)	Min. Cylinder Bore (in)
0	0.0021	0	0	0.0
1	0.0022	0	0	0.0
2	0.0023	0	0	0.0
3	0.0024	0	0	0.0
4	0.0026	0	0	0.0
5	0.0028	0	0	0.0
6	0.0030	0	0	0.0
7	0.0032	0	0	0.0
8	0.0035	0	0	0.0
9	0.0038	0	0	0.0
10	0.0042	5	232	0.3
11	0.0046	12	584	0.5
12	0.0052	21	1025	0.7
13	0.0059	33	1592	0.8
14	0.0069	49	2348	1.0
15	0.0083	71	3406	1.2
16	0.0104	104	4994	1.5
17	0.0138	159	7639	1.8
18	0.0208	269	12930	2.3
19	0.0415	598	28803	3.5
19.2	0.0519	763	36740	3.9

This calculation and data table was used to size the compaction cylinder bore. It showed the relationship between force exerted on loose plastic by the cylinder and the corresponding density achieved.

Appendix D - Compaction and Extrusion Calculations

Compaction and Extrusion Cylinder Calculations

INPUTS				
force_cyl	required force generated by cylinder	7639	lbs	"Plastic Compaction Data" file, "Work Prediction" spreadsheet
comp_stroke	compaction cylinder stroke	21	in	from autocad drawing
ext_stroke	extrusion cylinder stroke	15	in	from autocad drawing
press	maximum system hydraulic fluid pressure	3000	psi	assumed
initial_density	minimum plastic density before compaction	0.001	lb/in^3	"Plastic Compaction Data" file, "Drip Tape" spreadsheet (minimum)
final_density	minimum plastic density after compaction	0.010	lb/in^3	"CuttingDens_vs_KnifeTemp" file, "Cutting Density" spreadsheet
ext_height	extrusion chamber height	1.625	in	from autocad drawing
ext_width	extrusion chamber width	8.625	in	from autocad drawing
ext_depth	extrusion chamber depth	15.0	in	from autocad drawing
load_height	compaction chamber height	6.0	in	from autocad drawing
load_width	compaction chamber width	18.0	in	from autocad drawing
load_depth	compaction chamber depth	8.5	in	from autocad drawing
thruput	desired throughput of machine	500.0	lb/hr	design variable
pre_ext_height	pre-loading chamber height	6.0	in	from autocad drawing
pre_ext_width	pre-loading chamber width	2.5	in	from autocad drawing
pre_ext_depth	pre-loading chamber depth	8.5	in	from autocad drawing
INTERMEDIATE CALCULATIONS				
area_cyl_bore	bore area of cylinder	2.55	sq in	force_cyl/press
dia_cyl	cylinder bore diameter	1.80	in	SQRT(area_cyl_bore*4/PI())
ext_vol	volume of loading chamber	210	in^3	ext_height*ext_width*ext_depth
wt_ext	wieght of compacted plastic in loading chamber	2.10	lb	ext_vol*final_density
load_vol	volume of loading chamber	918	in^3	load_height*load_width*load_depth
load_weight	wieght of a single charge of plastic in loading chamber	0.918	lb	load_vol*initial_density
loads_per_ext	number of loads of plastic to reach required density in extrusion chamber	2.29	none	wt_ext/load_weight
loads	number of loads rounded up	3	none	ROUNDUP(loads_per_ext,0)
cycles_ext	number of times extrusion chamber must be filled per minute to meet goal	4	cycles/minute	(thruput/wt_ext)/60
cycles_comp	number of times compaction chamber must be filled per minute to meet goal	12	cycles/minute	cycles_ext*loads
COMPACTION CYLINDER SIZE SELECTION BASED ON INTERMEDIATE CALCULATIONS				
bore_dia	selected cylinder bore diameter	2.0	in	select this based on rounding up from dia_cyl
rod_dia	selected cylinder rod diameter	1.00	in	select this from catalogue
bore_area	cylinder bore area	3.14	in^2	PI()*bore_dia^2/4
annulus_area	cylinder annulus area	2.36	in^2	bore_area-PI()*rod_dia^2/4
oil_vol_per_cycle_comp	volume of oil required to cycle compaction cylinder	0.50	gal/cycle	(bore_area*comp_stroke+annulus_area*comp_stroke)/231
flowrate_comp	required flowrate to operate at desired compaction rate	5.9	gpm	oil_vol_per_cycle*cycles_comp
EXTRUSION CYLINDER SIZE SELECTION BASED ON INTERMEDIATE CALCULATIONS				
bore_dia	selected cylinder bore diameter	2.0	in	same as compacting cylinder
rod_dia	selected cylinder rod diameter	1.00	in	select this from catalogue
bore_area	cylinder bore area	3.14	in^2	PI()*bore_dia^2/4
annulus_area	cylinder annulus area	2.36	in^2	bore_area-PI()*rod_dia^2/4
oil_vol_per_cycle_ext	volume of oil required to cycle extrusion cylinder	0.36	gal/cycle	(bore_area*ext_stroke+annulus_area*ext_stroke)/231
flowrate_ext	required flowrate to operate at desired compaction rate	1.4	gpm	oil_vol_per_cycle_ext*cycles_ext
POWER REQUIREMENT OF CYLINDERS				
P_comp	Power requirement of the compacting cylinder at given throughput	10.40	hp	press*flowrate_comp/1714
P_ext	Power requirement of the extrusion cylinder at given throughput	2.5	hp	press*flowrate_ext/1714
P_comp_SI	Power requirement of the compacting cylinder at given throughput	7.76	kW	P_comp*746/1000
P_ext_SI	Power requirement of the extrusion cylinder at given throughput	1.85	kW	P_ext*746/1000

These calculations estimated power consumption by the compaction and extrusion cylinders. It was used to initially size the engine generator and hydraulic power unit

Appendix E - Cutting Cylinder Calculations

Cutting Cylinder(s) Calculations

INPUTS				
d_plastofuel	density of plastofuel	57	lb/ft^3	determined experimentally
dia_plastofuel	required diameter of plastofuel	1.5	in	assumed
time	time to create plastofuel	1.0	hr	assumed
w_plastofuel	weight of plastofuel	500	lb	assumed
n_die	number of plastofuel dies	4	none	assumed
l_nugget	desired nugget length	2.0	in	assumed
	Cutting Cylinder Assumptions			
d_cyl	cylinder bore	1.5	in	assumed
r_cyl	cylinder rod	0.75	in	assumed
press	hydraulic presure	3000	psi	assumed
s_cyl	cylinder stroke	2.5	in	assumed
INTERMEDIATE CALCULATIONS				
v_plastofuel	volume of plastofuel to achieve weight goal	15079	in^3	((1/d_plastofuel)*w_plastofuel)*12^3
n_cyl	number of cutting cylinders	4	none	n_die
f_cyl	force of cutting cylinder	5301	lbs	press*((PI()*d_cyl^2)/4)
v_cyl_ext	volume of cap end of cylinder	4	in^3	((PI()*d_cyl^2)/4)*s_cyl
v_cyl_ret	volume of rod end of cylinder	3	in^3	(((PI()*d_cyl^2)/4)-((PI()*r_cyl^2)/4))*s_cyl
v_tot	total volume of hydraulic fluid required for one cycle	0.033	gal	(v_cyl_ext+v_cyl_ret)/231
OUTPUTS				
l_plastofuel	length of single plastofuel "sausage" required to achieve goal	8533	in	(v_plastofuel/((PI()*dia_plastofuel^2)/4))
r_plastofuel	rate of plastic extrusion per die to achieve goal	0.59	in/sec	((v_plastofuel/((PI()*dia_plastofuel^2)/4))/(time*3600))/n_die
cuts	number of cuts per die per minute to make nuggets	18	none	(((l_plastofuel/l_nugget)/n_die))/(time*60)
cycles	number of cylinder cycles	18	cyc/min	cuts
hp_cut	hydraulic horsepower required per die to cut plastofuel	1.04	hp	cycles*v_tot*press/1714
hp_cut_total	total horsepower required for all dies	4.17	hp	hp_cut*n_die
kw_cut_total	total kW required for all dies	3.11	kW	hp_cut_total*0.746

This calculation estimated power consumption by the cutting cylinders. It was used to initially size the engine generator and hydraulic power unit

Appendix F – Estimated Heater Strip Power Requirement

Melting Calculations				
INPUTS				
thruput	desired throughput of machine	227.0	kg/hr	design variable
density_plast	density of plastofuel nugget	728.0	kg/m^3	determined experimentally (see MJL notebook)
per_melt	depth of melted plastic around nugget perimeter	0.002	m	assumed
face_melt	depth of melted plastic on each nugget face	0.002	m	assumed
outer_dia	diameter of plastofuel nugget	0.0381	m	assumed
length	length of plastofuel nugget	0.0508	m	assumed
T_initial	initial plastic temperature	21	C	assumed
T_final	final plastic temperature	135	C	assumed
dies	number of dies	4		assumed
Material Properties(Worst Case Values from PS, PP, and PE)				
density_LDPE	density of low density polyethylene	910	kg/m^3	found in literature review
SH_LDPE	specific heat of low density polyethylene	2300	J/K*kg	found in literature review
INTERMEDIATE CALCULATIONS				
area_face	area of face of plastofuel	0.0011	m^2	PI()*outer_dia^2/4
l_plastofuel	length of single plastofuel nugget per die to achieve goal per hour	68	m	(thruput/(area_face*density_plast))/dies
Melting the Entire Nugget Volume				
volume_tot	total volume of Plastofuel created	0.312	m^3	area_face*l_plastofuel*dies
m_dot_tot	total mass flow of Plastofuel created	0.063	kg/s	volume_tot*density_plast/3600
Melting the Nugget Perimeter				
inner_dia	diameter of unmelted plastic (inside nugget)	0.0341	m	outer_dia-2*per_melt
annulus_melt	area of melted annulus around perimeter	0.00023	m^2	PI()*((outer_dia^2/4-inner_dia^2/4))
vol_per_melt	total volume of melted plastic around perimeter per die per hour	0.016	m^3	annulus_melt*l_plastofuel
m_dot_per	mass flow of plastic per die for melting perimeter	0.004	kg/s	vol_per_melt*density_LDPE/3600
Melting the Nugget Faces				
cuts	number of cuts that must be made per die during an hour	336	none	l_plastofuel/length
faces	number of nugget faces that must be melted per die per hour	673	none	cuts*2
vol_cut	volume of plastic that is melted per face	2.28E-06	m^3	area_face*face_melt
vol_face_melt	total volume of plastic melted per die per hour for facing	0.002	m^3	vol_cut*faces
m_dot_face	mass flow of plastic per die for melting faces	0.0004	kg/s	vol_tot*density_LDPE/3600
OUTPUT				
Pkw_per	power requirement per die to bring nugget perimeters to final temperatu	1.03	kW	(m_dot_per*SH_LDPE*(T_final-T_initial))/1000
Pkw_face	power requirement per die to bring nugget faces to final temperature	0.1	kW	(m_dot_face*SH_LDPE*(T_final-T_initial))/1000
Pkw_tot	power required of all dies to bring perimeter and face to final temperatu	4.5	kW	dies*(Pkw_per+Pkw_face)
Php_tot	power required of all dies to bring perimeter and face to final temperatu	6.1	hp	Pkw_tot*1.34
Pkw_full_melt	power required if Plastofuel were completely melted	16.5	kW	(m_dot_tot*SH_LDPE*(T_final-T_initial))/1000
Php_full_melt	power required if Plastofuel were completely melted	22.2	hp	Pkw_full_melt*1.34

This calculation estimated power consumption by the heating strips. It was used to initially size the engine generator.

Appendix G – Melt Depth Calculations

Stefan-Neumann Problem - HDPE					Spreadsheet Directions:
MATSE 596	Matt Lawrence				1. Select "Enable Macros" when opening this spreadsheet.
INPUTS					2. Enter in liquid, solid, and heated die constants in the "Input" section.
	Liquid Properties				
rho_l	density	855	kg/m^3	given	
k_l	thermal conductivity	0.26	W/m^{o}K	given	3. Press "Ctrl+A" to solve for the K constant in the "Output" section. A goalseek macro enables this function.
alpha_l	themal diffusivity	1.36487E-07	m^2/s	given	
c_l	heat capacity	2228	J/kg^{o}K	given	
	Solid Properties				The depth of melt for a number of die throughput rates will be automatically generated in cells B7-B19 along in the "Chart Data" worksheet.
rho_s	density	950	kg/m^3	given	
k_s	thermal conductivity	0.4	W/m^{o}K	given	
alpha_s	thermal diffusivity	1.87135E-07	m^2/s	given	
c_s	heat capacity	2250	J/kg^{o}K	given	4. Copy and paste melt depths using the "Paste Special - Values" option into the table in the "Chart Data" worksheet.
delta_h	heat of fusion	-280,000	J/kg	assumed	
beta	liquid to solid ratio	1	none	assumed	
Tone	wall temperature	418	^{o}K	assumed	
To	intital core temperature	298	^{o}K	assumed	5. The Melt Depth vs. Throughput worksheet will change as new vlaues are pasted into the table.
Tm	melting temperature	408	^{o}K	assumed	
INTERMEDIATE CALCULATIONS					
Term1_num	numerator of first term on LHS in Stefan_Neumann equation	-2.6	?	((Tm-Tone)*k_l*EXP(-(K^2*beta^2)/(4*alpha_l)))	
Term1_den	demnomerator of first term on LHS in Stefan_Neumann equation	0.0000398	?	(SQRT(PI()*alpha_l))*ERF(K*beta/(2*SQRT(alpha_l)))	
Term2_num	numerator of second term on LHS of Stefan-Neumann equation	-43.9	?	((To-Tm)*k_s*EXP(-(K^2)/(4*alpha_s)))	
Term2_den	denomerator of second term on LHS of Stefan-Neumann equation	0.0007270	?	(SQRT(PI()*alpha_s))*ERFC(K/(2*SQRT(alpha_s)))	
LHS	left hand side of Stefan-Neumann equation	-4766.6267	J/kg-m^3	(Term1_num/Term1_den)-(Term2_num/Term2_den)	
RHS	right hand side of Stefan-Neumann equation	-4766.6267	J/kg-m^3	delta_h*rho_l*K*beta/2	
DIFF	difference of left hand side and right hand side	0.000	J/kg-m^3	LHS-RHS	
OUTPUTS					
K	unknown constant (used goal-seek to set DIFF=0 by changing K)	3.9821E-05	none	guess	

This is a spreadsheet solution to the Stefan-Neumann equation used to solve for the K term and predict melt depths of pure plastic types.

Melt Depth Calculations (continued)

Beta = 1 for this problem so Xs = Xl

K= 7.22E-05
Twall (°C)= 155

t (sec)	X (mm)
120	0.79
150	0.88
180	0.97
210	1.05
240	1.12
270	1.19
300	1.25
330	1.31
360	1.37
390	1.43
420	1.48

K=	2.11E-04	1.76E-04	1.25E-04	1.00E-04	7.22E-05
Twall (°C)=	220	200	175	165	155
thruput (kg/hr)			Melt Depth (mm)		
43	2.3	1.9	1.4	1.1	0.8
35	2.6	2.2	1.5	1.2	0.9
29	2.8	2.4	1.7	1.3	1.0
25	3.1	2.6	1.8	1.4	1.0
22	3.3	2.7	1.9	1.5	1.1
19	3.5	2.9	2.0	1.6	1.2
17	3.7	3.1	2.2	1.7	1.3
16	3.8	3.2	2.3	1.8	1.3
14	4.0	3.3	2.4	1.9	1.4
13	4.2	3.5	2.5	2.0	1.4
12	4.3	3.6	2.6	2.0	1.5

Appendix H – IQAN Control Algorithms

Control Algorithm 1

F:\plastofuel IQAN - Final\Plastofuel_Jan11.idt
No application description, version 0.00

Page 1 (7)
5/17/2007 3:32:44 PM

Channels

Voltage in, XS-A1												
A: Hydraulic Pressure [psi]	Error:	16.00	Min:	1000	Sc. min:	16.00	Adjustable:	No	Al. low:	No
Hydraulic Pressure [psi]	Sim:	No	Max:	5000	Sc. max:	5000.00	Filter:	0	Al. high:	No
B: Hydraulic Flow [gpm]	Error:	0.00	Min:	0	Sc. min:	0.00	Adjustable:	No	Al. low:	No
VIN-D:XS-A0 [gpm]	Sim:	No	Max:	5000	Sc. max:	20.00	Filter:	0	Al. high:	No
C: Comp. Cyl. Location [in]	Error:	0.00	Min:	92	Sc. min:	0.00	Adjustable:	No	Al. low:	No
Comp. Cyl. Location [in]	Sim:	No	Max:	3963	Sc. max:	21.00	Filter:	0	Al. high:	No
D: Ext. Cyl. Location [in]	Error:	0.00	Min:	34	Sc. min:	0.00	Adjustable:	No	Al. low:	No
Ext. Cyl. Location [in]	Sim:	No	Max:	5000	Sc. max:	15.00	Filter:	0	Al. high:	No

Digital in, XS-A1		
A: Main Switch	Sim:	No
On/Off Main Switch		
B: Auto/Man Switch	Sim:	No
Automatic Switch		
C: Auto Start/Stop Switch	Sim:	No
Auto Start/Stop Switch		
D: Comp. Cyl. Ext. Switch	Sim:	No
Comp. Cyl. Extend		
E: Comp. Cyl. Ret. Switch	Sim:	No
Comp. Cyl. Retract		
F: Ext. Cyl. Ext. Switch	Sim:	No
Ext. Cyl. Extend		
G: Ext. Cyl. Ret. Switch	Sim:	No
Ext. Cyl. Retract		
H: Cut Cyl. 1 Ext. Switch	Sim:	No
Cut Cyl. 1 Extend		
I: Cut Cyl. 2 Ext. Switch	Sim:	No
Cut Cyl. 2 Extend		
J: Cut Cyl. 3 Ext. Switch	Sim:	No
Cut Cyl. 3 Extend		
K: Cut Cyl. 4 Ext. Switch	Sim:	No
Cut Cyl. 4 Extend		
L: Nugget Length Sensor 1	Sim:	No
Nugget Length Sensor 1		
M: Nugget Length Sensor 2	Sim:	No
Nugget Length Sensor 2		
N: Nugget Length Sensor 3	Sim:	No
Nugget Length Sensor 3		
O: Nugget Length Sensor 4	Sim:	No
Nugget Length Sensor 4		
P: Temperature Alarm	Sim:	No
Temperature Alarm		

Function parameter, MDM							
1: Compaction Threshold [psi]	Min:	500	Value:	1000	Step small:	10	
Compaction Threshold [psi]	Max:	3000	Adjustable:	Yes	Step large:	100	
2: Temp Threshold [deg C]	Min:	100	Value:	200	Step small:	1	
Temp Threshold [C]	Max:	350	Adjustable:	Yes	Step large:	10	
3: Comp. Limit Switch Ext. [in]	Min:	18.00	Value:	20.50	Step small:	0.25	
Comp. Limit Switch Ext. [in]	Max:	22.00	Adjustable:	Yes	Step large:	1.00	
4: Comp. Limit Switch Ret. [in]	Min:	0.00	Value:	0.50	Step small:	0.25	
Comp. Limit Switch Ret. [in]	Max:	2.00	Adjustable:	Yes	Step large:	1.00	
5: Ext. Limit Switch Ext. [in]	Min:	13.00	Value:	14.50	Step small:	0.25	
Ext. Limit Switch Ext. [in]	Max:	15.00	Adjustable:	Yes	Step large:	1.00	
6: Ext. Limit Switch Ret. [in]	Min:	0.00	Value:	0.50	Step small:	0.25	
Ext. Limit Switch Ret. [in]	Max:	2.50	Adjustable:	Yes	Step large:	1.00	

Math, analog, MDM	
A: Hydraulic Power [hp]	A: (Hydraulic Pressure [psi]) * (Hydraulic Flow [gpm])
Hydraulic Power [hp]	B: A / 1714.00

Channels

Internal digital, MDM			
A: Auto compaction extend	Delay on: 0	Toggle: No	
auto compaction extend	Delay off: 0		
Activating objects (and)	(Auto/Man Switch) = High (Comp. Cyl Toggle) = True (Auto Start/Stop Switch) = High		
Blocking objects (or)	(Comp. Cyl. Retraction Sol) = High (Ext. Cyl. Extension Sol) = High (Ext Cyl. Retraction Sol.) = High (Ext. Cyl Toggle) = False (Temperature Alarm) = High		
B: Auto compaction retract	Delay on: 0	Toggle: No	
auto compaction retract	Delay off: 0		
Activating objects (and)	(Comp. Cyl Toggle) = False (Auto/Man Switch) = High		
Blocking objects (or)	(Comp. Cyl. Extension Sol) = High (Ext. Cyl. Extension Sol) = High (Ext Cyl. Retraction Sol.) = High (Temperature Alarm) = High		
C: Auto extrusion extend	Delay on: 0	Toggle: No	
Auto extrusion extend	Delay off: 0		
Activating objects (and)	(Hydraulic Pressure) > (Compaction Threshold) (Ext. Cyl Toggle) = True (Auto/Man Switch) = High		
Blocking objects (or)	(Ext Cyl. Retraction Sol.) = High (Temperature Alarm) = High		
D: Auto extrusion retract	Delay on: 0	Toggle: No	
Auto extrusion retract	Delay off: 0		
Activating objects (and)	(Ext. Cyl Toggle) = False (Auto/Man Switch) = High		
Blocking objects (or)	(Ext. Cyl. Extension Sol) = High (Temperature Alarm) = High		
E: Man compaction extend	Delay on: 0	Toggle: No	
Man compaction extend	Delay off: 0		
Activating objects (and)	(Auto/Man Switch) = Low (Comp. Cyl. Ext. Switch) = High		
F: Man compaction retract	Delay on: 0	Toggle: No	
Man compaction retract	Delay off: 0		
Activating objects (and)	(Auto/Man Switch) = Low (Comp. Cyl. Ret. Switch) = High		
G: Man extrusion extend	Delay on: 0	Toggle: No	
Man extrusion extend	Delay off: 0		
Activating objects (and)	(Auto/Man Switch) = Low (Ext. Cyl. Ext. Switch) = High		
H: Man extrusion retract	Delay on: 0	Toggle: No	
Man extrusion retract	Delay off: 0		
Activating objects (and)	(Auto/Man Switch) = Low (Ext. Cyl. Ret. Switch) = High		
I: Auto cutting cyl 1	Delay on: 0	Toggle: No	
Auto cutting cyl 1	Delay off: 0		
Activating objects (and)	(Auto/Man Switch) = High (Auto Start/Stop Switch) = High (Nugget Length Sensor 1) = High		
J: Auto cutting cyl 2	Delay on: 0	Toggle: No	
Auto cutting cyl 2	Delay off: 0		
Activating objects (and)	(Auto/Man Switch) = High (Auto Start/Stop Switch) = High (Nugget Length Sensor 2) = High		
K: Auto cutting cyl 3	Delay on: 0	Toggle: No	
Auto cutting cyl 3	Delay off: 0		
Activating objects (and)	(Auto/Man Switch) = High (Auto Start/Stop Switch) = High (Nugget Length Sensor 3) = High		

Channels

Internal digital, MDM			
L: Auto cutting cyl 4 Auto cutting cyl 4	Delay on: 0 Delay off: 0	Toggle: No	
Activating objects (and)	(Auto/Man Switch) = High (Auto Start/Stop Switch) = High (Nugget Length Sensor 4) = High		
M: Man cutting cyl 1 Man cutting cyl 1	Delay on: 0 Delay off: 0	Toggle: No	
Activating objects (and)	(Auto/Man Switch) = Low (Cut Cyl. 1 Ext. Switch) = High		
N: Man cutting cyl 2 Man cutting cyl 2	Delay on: 0 Delay off: 0	Toggle: No	
Activating objects (and)	(Auto/Man Switch) = Low (Cut Cyl. 2 Ext. Switch) = High		
O: Man cutting cyl 3 Man cutting cyl 3	Delay on: 0 Delay off: 0	Toggle: No	
Activating objects (and)	(Auto/Man Switch) = Low (Cut Cyl. 3 Ext. Switch) = High		
P: Man cutting cyl 4 Man cutting cyl 4	Delay on: 0 Delay off: 0	Toggle: No	
Activating objects (and)	(Auto/Man Switch) = Low (Cut Cyl. 4 Ext. Switch) = High		
Q: Comp. Cyl Toggle Comp. Cyl Toggle	Delay on: 0 Delay off: 0	Toggle: Yes	
Activating objects (or)	(Comp. Cyl. Location) > (Comp. Limit Switch Ext.) (Comp. Cyl. Location) < (Comp. Limit Switch Ret.)		
Blocking objects (or)	(Auto/Man Switch) = Low		
R: Ext. Cyl Toggle Ext. Cyl Toggle	Delay on: 0 Delay off: 0	Toggle: Yes	
Activating objects (or)	(Ext. Cyl. Location) > (Ext. Limit Switch Ext.) (Ext. Cyl. Location) < (Ext. Limit Switch Ret.)		
Blocking objects (or)	(Auto/Man Switch) = Low		

Event counter, MDM		
A: Nugget Counter Nugget Counter		
Increasing objects (or)	(Cutting Cyl 2 Sol.) = High (Cutting Cyl 1 Sol.) = High (Cutting Cyl 3 Sol.) = High (Cutting Cyl 4 Sol.) = High	
Resetting objects (or)	(Counter reset msg) = F1: YES	
B: Lifetime Nugget Counter Lifetime Nugget Counter		
Increasing objects (or)	(Cutting Cyl 2 Sol.) = High (Cutting Cyl 1 Sol.) = High (Cutting Cyl 3 Sol.) = High (Cutting Cyl 4 Sol.) = High	

Hour counter, MDM		
A: Hour Meter [h] Hour Meter [h]	Adjustable: No	
Activating objects (or)	(Auto/Man Switch) = High	

Digital out, XP-A0		
A1: Cutting Cyl 1 Sol. Cutting Cyl 1 Sol.	Delay on: 0 Delay off: 0	
Activating objects (or)	(Auto cutting cyl 1) = True (Man cutting cyl 1) = True	
Blocking objects (or)	(Main Switch) = Low	
B1: Cutting Cyl 2 Sol. Cutting Cyl 2 Sol.	Delay on: 0 Delay off: 0	
Activating objects (or)	(Auto cutting cyl 2) = True (Man cutting cyl 2) = True	
Blocking objects (or)	(Main Switch) = Low	

Channels

Digital out, XP-A0		
C1: Cutting Cyl 3 Sol.	Delay on: 0	
Cutting Cyl 3 Sol.	Delay off: 0	
Activating objects (or)	(Auto cutting cyl 3) = True	
	(Man cutting cyl 3) = True	
Blocking objects (or)	(Main Switch) = Low	
D1: Cutting Cyl 4 Sol.	Delay on: 0	
Cutting Cyl 4 Sol.	Delay off: 0	
Activating objects (or)	(Auto cutting cyl 4) = True	
	(Man cutting cyl 4) = True	
Blocking objects (or)	(Main Switch) = Low	
E1: Heaters Ready Light	Delay on: 0	
Heaters Ready Light	Delay off: 0	
Activating objects (and)	(Main Switch) = High	
	(Temperature Alarm) = Low	

Digital out, XS-A1		
A1: Comp. Cyl. Extension Sol	Delay on: 0	
Compaction Extension Sol	Delay off: 0	
Activating objects (or)	(Man compaction extend) = True	
	(Auto compaction extend) = True	
Blocking objects (or)	(Main Switch) = Low	
B1: Comp. Cyl. Retraction Sol	Delay on: 0	
Compaction Retraction Sol	Delay off: 0	
Activating objects (or)	(Auto compaction retract) = True	
	(Man compaction retract) = True	
Blocking objects (and)	(Main Switch) = Low	
C1: Ext. Cyl. Extension Sol	Delay on: 0	
Extrusion Extension Sol	Delay off: 0	
Activating objects (or)	(Auto extrusion extend) = True	
	(Man extrusion extend) = True	
Blocking objects (or)	(Main Switch) = Low	
D1: Ext Cyl. Retraction Sol.	Delay on: 0	
Copy of Extrusion Extensi	Delay off: 0	
Activating objects (or)	(Auto extrusion retract) = True	
	(Man extrusion retract) = True	
Blocking objects (or)	(Main Switch) = Low	

Conditional message, MDM				
A: Hyd. Press. Disp.	Delay on: 0	Text and channel		
Hyd. Press Disp.	Delay off: 0	Show always	Dual channels	
	Comp. Cylinder			
	Comp. Cyl. Location [in]		Comp. Cyl. Location [in]	
	Ext. Cylinder			
	Ext. Cyl. Location [in]		Ext. Cyl. Location [in]	
Activating objects (or)	True			

Interactive message, MDM		
A: Counter reset msg	Text only	
Counter reset msg		
	Reset Nugget Counter?	
	F1=YES, F2=NO, F3=	F1=, F2=, F3=
Activating objects (or)	True	

IQAN MDM

Serial number: 611260015
Hardware version: 18.00
Software version: 4.06

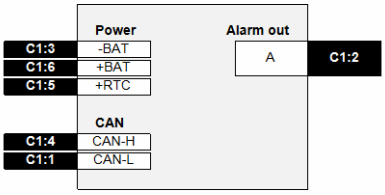

IQAN XP-A0

Serial number: 548230011
Hardware version: 56.00
Software version: 1.68

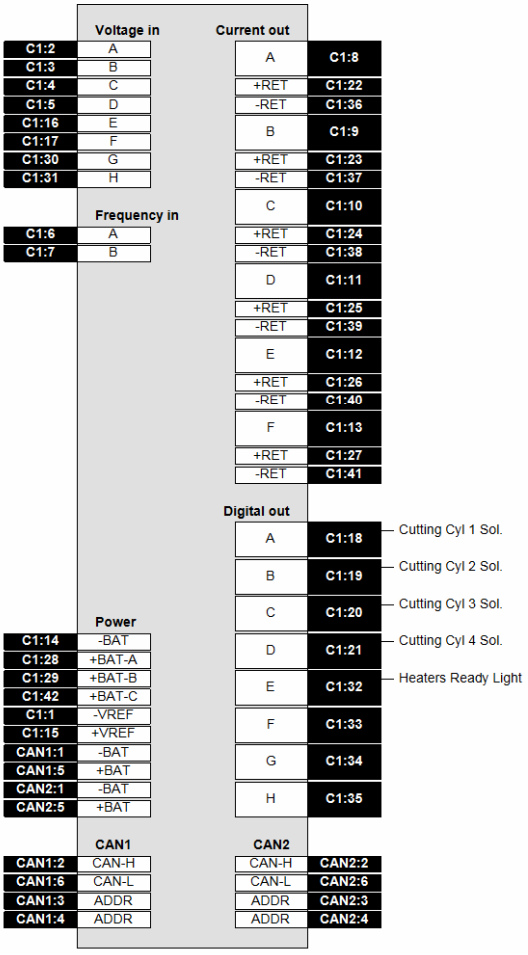

IQAN XS-A1

Serial number: 608230174
Hardware version: 45.00
Software version: 1.43

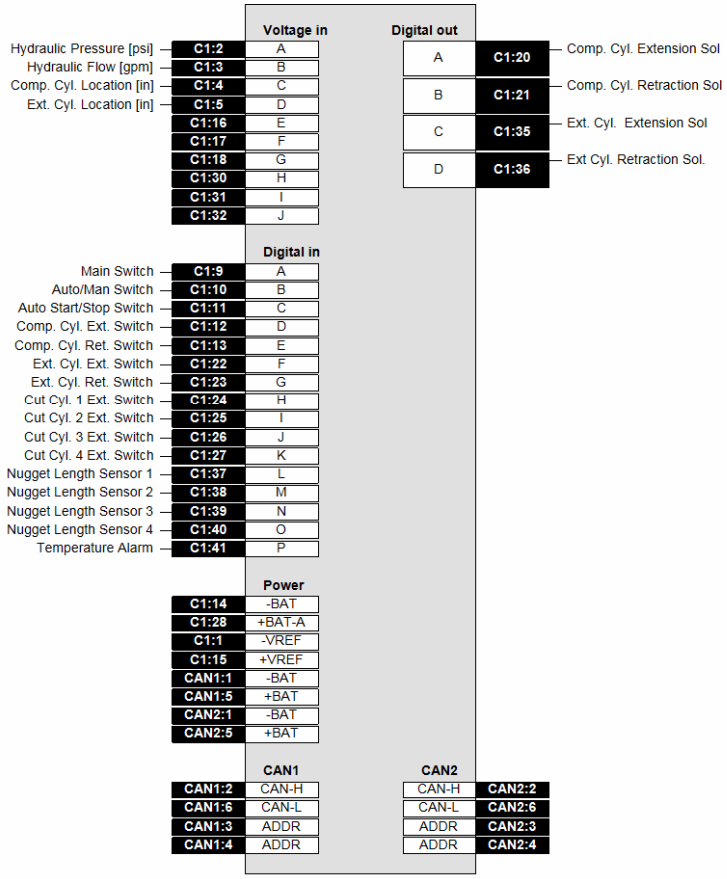

Control Algorithm 2

Channels

Voltage in, XS-A1												
A: Hydraulic Pressure [psi]	Error:	16.00	Min:	1000	Sc. min:	16.00	Adjustable:	No	Al. low:	No
Hydraulic Pressure [psi]	Sim:	No	Max:	5000	Sc. max:	5000.00	Filter:	0	Al. high:	No
B: Hydraulic Flow [gpm]	Error:	0.00	Min:	0	Sc. min:	0.00	Adjustable:	No	Al. low:	No
VIN-D:XS-A0 [gpm]	Sim:	No	Max:	5000	Sc. max:	20.00	Filter:	0	Al. high:	No
C: Comp. Cyl. Location [in]	Error:	0.00	Min:	83	Sc. min:	0.00	Adjustable:	No	Al. low:	No
Comp. Cyl. Location [in]	Sim:	No	Max:	3983	Sc. max:	21.00	Filter:	0	Al. high:	No
D: Ext. Cyl. Location [in]	Error:	0.00	Min:	24	Sc. min:	0.00	Adjustable:	No	Al. low:	No
Ext. Cyl. Location [in]	Sim:	No	Max:	2785	Sc. max:	15.00	Filter:	0	Al. high:	No

Digital in, XS-A1		
A: Main Switch	Sim:	No
On/Off Main Switch		
B: Auto/Man Switch	Sim:	No
Automatic Switch		
C: Auto Start/Stop Switch	Sim:	No
Auto Start/Stop Switch		
D: Comp. Cyl. Ext. Switch	Sim:	No
Comp. Cyl. Extend		
E: Comp. Cyl. Ret. Switch	Sim:	No
Comp. Cyl. Retract		
F: Ext. Cyl. Ext. Switch	Sim:	No
Ext. Cyl. Extend		
G: Ext. Cyl. Ret. Switch	Sim:	No
Ext. Cyl. Retract		
H: Cut Cyl. 1 Ext. Switch	Sim:	No
Cut Cyl. 1 Extend		
I: Cut Cyl. 2 Ext. Switch	Sim:	No
Cut Cyl. 2 Extend		
J: Cut Cyl. 3 Ext. Switch	Sim:	No
Cut Cyl. 3 Extend		
K: Cut Cyl. 4 Ext. Switch	Sim:	No
Cut Cyl. 4 Extend		
L: Nugget Length Sensor 1	Sim:	No
Nugget Length Sensor 1		
M: Nugget Length Sensor 2	Sim:	No
Nugget Length Sensor 2		
N: Nugget Length Sensor 3	Sim:	No
Nugget Length Sensor 3		
O: Nugget Length Sensor 4	Sim:	No
Nugget Length Sensor 4		
P: Temperature Alarm	Sim:	No
Temperature Alarm		

Function parameter, MDM							
1: Compaction Threshold [psi]	Min:	500	Value:	1000	Step small:	10	
Compaction Threshold [psi]	Max:	3000	Adjustable:	Yes	Step large:	100	
2: Temp Threshold [deg C]	Min:	100	Value:	200	Step small:	1	
Temp Threshold [C]	Max:	350	Adjustable:	Yes	Step large:	10	
3: Comp. Limit Switch Ext. [in]	Min:	18.00	Value:	19.50	Step small:	0.10	
Comp. Limit Switch Ext. [in]	Max:	22.00	Adjustable:	Yes	Step large:	1.00	
4: Comp. Limit Switch Ret. [in]	Min:	0.00	Value:	1.00	Step small:	0.10	
Comp. Limit Switch Ret. [in]	Max:	2.00	Adjustable:	Yes	Step large:	1.00	
5: Ext. Limit Switch Ext. [in]	Min:	13.00	Value:	14.80	Step small:	0.10	
Ext. Limit Switch Ext. [in]	Max:	15.00	Adjustable:	Yes	Step large:	1.00	
6: Ext. Limit Switch Ret. [in]	Min:	0.00	Value:	0.15	Step small:	0.10	
Ext. Limit Switch Ret. [in]	Max:	2.50	Adjustable:	Yes	Step large:	0.10	

Math, analog, MDM	
A: Hydraulic Power [hp]	A: (Hydraulic Pressure [psi]) * (Hydraulic Flow [gpm])
Hydraulic Power [hp]	B: A / 1714.00

Channels

Internal digital, MDM			
A: Auto compaction extend auto compaction extend	Delay on: 0 Delay off: 0	Toggle: No	
Activating objects (and)	(Auto/Man Switch) = High (Auto Start/Stop Switch) = High (Comp. Cyl. Location) < (Comp. Limit Switch Ext.)		
Blocking objects (or)	(Comp. Cyl. Retraction Sol) = High (Heaters Ready Light) = Low		
B: Auto compaction retract auto compaction retract	Delay on: 0 Delay off: 0	Toggle: No	
Activating objects (and)	(Auto/Man Switch) = High (Auto Start/Stop Switch) = High (Comp. Cyl. Location) > (Comp. Limit Switch Ret.)		
Blocking objects (or)	(Comp. Cyl. Extension Sol) = High (Ext. Cyl. Extension Sol) = High (Heaters Ready Light) = Low		
C: Auto extrusion extend Auto extrusion extend	Delay on: 0 Delay off: 0	Toggle: No	
Activating objects (and)	(Auto/Man Switch) = High (Auto Start/Stop Switch) = High (Ext. Cyl. Location) < (Ext. Limit Switch Ext.) (Comp. Cyl. Location) > (Comp. Limit Switch Ext.)		
Blocking objects (or)	(Ext Cyl. Retraction Sol.) = High (Heaters Ready Light) = Low		
D: Auto extrusion retract Auto extrusion retract	Delay on: 0 Delay off: 0	Toggle: No	
Activating objects (and)	(Auto/Man Switch) = High (Ext. Cyl. Location) > (Ext. Limit Switch Ret.) (Auto Start/Stop Switch) = High		
Blocking objects (or)	(Ext. Cyl. Extension Sol) = High (Heaters Ready Light) = Low		
E: Man compaction extend Man compaction extend	Delay on: 0 Delay off: 0	Toggle: No	
Activating objects (and)	(Auto/Man Switch) = Low (Comp. Cyl. Ext. Switch) = High		
F: Man compaction retract Man compaction retract	Delay on: 0 Delay off: 0	Toggle: No	
Activating objects (and)	(Auto/Man Switch) = Low (Comp. Cyl. Ret. Switch) = High		
G: Man extrusion extend Man extrusion extend	Delay on: 0 Delay off: 0	Toggle: No	
Activating objects (and)	(Auto/Man Switch) = Low (Ext. Cyl. Ext. Switch) = High		
H: Man extrusion retract Man extrusion retract	Delay on: 0 Delay off: 0	Toggle: No	
Activating objects (and)	(Auto/Man Switch) = Low (Ext. Cyl. Ret. Switch) = High		
I: Auto cutting cyl 1 Auto cutting cyl 1	Delay on: 0 Delay off: 0	Toggle: No	
Activating objects (and)	(Auto/Man Switch) = High (Auto Start/Stop Switch) = High (Nugget Length Sensor 1) = High		
J: Auto cutting cyl 2 Auto cutting cyl 2	Delay on: 0 Delay off: 0	Toggle: No	
Activating objects (and)	(Auto/Man Switch) = High (Auto Start/Stop Switch) = High (Nugget Length Sensor 2) = High		
K: Auto cutting cyl 3 Auto cutting cyl 3	Delay on: 0 Delay off: 0	Toggle: No	
Activating objects (and)	(Auto/Man Switch) = High (Auto Start/Stop Switch) = High (Nugget Length Sensor 3) = High		

Channels

Internal digital, MDM			
L: Auto cutting cyl 4 Auto cutting cyl 4	Delay on: 0 Delay off: 0	Toggle: No	
Activating objects (and)	(Auto/Man Switch) = High (Auto Start/Stop Switch) = High (Nugget Length Sensor 4) = High		
M: Man cutting cyl 1 Man cutting cyl 1	Delay on: 0 Delay off: 0	Toggle: No	
Activating objects (and)	(Cut Cyl. 1 Ext. Switch) = High		
N: Man cutting cyl 2 Man cutting cyl 2	Delay on: 0 Delay off: 0	Toggle: No	
Activating objects (and)	(Cut Cyl. 2 Ext. Switch) = High		
O: Man cutting cyl 3 Man cutting cyl 3	Delay on: 0 Delay off: 0	Toggle: No	
Activating objects (and)	(Cut Cyl. 3 Ext. Switch) = High		
P: Man cutting cyl 4 Man cutting cyl 4	Delay on: 0 Delay off: 0	Toggle: No	
Activating objects (and)	(Cut Cyl. 4 Ext. Switch) = High		
Q: Comp. Cyl Toggle Comp. Cyl Toggle	Delay on: 0 Delay off: 0	Toggle: Yes	
Activating objects (or)	(Comp. Cyl. Location) > (Comp. Limit Switch Ext.) (Comp. Cyl. Location) < (Comp. Limit Switch Ret.)		
Blocking objects (or)	(Auto/Man Switch) = Low		
R: Ext. Cyl Toggle Ext. Cyl Toggle	Delay on: 0 Delay off: 0	Toggle: Yes	
Activating objects (or)	(Ext. Cyl. Location) > (Ext. Limit Switch Ext.) (Ext. Cyl. Location) < (Ext. Limit Switch Ret.)		
Blocking objects (or)	(Auto/Man Switch) = Low		

Event counter, MDM		
B: Lifetime Nugget Counter Lifetime Nugget Counter		
Increasing objects (or)	(Cutting Cyl 2 Sol.) = High (Cutting Cyl 1 Sol.) = High (Cutting Cyl 3 Sol.) = High (Cutting Cyl 4 Sol.) = High	

Digital out, XP-A0		
A1: Cutting Cyl 1 Sol. Cutting Cyl 1 Sol.	Delay on: 0 Delay off: 0	
Activating objects (or)	(Auto cutting cyl 1) = True (Man cutting cyl 1) = True	
Blocking objects (or)	(Main Switch) = Low	
B1: Cutting Cyl 2 Sol. Cutting Cyl 2 Sol.	Delay on: 0 Delay off: 0	
Activating objects (or)	(Auto cutting cyl 2) = True (Man cutting cyl 2) = True	
Blocking objects (or)	(Main Switch) = Low	
C1: Cutting Cyl 3 Sol. Cutting Cyl 3 Sol.	Delay on: 0 Delay off: 0	
Activating objects (or)	(Auto cutting cyl 3) = True (Man cutting cyl 3) = True	
Blocking objects (or)	(Main Switch) = Low	
D1: Cutting Cyl 4 Sol. Cutting Cyl 4 Sol.	Delay on: 0 Delay off: 0	
Activating objects (or)	(Auto cutting cyl 4) = True (Man cutting cyl 4) = True	
Blocking objects (or)	(Main Switch) = Low	
E1: Heaters Ready Light Heaters Ready Light	Delay on: 0 Delay off: 0	
Activating objects (and)	(Main Switch) = High (Temperature Alarm) = Low	

Channels

Digital out, XS-A1		
A1: Comp. Cyl. Extension Sol Compaction Extension Sol	Delay on: 0 Delay off: 0	
Activating objects (or)	(Man compaction extend) = True (Auto compaction extend) = True	
Blocking objects (or)	(Main Switch) = Low	
B1: Comp. Cyl. Retraction Sol Compaction Retraction Sol	Delay on: 0 Delay off: 0	
Activating objects (or)	(Man compaction retract) = True (Auto compaction retract) = True	
Blocking objects (or)	(Main Switch) = Low	
C1: Ext. Cyl. Extension Sol Extrusion Extension Sol	Delay on: 0 Delay off: 0	
Activating objects (or)	(Man extrusion extend) = True (Auto extrusion extend) = True	
Blocking objects (or)	(Main Switch) = Low	
D1: Ext Cyl. Retraction Sol. Copy of Extrusion Extensi	Delay on: 0 Delay off: 0	
Activating objects (or)	(Man extrusion retract) = True (Auto extrusion retract) = True	
Blocking objects (or)	(Main Switch) = Low	

Conditional message, MDM				
A: Hyd. Press. Disp. Hyd. Press Disp.	Delay on: 0 Delay off: 0	Text and channel Show always	Dual channels	
	Comp. Cylinder Comp. Cyl. Location [in]		Comp. Cyl. Location [in]	
	Ext. Cylinder Ext. Cyl. Location [in]		Ext. Cyl. Location [in]	
Activating objects (or)	True			

Interactive message, MDM		
A: Counter reset msg Counter reset msg	Text only	
	Reset Nugget Counter? F1=YES, F2=NO, F3=	F1=, F2=, F3=

IQAN MDM

Serial number: 611260015
Hardware version: 18.00
Software version: 4.06

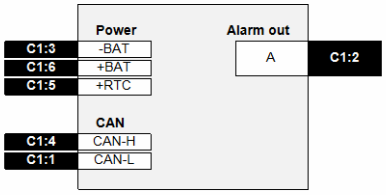

IQAN XP-A0

Serial number: 548230011
Hardware version: 56.00
Software version: 1.68

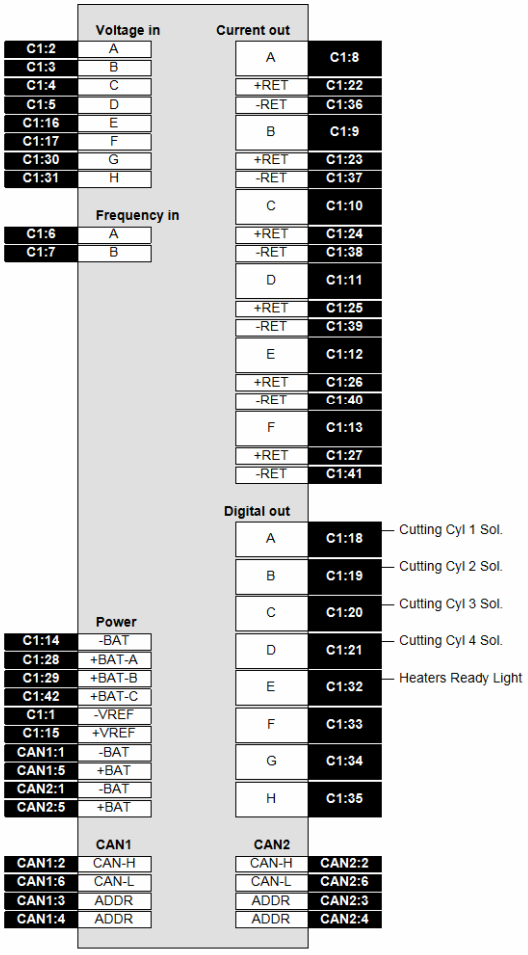

IQAN XS-A1

Serial number: 608230174
Hardware version: 45.00
Software version: 1.43

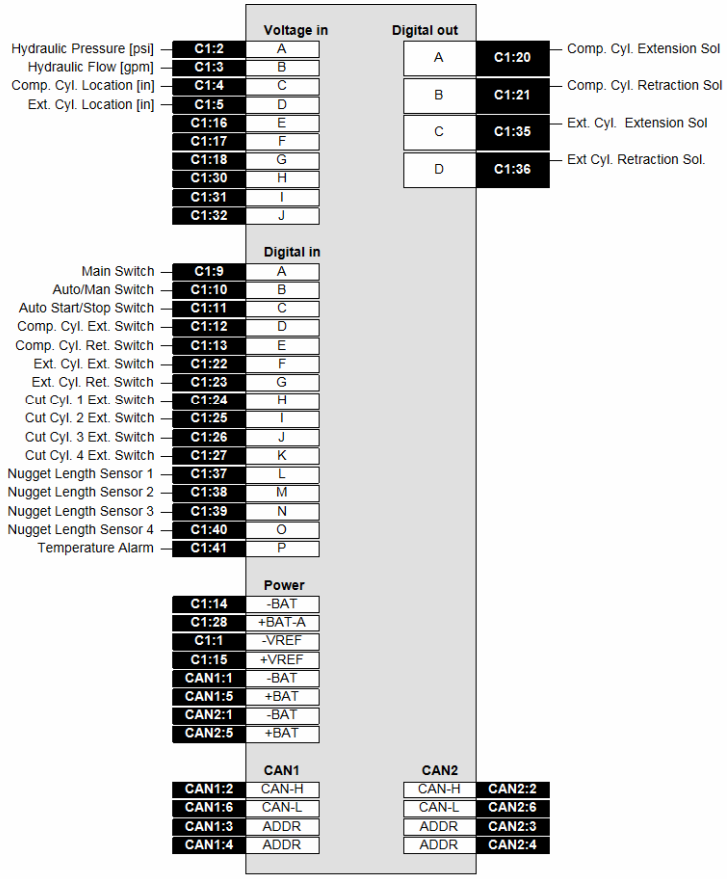

Control Algorithm 3

Channels

Voltage in, XS-A1												
A: Hydraulic Pressure [psi]	Error:	16.00	Min:	1000	Sc. min:	16.00	Adjustable:	No	Al. low:	No
Hydraulic Pressure [psi]	Sim:	No	Max:	5000	Sc. max:	5000.00	Filter:	0	Al. high:	No
B: Hydraulic Flow [gpm]	Error:	0.00	Min:	0	Sc. min:	0.00	Adjustable:	No	Al. low:	No
VIN-D:XS-A0 [gpm]	Sim:	No	Max:	5000	Sc. max:	20.00	Filter:	0	Al. high:	No
C: Comp. Cyl. Location [in]	Error:	0.00	Min:	29	Sc. min:	0.00	Adjustable:	No	Al. low:	No
Comp. Cyl. Location [in]	Sim:	No	Max:	3910	Sc. max:	21.00	Filter:	0	Al. high:	No
D: Ext. Cyl. Location [in]	Error:	0.00	Min:	24	Sc. min:	0.00	Adjustable:	No	Al. low:	No
Ext. Cyl. Location [in]	Sim:	No	Max:	2785	Sc. max:	15.00	Filter:	0	Al. high:	No

Digital in, XS-A1		
A: Main Switch	Sim:	No
On/Off Main Switch		
B: Auto/Man Switch	Sim:	No
Automatic Switch		
C: Auto Start/Stop Switch	Sim:	No
Auto Start/Stop Switch		
D: Comp. Cyl. Ext. Switch	Sim:	No
Comp. Cyl. Extend		
E: Comp. Cyl. Ret. Switch	Sim:	No
Comp. Cyl. Retract		
F: Ext. Cyl. Ext. Switch	Sim:	No
Ext. Cyl. Extend		
G: Ext. Cyl. Ret. Switch	Sim:	No
Ext. Cyl. Retract		
H: Cut Cyl. 1 Ext. Switch	Sim:	No
Cut Cyl. 1 Extend		
I: Cut Cyl. 2 Ext. Switch	Sim:	No
Cut Cyl. 2 Extend		
J: Cut Cyl. 3 Ext. Switch	Sim:	No
Cut Cyl. 3 Extend		
K: Cut Cyl. 4 Ext. Switch	Sim:	No
Cut Cyl. 4 Extend		
L: Nugget Length Sensor 1	Sim:	No
Nugget Length Sensor 1		
M: Nugget Length Sensor 2	Sim:	No
Nugget Length Sensor 2		
N: Nugget Length Sensor 3	Sim:	No
Nugget Length Sensor 3		
O: Nugget Length Sensor 4	Sim:	No
Nugget Length Sensor 4		
P: Temperature Alarm	Sim:	No
Temperature Alarm		

Function parameter, MDM							
1: Compaction Threshold [psi]	Min:	500	Value:	1000	Step small:	10	
Compaction Threshold [psi]	Max:	3000	Adjustable:	Yes	Step large:	100	
2: Temp Threshold [deg C]	Min:	100	Value:	200	Step small:	1	
Temp Threshold [C]	Max:	350	Adjustable:	Yes	Step large:	10	
3: Comp. Limit Switch Ext. [in]	Min:	18.00	Value:	19.50	Step small:	0.10	
Comp. Limit Switch Ext. [in]	Max:	22.00	Adjustable:	Yes	Step large:	1.00	
4: Comp. Limit Switch Ret. [in]	Min:	0.00	Value:	1.00	Step small:	0.10	
Comp. Limit Switch Ret. [in]	Max:	2.00	Adjustable:	Yes	Step large:	1.00	
5: Ext. Limit Switch Ext. [in]	Min:	13.00	Value:	14.80	Step small:	0.10	
Ext. Limit Switch Ext. [in]	Max:	15.00	Adjustable:	Yes	Step large:	1.00	
6: Ext. Limit Switch Ret. [in]	Min:	0.00	Value:	0.15	Step small:	0.10	
Ext. Limit Switch Ret. [in]	Max:	2.50	Adjustable:	Yes	Step large:	0.10	

Math, analog, MDM	
A: Hydraulic Power [hp]	A: (Hydraulic Pressure [psi]) * (Hydraulic Flow [gpm])
Hydraulic Power [hp]	B: A / 1714.00

Channels

Internal digital, MDM			
A: Auto compaction extend	Delay on: 0	Toggle: No	
auto compaction extend	Delay off: 0		
Blocking objects (or)	(Comp. Cyl. Retraction Sol) = High		
	(Heaters Ready Light) = Low		
B: Auto compaction retract	Delay on: 0	Toggle: No	
auto compaction retract	Delay off: 0		
Activating objects (and)	(Auto/Man Switch) = High		
	(Auto Start/Stop Switch) = High		
	(Comp. Cyl. Location) > (Comp. Limit Switch Ret.)		
Blocking objects (or)	(Comp. Cyl. Extension Sol) = High		
	(Ext. Cyl. Extension Sol) = High		
	(Heaters Ready Light) = Low		
C: Auto extrusion extend	Delay on: 0	Toggle: No	
Auto extrusion extend	Delay off: 0		
Activating objects (and)	(Auto/Man Switch) = High		
	(Auto Start/Stop Switch) = High		
	(Ext. Cyl. Location) < (Ext. Limit Switch Ext.)		
Blocking objects (or)	(Ext Cyl. Retraction Sol.) = High		
	(Heaters Ready Light) = Low		
D: Auto extrusion retract	Delay on: 0	Toggle: No	
Auto extrusion retract	Delay off: 0		
Activating objects (and)	(Auto/Man Switch) = High		
	(Ext. Cyl. Location) > (Ext. Limit Switch Ret.)		
	(Auto Start/Stop Switch) = High		
Blocking objects (or)	(Ext. Cyl. Extension Sol) = High		
	(Heaters Ready Light) = Low		
E: Man compaction extend	Delay on: 0	Toggle: No	
Man compaction extend	Delay off: 0		
Activating objects (and)	(Auto/Man Switch) = Low		
	(Comp. Cyl. Ext. Switch) = High		
F: Man compaction retract	Delay on: 0	Toggle: No	
Man compaction retract	Delay off: 0		
Activating objects (and)	(Auto/Man Switch) = Low		
	(Comp. Cyl. Ret. Switch) = High		
G: Man extrusion extend	Delay on: 0	Toggle: No	
Man extrusion extend	Delay off: 0		
Activating objects (and)	(Auto/Man Switch) = Low		
	(Ext. Cyl. Ext. Switch) = High		
H: Man extrusion retract	Delay on: 0	Toggle: No	
Man extrusion retract	Delay off: 0		
Activating objects (and)	(Auto/Man Switch) = Low		
	(Ext. Cyl. Ret. Switch) = High		
I: Auto cutting cyl 1	Delay on: 0	Toggle: No	
Auto cutting cyl 1	Delay off: 0		
Activating objects (and)	(Auto/Man Switch) = High		
	(Auto Start/Stop Switch) = High		
	(Nugget Length Sensor 1) = High		
J: Auto cutting cyl 2	Delay on: 0	Toggle: No	
Auto cutting cyl 2	Delay off: 0		
Activating objects (and)	(Auto/Man Switch) = High		
	(Auto Start/Stop Switch) = High		
	(Nugget Length Sensor 2) = High		
K: Auto cutting cyl 3	Delay on: 0	Toggle: No	
Auto cutting cyl 3	Delay off: 0		
Activating objects (and)	(Auto/Man Switch) = High		
	(Auto Start/Stop Switch) = High		
	(Nugget Length Sensor 3) = High		
L: Auto cutting cyl 4	Delay on: 0	Toggle: No	
Auto cutting cyl 4	Delay off: 0		
Activating objects (and)	(Auto/Man Switch) = High		
	(Auto Start/Stop Switch) = High		
	(Nugget Length Sensor 4) = High		

Channels

Internal digital, MDM				
M: Man cutting cyl 1	Delay on:	0	Toggle:	No
Man cutting cyl 1	Delay off:	0		
Activating objects (and)	(Cut Cyl. 1 Ext. Switch) = High			
N: Man cutting cyl 2	Delay on:	0	Toggle:	No
Man cutting cyl 2	Delay off:	0		
Activating objects (and)	(Cut Cyl. 2 Ext. Switch) = High			
O: Man cutting cyl 3	Delay on:	0	Toggle:	No
Man cutting cyl 3	Delay off:	0		
Activating objects (and)	(Cut Cyl. 3 Ext. Switch) = High			
P: Man cutting cyl 4	Delay on:	0	Toggle:	No
Man cutting cyl 4	Delay off:	0		
Activating objects (and)	(Cut Cyl. 4 Ext. Switch) = High			
Q: Comp. Cyl Toggle	Delay on:	0	Toggle:	Yes
Comp. Cyl Toggle	Delay off:	0		
Activating objects (or)	(Comp. Cyl. Location) > (Comp. Limit Switch Ext.)			
	(Comp. Cyl. Location) < (Comp. Limit Switch Ret.)			
Blocking objects (or)	(Auto/Man Switch) = Low			
R: Ext. Cyl Toggle	Delay on:	0	Toggle:	Yes
Ext. Cyl Toggle	Delay off:	0		
Activating objects (or)	(Ext. Cyl. Location) > (Ext. Limit Switch Ext.)			
	(Ext. Cyl. Location) < (Ext. Limit Switch Ret.)			
Blocking objects (or)	(Auto/Man Switch) = Low			

Event counter, MDM		
B: Lifetime Nugget Counter		
Lifetime Nugget Counter		
Increasing objects (or)	(Cutting Cyl 2 Sol.) = High	
	(Cutting Cyl 1 Sol.) = High	
	(Cutting Cyl 3 Sol.) = High	
	(Cutting Cyl 4 Sol.) = High	

Digital out, XP-A0			
A1: Cutting Cyl 1 Sol.	Delay on:	0	
Cutting Cyl 1 Sol.	Delay off:	0	
Activating objects (or)	(Auto cutting cyl 1) = True		
	(Man cutting cyl 1) = True		
Blocking objects (or)	(Main Switch) = Low		
B1: Cutting Cyl 2 Sol.	Delay on:	0	
Cutting Cyl 2 Sol.	Delay off:	0	
Activating objects (or)	(Auto cutting cyl 2) = True		
	(Man cutting cyl 2) = True		
Blocking objects (or)	(Main Switch) = Low		
C1: Cutting Cyl 3 Sol.	Delay on:	0	
Cutting Cyl 3 Sol.	Delay off:	0	
Activating objects (or)	(Auto cutting cyl 3) = True		
	(Man cutting cyl 3) = True		
Blocking objects (or)	(Main Switch) = Low		
D1: Cutting Cyl 4 Sol.	Delay on:	0	
Cutting Cyl 4 Sol.	Delay off:	0	
Activating objects (or)	(Auto cutting cyl 4) = True		
	(Man cutting cyl 4) = True		
Blocking objects (or)	(Main Switch) = Low		
E1: Heaters Ready Light	Delay on:	0	
Heaters Ready Light	Delay off:	0	
Activating objects (and)	(Main Switch) = High		
	(Temperature Alarm) = Low		

Digital out, XS-A1			
A1: Comp. Cyl. Extension Sol	Delay on:	0	
Compaction Extension Sol	Delay off:	0	
Activating objects (or)	(Man compaction extend) = True		
	(Auto compaction extend) = True		
Blocking objects (or)	(Main Switch) = Low		

Channels

Digital out, XS-A1		
B1: Comp. Cyl. Retraction Sol Compaction Retraction Sol	Delay on: 0 Delay off: 0	
Activating objects (or)	(Man compaction retract) = True (Auto compaction retract) = True	
Blocking objects (or)	(Main Switch) = Low	
C1: Ext. Cyl. Extension Sol Extrusion Extension Sol	Delay on: 0 Delay off: 0	
Activating objects (or)	(Man extrusion extend) = True (Auto extrusion extend) = True	
Blocking objects (or)	(Main Switch) = Low	
D1: Ext Cyl. Retraction Sol. Copy of Extrusion Extensi	Delay on: 0 Delay off: 0	
Activating objects (or)	(Man extrusion retract) = True (Auto extrusion retract) = True	
Blocking objects (or)	(Main Switch) = Low	

Conditional message, MDM				
A: Hyd. Press. Disp. Hyd. Press Disp.	Delay on: 0 Delay off: 0	Text and channel Show always	Dual channels	
	Comp. Cylinder Comp. Cyl. Location [in]		Comp. Cyl. Location [in]	
	Ext. Cylinder Ext. Cyl. Location [in]		Ext. Cyl. Location [in]	
Activating objects (or)	True			

Interactive message, MDM		
A: Counter reset msg Counter reset msg	Text only	
	Reset Nugget Counter? F1=YES, F2=NO, F3=	F1=, F2=, F3=

IQAN MDM

Serial number: 611260015
Hardware version: 18.00
Software version: 4.06

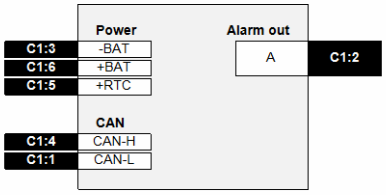

IQAN XP-A0

Serial number: 548230011
Hardware version: 56.00
Software version: 1.68

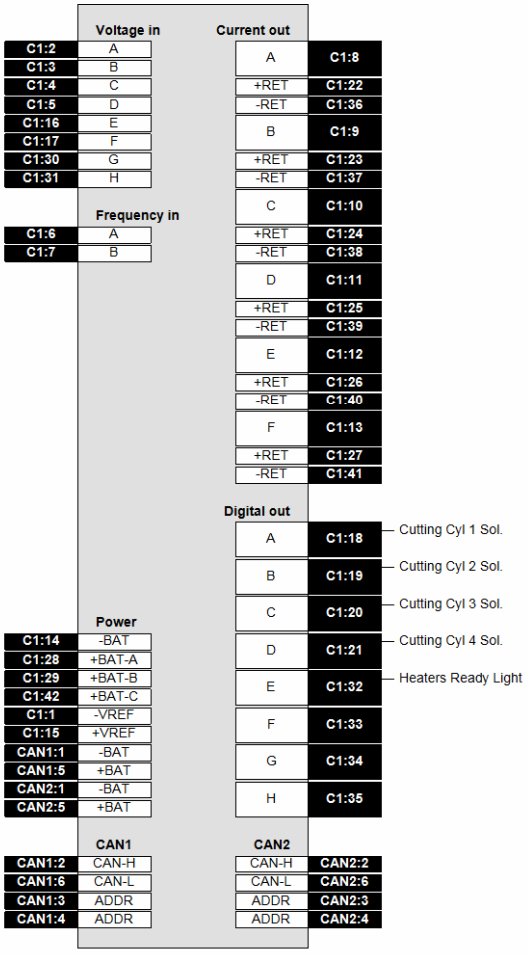

IQAN XS-A1

Serial number: 608230174
Hardware version: 45.00
Software version: 1.43

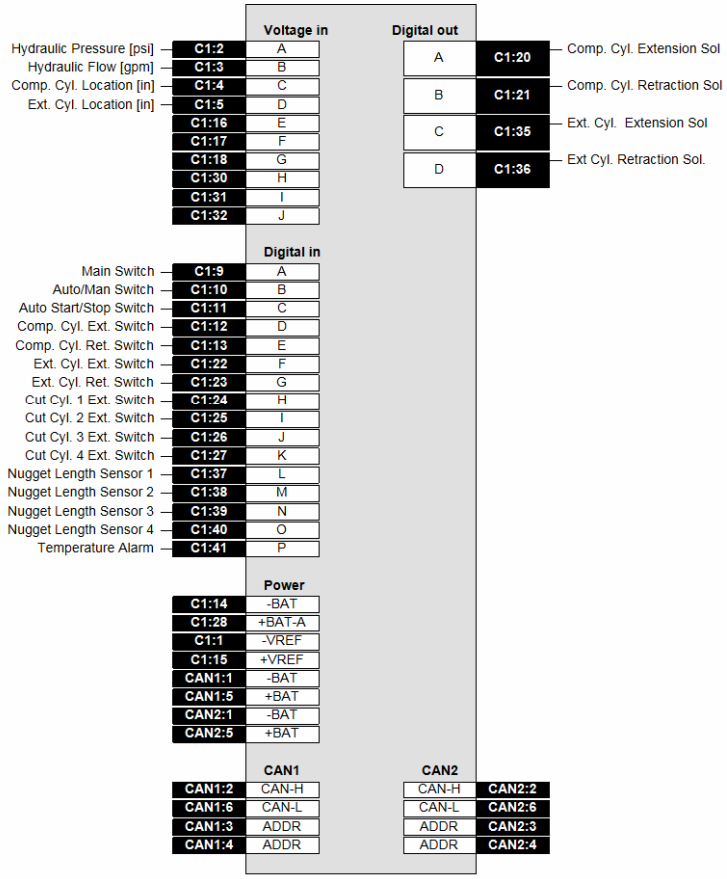

Appendix I – Wiring Diagrams for Control Box Components

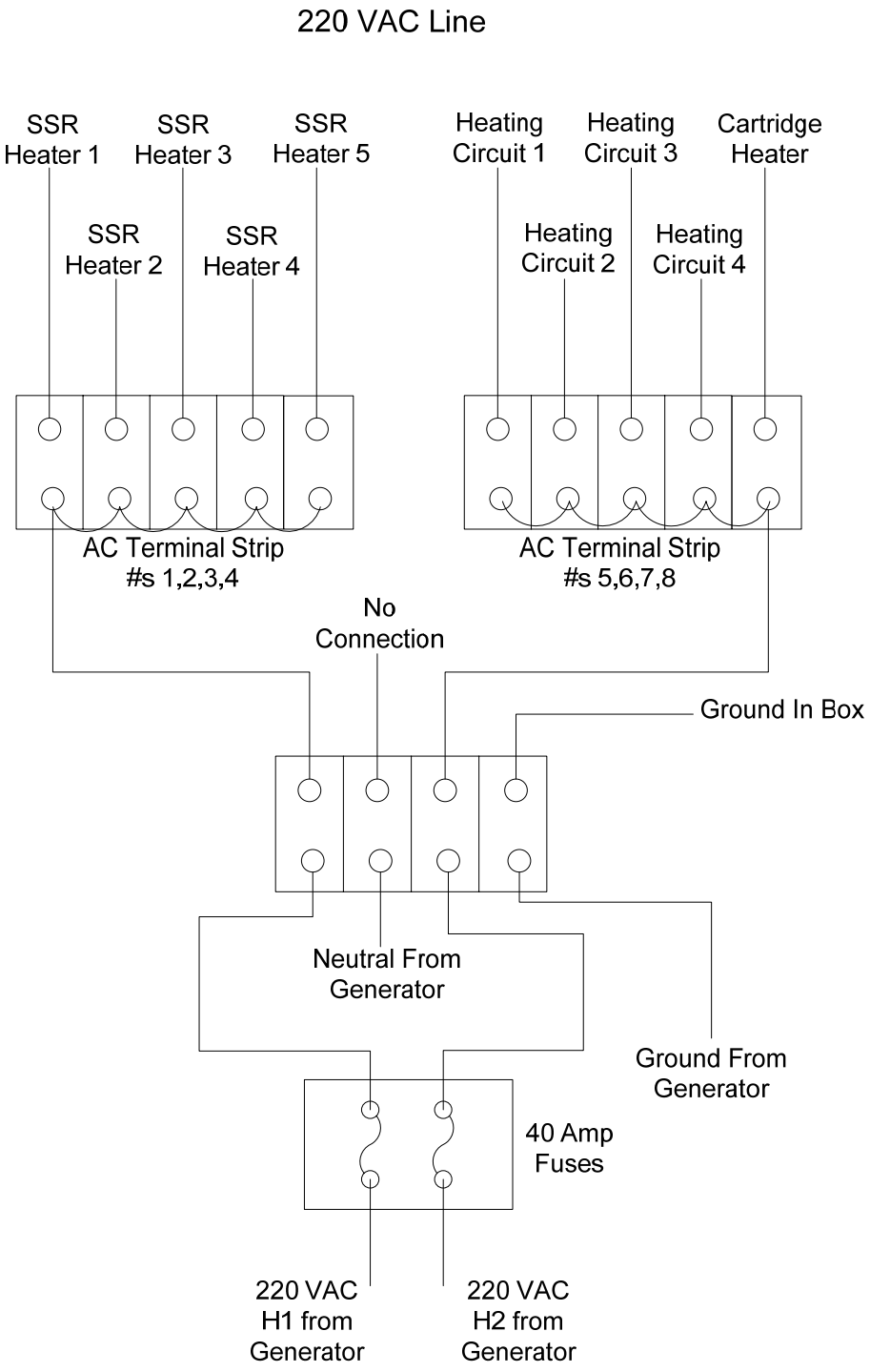

115 VAC Line

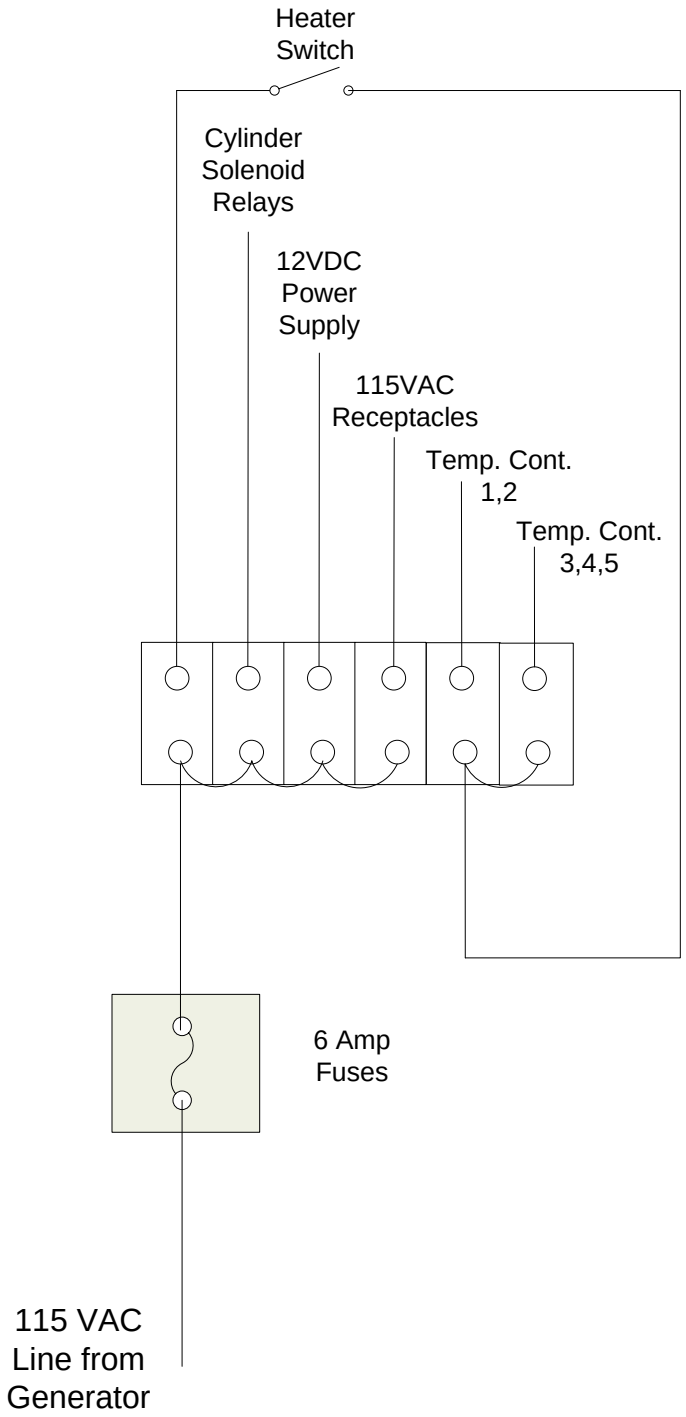
Heater
Switch
Cylinder
Solenoid
Relays
12VDC
Power
Supply
115VAC
Receptacles
Temp. Cont.
1,2
Temp. Cont.
3,4,5
6 Amp
Fuses
115 VAC
Line from
Generator

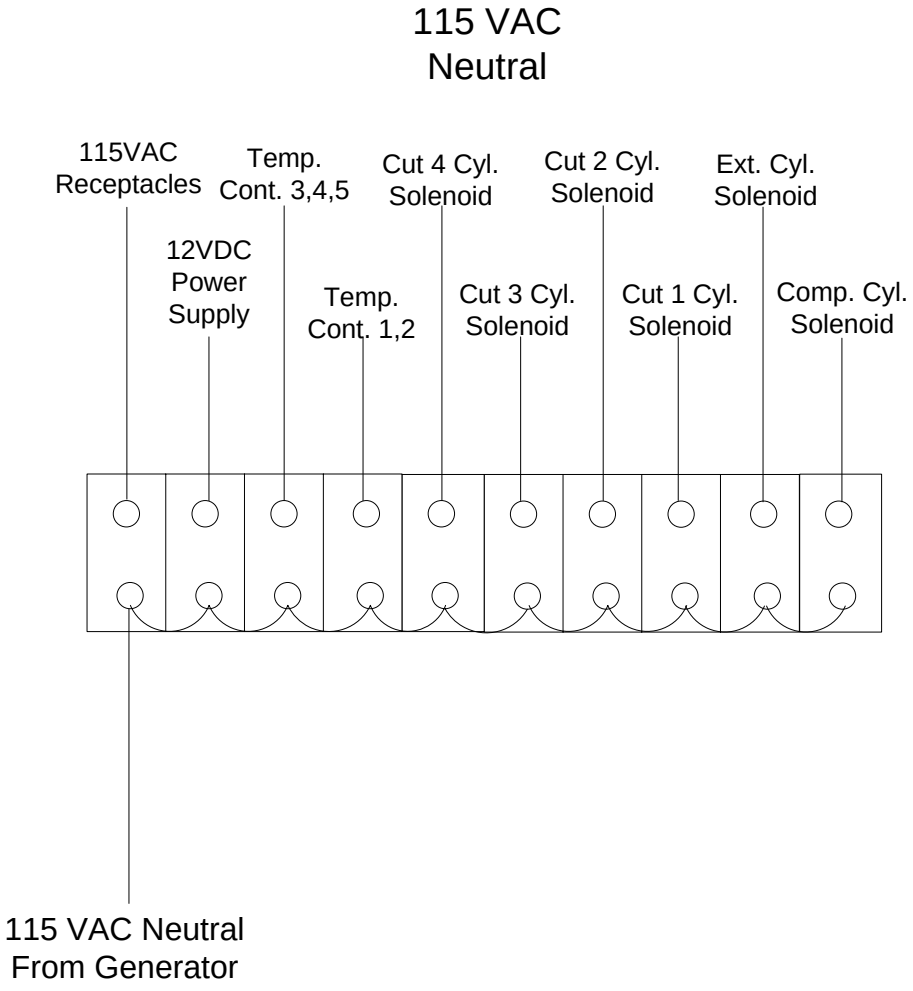
115 VAC
Neutral
115VAC
Receptacles
Temp.
Cont. 3,4,5
Cut 4 Cyl.
Solenoid
Cut 2 Cyl.
Solenoid
Ext. Cyl.
Solenoid
12VDC
Power
Supply
Temp.
Cont. 1,2
Cut 3 Cyl.
Solenoid
Cut 1 Cyl.
Solenoid
Comp. Cyl.
Solenoid
115 VAC Neutral
From Generator

12 VDC “+”

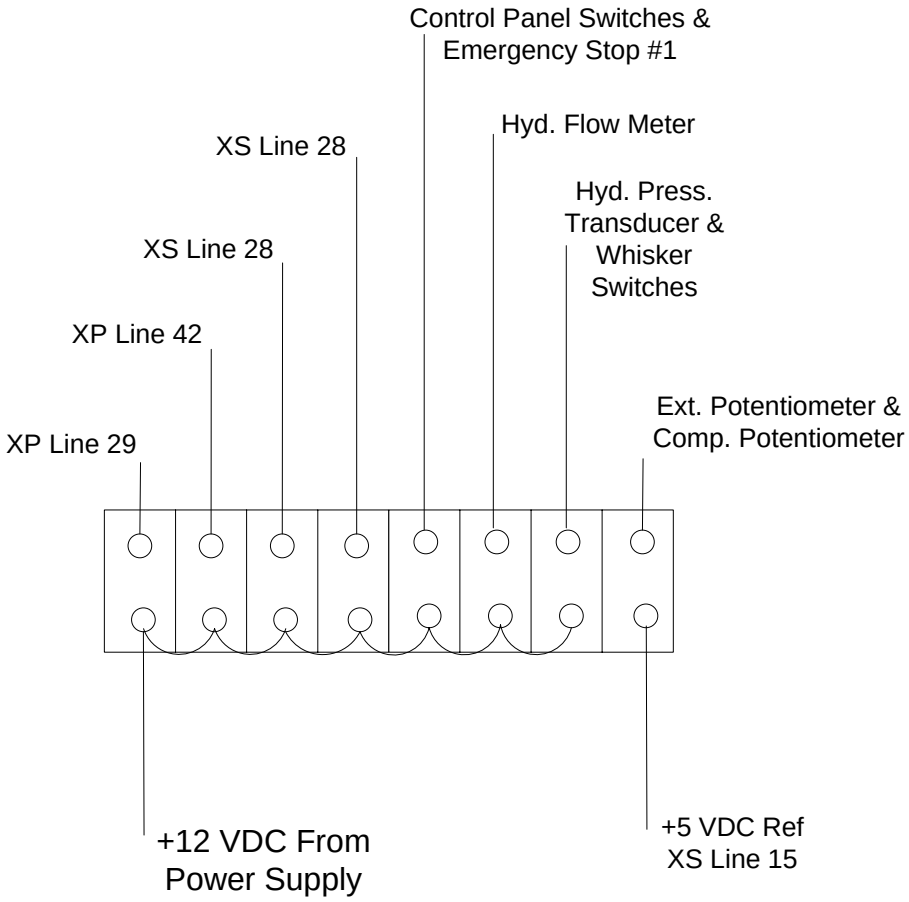
Control Panel Switches &
Emergency Stop #1
Hyd. Flow Meter
XS Line 28
Hyd. Press.
Transducer &
Whisker
Switches
XS Line 28
XP Line 42
Ext. Potentiometer &
Comp. Potentiometer
XP Line 29
+12 VDC From
Power Supply
+5 VDC Ref
XS Line 15

Grounding Terminal Strip

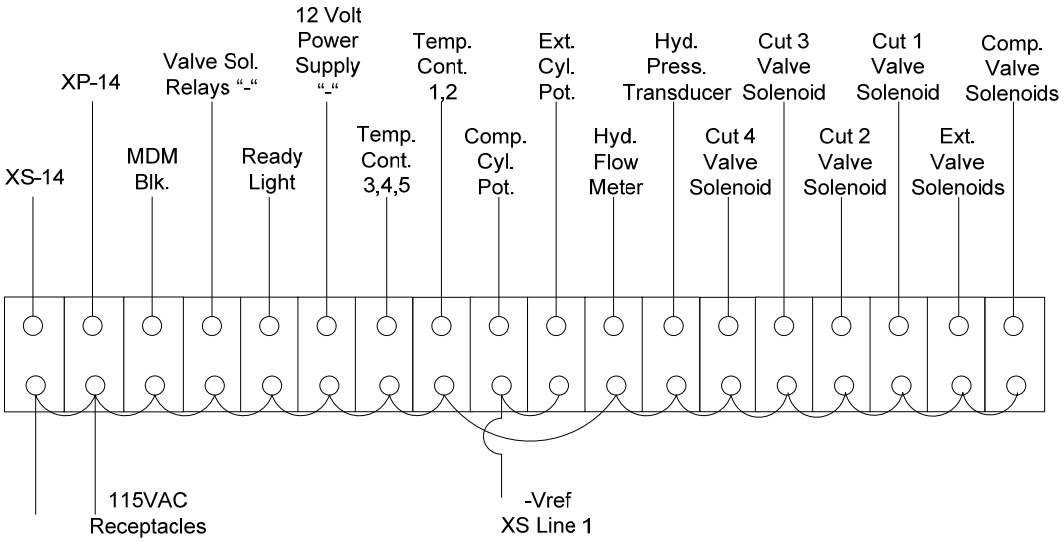

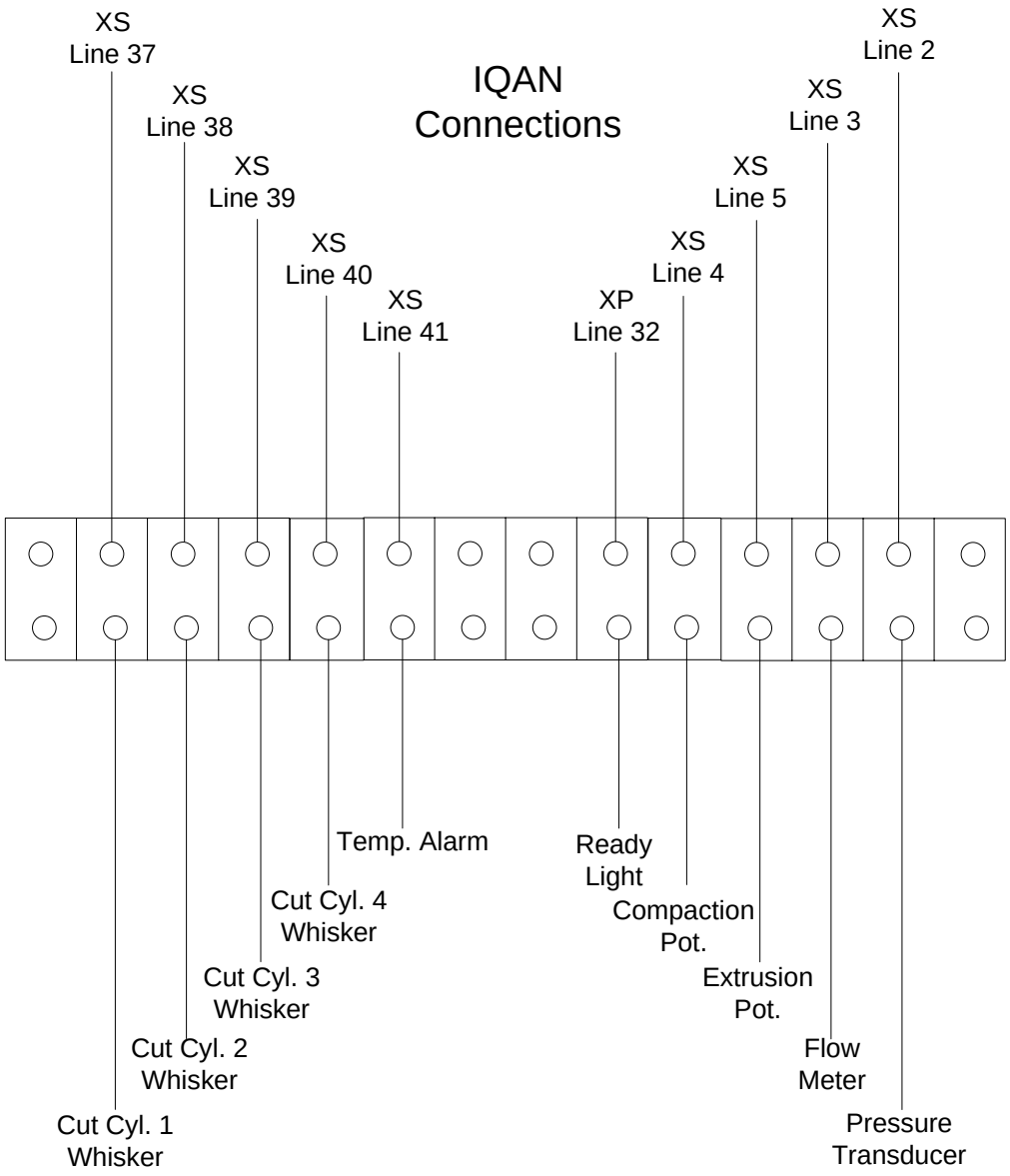
IQAN
Connections
XS
Line 37
XS
Line 38
XS
Line 39
XS
Line 40
XS
Line 41
XP
Line 32
XS
Line 4
XS
Line 5
XS
Line 3
XS
Line 2
Cut Cyl. 1
Whisker
Cut Cyl. 2
Whisker
Cut Cyl. 3
Whisker
Cut Cyl. 4
Whisker
Temp. Alarm
Ready
Light
Compaction
Pot.
Extrusion
Pot.
Flow
Meter
Pressure
Transducer

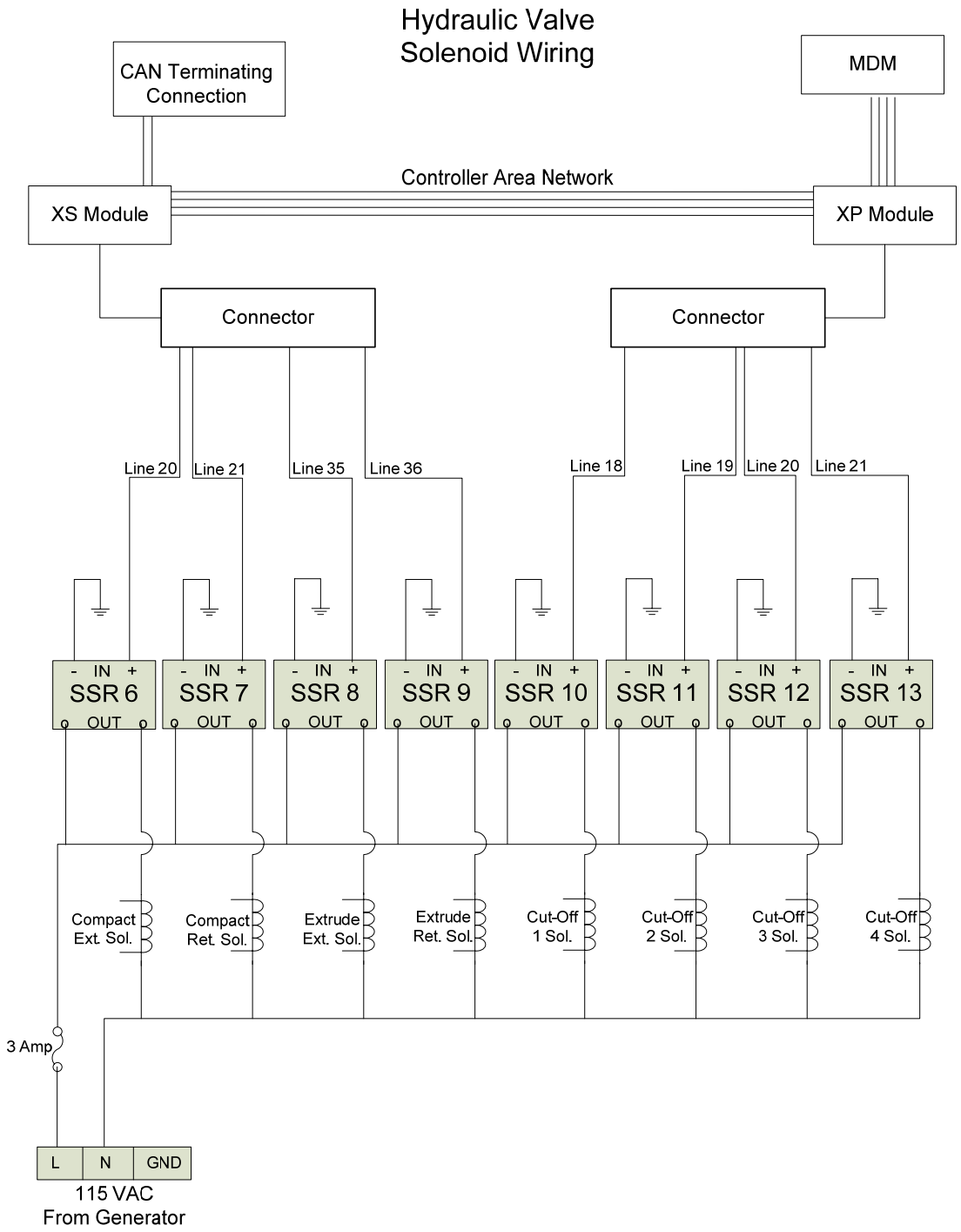
Hydraulic Valve
Solenoid Wiring
CAN Terminating Connection
MDM
Controller Area Network
XS Module
XP Module
Connector
Connector
Line 20
Line 21
Line 35
Line 36
Line 18
Line 19
Line 20
Line 21
- IN +
SSR 6
OUT
SSR 7
SSR 8
SSR 9
SSR 10
SSR 11
SSR 12
SSR 13
Compact Ext. Sol.
Compact Ret. Sol.
Extrude Ext. Sol.
Extrude Ret. Sol.
Cut-Off 1 Sol.
Cut-Off 2 Sol.
Cut-Off 3 Sol.
Cut-Off 4 Sol.
3 Amp
L
N
GND
115 VAC
From Generator

Heater Strip Wiring

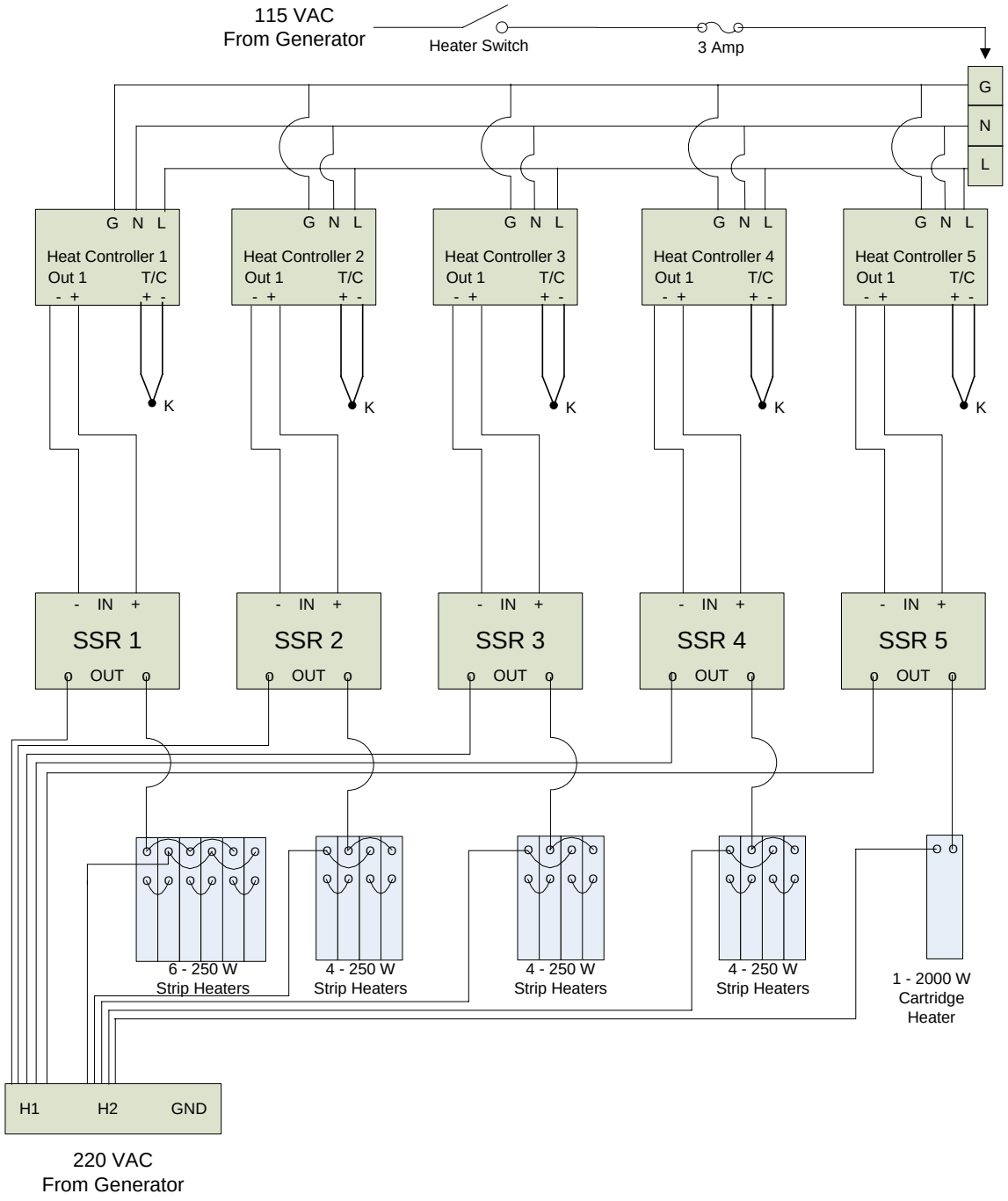

Appendix J – Sample Data from the ElitePro Power Meter

Sample Data From the ElitePro Power Meter

Date	Time	115VAC Power (kW)	220VAC Power (kW)
4/21/2007	9:20:12	0.028	1.446
4/21/2007	9:20:15	0.028	1.449
4/21/2007	9:20:18	0.028	1.447
4/21/2007	9:20:21	0.029	1.441
4/21/2007	9:20:24	0.028	1.448
4/21/2007	9:20:27	0.028	1.446
4/21/2007	9:20:30	0.029	2.413
4/21/2007	9:20:33	0.027	2.414
4/21/2007	9:20:36	0.028	2.408
4/21/2007	9:20:39	0.049	2.406
4/21/2007	9:20:42	0.049	2.402
4/21/2007	9:20:45	0.049	2.396
4/21/2007	9:20:48	0.049	2.397
4/21/2007	9:20:51	0.05	2.39
4/21/2007	9:20:54	0.049	2.395
4/21/2007	9:20:57	0.049	2.398
4/21/2007	9:21:00	0.049	2.397
4/21/2007	9:21:03	0.05	2.394
4/21/2007	9:21:06	0.068	1.444
4/21/2007	9:21:09	0.068	1.443
4/21/2007	9:21:12	0.049	1.442
4/21/2007	9:21:15	0.069	1.446
4/21/2007	9:21:18	0.048	1.44
4/21/2007	9:21:21	0.05	1.442
4/21/2007	9:21:24	0.049	1.441
4/21/2007	9:21:27	0.05	1.442
4/21/2007	9:21:30	0.049	1.437

Sample Analyzed Data from the ElitePro Power Meter

Test Run 1 April 21

Start Time	4/21/07 8:17 AM	
End Time	4/21/07 8:27 AM	
Plastofuel Formed	3.6	kg
Avg. Power Used	1.61	kW
Total Energy Used	0.27	kW-hr

Record Date	Record End Time	115VAC Circuit (kW)	220VAC Circuit (kW)	Total Power Use (kW)	Energy Consumption (kW-hr)	
4/21/2007	8:17:09	0.03	2.421	2.451	0.0020	
4/21/2007	8:17:12	0.028	2.426	2.454	0.0020	
4/21/2007	8:17:15	0.028	2.416	2.444	0.0020	
4/21/2007	8:17:18	0.028	2.418	2.446	0.0020	
4/21/2007	8:17:21	0.029	2.423	2.452	0.0020	
4/21/2007	8:17:24	0.028	2.419	2.447	0.0020	
4/21/2007	8:17:27	0.028	1.458	1.486	0.0012	
4/21/2007	8:17:30	0.029	1.456	1.485	0.0012	
4/21/2007	8:17:33	0.028	1.457	1.485	0.0012	
4/21/2007	8:17:36	0.027	1.453	1.48	0.0012	
.	.	.	.	.	.	
.	.	.	.	.	.	
.	.	.	.	.	.	
4/21/2007	8:27:18	0.028	1.928	1.956	0.0016	
4/21/2007	8:27:21	0.028	1.936	1.964	0.0016	
4/21/2007	8:27:24	0.028	1.93	1.958	0.0016	
4/21/2007	8:27:27	0.029	1.45	1.479	0.0012	
4/21/2007	8:27:30	0.028	1.45	1.478	0.0012	
4/21/2007	8:27:33	0.05	1.455	1.505	0.0013	
4/21/2007	8:27:36	0.03	1.452	1.482	0.0012	
4/21/2007	8:27:39	0.028	1.449	1.477	0.0012	
4/21/2007	8:27:42	0.028	1.449	1.477	0.0012	
4/21/2007	8:27:45	0.028	1.454	1.482	0.0012	
			Calculated Average -->	1.82	0.3223	<-- Calculated Sum

Appendix K – Sample Data from MDM Data Logger

Sample Data from the MDM Data Logger

Appl. description	
Appl. version	0
Start time	4/21/2007 8:33
Total time	10.1 minutes
Comment	

Time [s]	Hydraulic Pressure [psi]	Hydraulic Flow [gpm]	Comp. Cyl. Location [in]	Ext. Cyl. Location [in]	Cutting Cyl 1 Sol.	Cutting Cyl 2 Sol.	Cutting Cyl 3 Sol.	Cutting Cyl Heaters	Ready Light
33050	991	0	0.89	14.83	0	1	0	0	1
33100	919	0	0.89	14.83	0	1	0	0	1
33150	499	0	0.89	14.83	0	1	0	0	1
33200	286	0	0.89	14.83	0	1	0	0	1
33250	510	0	0.89	14.83	0	1	0	0	1
33300	1156	0	0.89	14.83	0	1	0	0	1
33350	1965	0	0.89	14.83	0	1	0	0	1
33400	2606	0	0.89	14.83	0	1	0	0	1
33450	3038	0	0.89	14.83	0	1	0	0	1
33500	2916	0	0.89	14.83	0	0	0	0	1
33550	2843	0	0.89	14.83	0	0	0	0	1
33600	2344	0	0.89	14.83	0	0	0	0	1
33650	1710	0	0.89	14.83	0	0	0	0	1
33700	2448	0	0.92	14.83	0	0	0	0	1
33750	2886	0	0.92	14.83	0	0	0	0	1
33800	2800	0	0.92	14.83	0	0	0	0	1
33850	2672	0	0.92	14.83	0	0	0	0	1
33900	2490	0	0.92	14.83	0	0	0	0	1
33950	2094	0	0.92	14.83	0	0	0	0	1
34000	1735	0	0.92	14.83	0	0	0	0	1
34050	1564	0	0.92	14.83	0	0	0	0	1
34100	1455	0	0.92	14.83	0	0	0	0	1
34150	1345	0	0.92	14.83	0	0	0	0	1
34200	1248	0	0.92	14.83	0	0	0	0	1
34250	1162	0	0.92	14.83	0	0	1	0	1
34300	1077	0	0.92	14.83	0	0	1	0	1
34350	571	0	0.92	14.83	0	0	1	0	1
34400	322	0	0.92	14.83	0	0	1	0	1
34450	529	0	0.92	14.83	0	0	1	0	1
34500	1516	0	0.92	14.83	0	0	1	0	1
34550	2283	0	0.92	14.83	0	0	1	0	1
34600	2904	0	0.92	14.83	0	0	1	0	1
34650	3081	0	0.92	14.83	0	0	0	0	1

Sample Analyzed Data from MDM

Test 2 Apr 21

Start time	4/21/07 8:33 AM	
Total time	10	minutes
Plastofuel Formed	3.5	kg
Avg. Hyd. Power	2.10	kW
% Energy for Compaction	0.5	%
% Energy for Extrusion	93.1	%
% Energy for Cutting	6.4	%
Total Energy Used	0.35	kw-hr

Comp. and Ext. Cylinders

cyl_bore	5.08	cm	given
bore_area	20.27	sq_cm	PI()*(cyl_bore/2)^2
cyl_rod	2.54	cm	given
rod_area	5.07	sq_cm	PI()*(cyl_rod/2)^2
annulus_area	15.20	sq_cm	bore_area-rod_area

Cutting Cylinders

cut_cyl_bore	3.81	cm	given
cut_cyl_bore_area	11.40	sq_cm	PI()*(cut_cyl_bore/2)^2
cut_cyl_rod	1.98	cm	given
cut_cyl_rod_area	3.08	sq_cm	PI()*(cut_cyl_rod/2)^2
cut_annulus_area	8.32	sq_cm	cut_cyl_bore_area-cut_cyl_rod_area
cut_cyl_stroke	6.35	cm	given
extend_volume	72.40	cubic_cm	cut_cyl_bore_area*cut_cyl_stroke
retract_volume	52.84	cubic_cm	cut_annulus_area*cut_cyl_stroke
extend_time	0.4	sec	observed
retract_time	0.3	sec	observed
cut_extend_flow	180.99	cubic_cm/sec	extend_volume/extend_time
cut_retract_flow	176.15	cubic_cm/sec	retract_volume/retract_time
lpm_extend	10.86	lpm	cut_extend_flow*60/1000
lpm_retract	10.57	lpm	cut_retract_flow*60/1000

Calculations I added

Output directly from IQAN

Time [ms]	Hydraulic Pressure [psi]	Hydraulic Pressure (kPa)	Hydraulic Flow [gpm]	Comp. Cyl. Location [in]	Calculated Comp. Cyl. Flow [lpm]	Calculated Comp. Cyl. Energy (kW-hr)	Ext. Cyl. Location [in]	Calculated Ext. Cyl. Flow [lpm]	Calculated Ext. Cyl. Energy (kW-hr)	Calc. Comp. and Ext. Flow [lpm]
542550	1205	8308	0	0.84			14.97			0.00
542600	1156	7970	0	0.84	0.00	0.0000	14.97	0.00	0.0000	0.00
542650	712	4909	0	0.84	0.00	0.0000	14.97	0.00	0.0000	0.00
542700	339	2337	0	0.84	0.00	0.0000	14.97	0.00	0.0000	0.00
542750	559	3854	0	0.84	0.00	0.0000	14.97	0.00	0.0000	0.00
542800	1577	10873	0	0.84	0.00	0.0000	14.97	0.00	0.0000	0.00
542850	2393	16499	0	0.84	0.00	0.0000	14.97	0.00	0.0000	0.00
542900	2971	20484	0	0.84	0.00	0.0000	14.97	0.00	0.0000	0.00
542950	3020	20822	0	0.84	0.00	0.0000	14.97	0.00	0.0000	0.00
543000	2855	19685	0	0.84	0.00	0.0000	14.97	0.00	0.0000	0.00
543050	2258	15568	0	0.87	1.85	0.0000	14.97	0.00	0.0000	1.85
543100	1911	13176	0	0.87	0.00	0.0000	14.97	0.00	0.0000	0.00
543150	2539	17506	0	0.84	1.39	0.0000	14.97	0.00	0.0000	1.39
543200	2904	20022	0	0.87	1.85	0.0000	14.97	0.00	0.0000	1.85
543250	2825	19478	0.76	0.87	0.00	0.0000	14.97	0.00	0.0000	0.00
					Column Sum------->	0.0016		Column Sum--->	0.324	

This is an example of the spreadsheet used to solve for total hydraulic power consumption for the machine during operation.

(continued from previous page)

Sample Analyzed Data from MDM

Test 2 Apr 21

Cutting Cyl 1 Sol.	Cyl 1 Flowrate (lpm)	Cutting Cyl 2 Sol.	Cyl 2 Flowrate (lpm)	Cutting Cyl 3 Sol.	Cyl 3 Flowrate (lpm)	Cutting Cyl 4 Sol.	Cyl 4 Flowrate (lpm)	Total Cut Cyl. Flowrate (lpm)	Calculated Cutting Cyl. Energy (kW-hr)	Total Flowrate (lpm)	Hyd. Power Consumed (kW)	Hyd. Energy Consumed (kW-hr)	Heaters Ready Light
0		0		1	10.86	0		10.86		10.86	1.5		1
0		0		1	10.86	0		10.86	0.0000	10.86	1.4	0.000	1
0		0		1	10.86	0		10.86	0.0000	10.86	0.9	0.000	1
0		0		1	10.86	0		10.86	0.0000	10.86	0.4	0.000	1
0		0		1	10.86	0		10.86	0.0000	10.86	0.7	0.000	1
0		0		1	10.86	0		10.86	0.0000	10.86	2.0	0.000	1
0		0		1	10.86	0		10.86	0.0000	10.86	3.0	0.000	1
0		0		1	10.86	0		10.86	0.0001	10.86	3.7	0.000	1
0		0		0	10.57	0		10.57	0.0001	10.57	3.7	0.000	1
0		0		0	10.57	0		10.57	0.0000	10.57	3.5	0.000	1
0		0		0	10.57	0		10.57	0.0000	12.42	3.2	0.000	1
0		0		0	10.57	0		10.57	0.0000	10.57	2.3	0.000	1
0		0		0	10.57	0		10.57	0.0000	11.96	3.5	0.000	1
0		0		0	10.57	0		10.57	0.0000	12.42	4.1	0.000	1
0		0		0		0		0.00	0.0000	0.00	0.0	0.000	1
								Column Sum--->	0.0224	Column Avg.----->	2.08	0.348	<---Column Sum

Appendix L – Temperature Distribution in Plastofuel™ Melt Zone Calculations

This is a spreadsheet solution and data table to solve for and graph the temperature distribution in the melted portion of the Plastofuel™ nugget.

Temperature Profile of Liquid Portion - Tadmore Eqn 9.3-37

MATSE 596	Matt Lawrence			
INPUTS				
alpha_l	thermal diffusivity	1.13E-07	m^2/s	solved using Appendix G spreadsheet
beta	liquid to solid ratio	1	none	given
Tone	wall temperature	448	°K	assumed
Tm	melting temperature	393	°K	assumed
t	time in contact with hot plate	120	s	assumed
x_l	depth in melt at which temp is measure	0.00025	m	assumed
K	constant for wall temperature of 448°K	1.43E-04	none	solved using Appendix G spreadsheet
OUTPUT				
				(((1-((ERF(x_l/(2*SQRT(alpha_l*t))))/(ERF(K*beta/(2*SQRT(alpha_l))))))*(Tone-Tm))+Tm)-273
	temperature of liquid at depth x after			
Tl	time t	166.1	°C	

time (s)	Depth within melt at which temperature is measured (m)								
166.1	0.00025	0.0005	0.00075	0.001	0.00125	0.0015	0.00175	0.002
120	166.1	157.2	148.4	139.6	130.9	122.3	113.8	105.4
150	167.0	159.1	151.2	143.3	135.5	127.7	120.0	112.5
180	167.7	160.5	153.2	146.0	138.9	131.7	124.7	117.7
210	168.3	161.5	154.8	148.2	141.5	134.9	128.4	121.9
240	168.7	162.4	156.1	149.9	143.6	137.5	131.3	125.2
270	169.1	163.1	157.2	151.3	145.4	139.6	133.8	128.0
300	169.4	163.7	158.1	152.5	146.9	141.4	135.8	130.4
330	169.6	164.3	158.9	153.6	148.2	142.9	137.6	132.4
360	169.9	164.7	159.6	154.5	149.4	144.3	139.2	134.2
390	170.1	165.1	160.2	155.3	150.4	145.5	140.6	135.8
420	170.2	165.5	160.7	156.0	151.3	146.5	141.8	137.2

Appendix M – Temperature Distribution Calculations for Plastofuel™ Solid Zone

This is a spreadsheet solution and data table to solve for and graph the temperature distribution in the unmelted portion of the Plastofuel™ nugget.

Temperature Profile of Solid Portion - Tadmore Eqn 9.3-38

MATSE 596 Matt Lawrence

INPUTS

alpha_s	thermal diffusivity	1.13E-07 m^2/s	given
To	intital core temperature	298 °K	given
Tm	melting temperature	393 °K	given
t	time in contact with hot plate	120 s	given
x_s	depth in solid portion at which temp is measure	0 m	assumed
K	constant for wall temperature of 448°K	1.43E-04 none	determined in "K calcs" spreadsheet

OUTPUT

Ts	temperature of solid at a distance x from the melt after time t	149.4 °K	((1-((ERFC(x_s/(2*SQRT(alpha_s*t))))/(ERFC(K/(2*SQRT(alpha_s))))))*(To-

time (s)	Temperature at depth from melt/solid transition (m)								
149.4	0.0020	0.0025	0.0050	0.0075	0.0100	0.0125	0.0150	0.0190
120	112.2	103.5	66.9	43.6	31.8	27.0	25.5	25.0
150	116.0	108.1	73.6	49.6	35.7	29.0	26.2	25.1
180	118.8	111.5	78.9	54.8	39.5	31.2	27.3	25.4
210	121.0	114.2	83.2	59.4	43.2	33.7	28.7	25.7
240	122.8	116.4	86.9	63.4	46.7	36.2	30.2	26.2
270	124.3	118.2	90.0	66.9	49.9	38.6	31.8	26.9
300	125.5	119.7	92.6	70.1	52.9	41.0	33.5	27.6
330	126.6	121.1	95.0	72.9	55.7	43.4	35.3	28.5
360	127.6	122.3	97.1	75.5	58.3	45.6	37.0	29.4
390	128.4	123.3	98.9	77.8	60.7	47.8	38.7	30.3
420	129.2	124.2	100.6	79.9	62.9	49.8	40.4	31.4

Appendix N – Energy Required to Heat Unmelted Nugget Interior

INPUTS				
width	nugget width	0.038	m	given
height	nugget height	0.038	m	given
fillet_area	area of four edge fillets	3.46E-05	m^2	given
melt	depth of melt	0.002	m	given
prod_rate	production rate of plastofuel	19	kg/hr	assumed
sh_plastofuel	heat capacity of plastofuel	2217	J/kg°K	assumed
time	duration for test 20	0.17	hrs	given
radius	radius of unmelted nugget interior	0.017	m	given
length	nugget length	0.050	m	given
rho	density of plastofuel	708	kg/m^3	assumed
INTERMEDIATE CALCULATIONS				
area_total	area of nugget face	0.0014	m^2	width*height-fillet_area
nugget_volume	volume of each nugget	0.00007	m^3	area_total*length
nuggets_produced	number of nuggets produced in test run	65	none	(prod_rate*time)/(rho*nugget_volume)
energy_per_nugget	energy required to warm each nugget interior	0.0010	kW-hr	(2*PI()*length*rho*sh_plastofuel*(97500*radius^4-4600*radius^3+75*radius^2))/3600(
OUTPUT				
total_energy	total energy to raise unmelted interior temperatu	0.064	kW-hr	energy_per_nugget*nuggets_produced

This calculation was used to estimate the energy wasted during nugget formation by heating the unmelted nugget interior.

VITA
MATTHEW J. LAWRENCE

967 Runville Road
Bellefonte, PA 16823
http://www.personal.psu.edu/mjl145
814-355-0777

mjl145@psu.edu

EDUCATION

The Pennsylvania State University, University Park, PA

Ph.D. in Agricultural and Biological Engineering, August 2007
GPA 3.80
M.S. in Agricultural and Biological Engineering, December 2004
GPA 3.88
B.S. in Agricultural Engineering, August 1997
GPA 3.16

PROFESSIONAL EXPERIENCE

The Pennsylvania State University, University Park, PA
Teaching Assistant, Fall 2004 and Spring 2006

Cisco Systems, San Jose, CA and Arlington, VA
Technical Marketing Engineer, February 1999-August 2003

Parker Hannifin, Clovis, CA
Pneumatic Territory Manager, August 1997-February 1999

Cummins Engine, Jamestown, NY
Plant Engineer, Spring 1995 and Summer 1996

CERTIFICATIONS

Certified Hydraulic Specialist, International Fluid Power Society
Penn State College Teaching Certificate
Certified Pennsylvania Engineer-In-Training

HONORS

Harold V. and Velma B. Walton Doctoral Student Endowment Recipient
First Place – Penn State Gamma Sigma Delta 2005 Research Expo
Third Place – Penn State 2005 Graduate Exhibition
Alpha Epsilon, The Honor Society of Agricultural, Food, and Biological Engineering